SOIL PHOSPHORUS BIOGEOCHEMISTRY IN THE CALHOUN CRITICAL ZONE OBSERVATORY, SOUTH CAROLINA: EFFECTS OF LAND USE, TOPOGRAPHY, AND TIME

by

MARYAM FOROUGHI

(Under the Direction of Daniel Markewitz)

ABSTRACT

Soil phosphorus (P) biogeochemistry is fundamental to how terrestrial ecosystems function and cycling of soil P can modulate P bioavailability as can human actions. The Calhoun Critical Zone Observatory is an ancient landscape that has a modern (1750-1950) history of forest clearing for agriculture that included P fertilization and severe surface erosion followed by reforestation. I hypothesized that historic P fertilization impacts current P biogeochemistry and that soil P supply for afforestation is buffered by fertilizer P. My investigations of P pool changes with topography and with agricultural land use found that historically farmed hillslopes have more extractable P relative to forests without farming down through 2m depth. Further, in toe slope locations, organic P (P_o) is elevated compared to ridges. Phosphorus in soil solution and on ion exchange resins were higher in reference areas but were low in [P] similar to local streams. My analysis of soil P bioavailability under afforestation from 1957 to 2017, cataloged changes in 0-60 cm mineral soil P fractions in plots uncut since planting and plots cut in 2007. I found extractable P decreased in uncut and cut plots in 0-7.5 cm. Further, between 2005 to 2017 the slowly cycling P_o did not increase in the uncut plots but increased in 0-7.5 cm soil of cut plots. Changes in soil P fractions relative to tree P-demand suggest Ca-P and P_o pools are supplying soil P. To investigate the effect of different land uses on P losses over time I combined multiple years of soil, soil solution, and stream water data from two small watersheds with the soil and water assessment tool (SWAT). I found annual total P loss under 100% agriculture was six times greater than under 100% forest cover while intermediate conditions were three times less than under agriculture. Further, the model predicted rates of soil P leaching that were consistent with the observed increases in extractable soil P. Simulation indicated high rainfall years or events (i.e., hurricanes) may have historically facilitated P movement. After 60+ years since agricultural abandonment the Calhoun Critical Zone Observatory retains a legacy on soil P biogeochemistry.

INDEX WORDS: Phosphorus, slowly cycling P, Calhoun Critical Zone Observatory, P distribution, land use changes, SWAT

SOIL PHOSPHORUS BIOGEOCHEMISTRY IN THE CALHOUN CRITICAL ZONE OBSERVATORY, SOUTH CAROLINA: EFFECTS OF LAND USE, TOPOGRAPHY, AND TIME

by

MARYAM FOROUGHI

BS, Isfahan University of Technology, IRAN, 2006

MS, Khorasgan Azad University, IRAN, 2009

A Dissertation Submitted to the Graduate Faculty of The University of Georgia in Partial Fulfillment of the Requirements for the Degree

DOCTOR OF PHILOSOPHY

ATHENS, GEORGIA

2019

SOIL PHOSPHORUS BIOGEOCHEMISTRY IN THE CALHOUN CRITICAL ZONE OBSERVATORY, SOUTH CAROLINA: EFFECTS OF LAND USE, TOPOGRAPHY, AND TIME

by

MARYAM FOROUGHI

Major Professor: Daniel Markewitz
Committee: Lawrence Morris
Miguel Cabrera
Aaron Thompson

Electronic Version Approved:

Ron Walcott
Interim Dean of the Graduate School
The University of Georgia
December 2019

DEDICATION

This work is dedicated to my lovely husband without his caring support it would not have been possible and to my delightful parents for their endless love, support, and encouragement. To my brother who has never left my side and is very special.

ACKNOWLEDGEMENTS

Sincere appreciation and gratitude are extended to my advisor, Dr. Daniel Markewitz, for his insightful guidance, immense help and support, and constructive criticism throughout the preparation and completion of this PhD dissertation. Thanks also go to other members of my advisory committee, Dr. Lawrence Morris, Dr. Miguel Cabrera, and Dr. Aaron Thompson for their support and helpful discussions during my program. I'm extremely grateful to Dr. Lori Sutter for her guidance, the support many hours in field and lab, and editing.

I need to send out special thanks to Ji (Jill) Qi, Rachel Ryland, Matthew Thibodeaux, Brandon Varner, George Matthews, Lewis Craghead, Nahal Hoghooghi, Saime Carvalho, Ruan Mateus Guimaraes Dias, Nehru Mantripragada, Zhine Wang, Caitlin Hodges, Aaron Joslin, Nadia Noor, Melissa Martin, Tierra Sanford, Carla Gann, Paul Heine, Will Cook, John Mallard for their help within the field and laboratory, advice, and camaraderie.

Thanks should also go to the National Science Foundation (NSF) through the Critical Zone Observatories for providing the financial support for this research. In addition, thank you to NSF Science Across Virtual Institutes for providing Scholarship to participate in "Environmental Monitoring Techniques in the Critical Zone Observatory" field course hosted by the National Autonomous University of Mexico (UNAM). My deepest appreciation my parents and husband for their constant support and encouragement over the past years.

TABLE OF CONTENTS

LIST OF TABLES

Page

LIST OF FIGURES

Page

CHAPTER 1

INTRODUCTION

Soils are a key component of ecosystems. Studying soils and the associated nutrient cycling processes at and below Earth's surface is a key purpose of the Critical Zone Observatory (CZO) network. Soil cycling of the essential and often co-limiting element phosphorus (P) is a critical attribute governing ecosystem structure and function. Phosphorus is the least available and least mobile of the plant macro-nutrients in most soil orders, and its form (e.g., organic or inorganic), and spatial distribution vertically and horizontally also affects ecosystem processes. The distribution and conversion of soil P is dynamic and driven by both biological and pedological pathways and is well suited to investigation under the CZO context.

In this dissertation I focus on soil P dynamics as it relates to hillslope position, reforestation, and historical land use changes. The entirety of my research is undertaken in the Calhoun Experimental Forest that was established in 1947 in the Sumter National Forest in the Piedmont of South Carolina, USA and in 2015 became the Calhoun Critical Zone Observatory (Calhoun CZO). The southern Piedmont is dominated by Ultisols derived from granitic gneiss. The Calhoun CZO area has a history of forest clearing and burning in the early 1800s, which initiated an era of soil degradation and increased erosion rates. Severe surface erosion (~17 cm) resulted from cotton, corn, wheat, and other crops that were cultivated from 1800 until the early twentieth century when many agricultural lands were abandoned. During cultivation some lands were fertilized with lime and P for crop production. After abandonment, some lands were converted to pasture and many others regenerated to forest.

My overall dissertation objective is to better quantify how soil P has been modified by a history of agricultural fertilizer P input, how this P is being redistributed across the landscape, and how P forms are changing in the soils.

In Chapter 2, I provide a brief introduction and literature review for a range of topics on soil P.

In Chapter 3, I investigate the impact of long periods of land use changes within hillslope positions in watersheds of the Calhoun CZO. Soil P distribution was established using soil samples collected from three hillslope transects in three watersheds with a history of agricultural activity and compared to three hillslope transects one each from three areas where no farming use was evident. Soil solutions were collected over two years from four different hillslope positions through 60 cm from the hillslopes within these different land use histories to investigate how P moves in the watershed with and without historical cultivation. In addition, stream samples were collected from 17 different stream locations to measure the quantity of P in different stream orders.

In Chapter 4, I focus on soil P distribution during 60 years of forest regeneration from seedling to mature trees when farmland was abandoned. To investigate how slow cycling soil P fractions support the labile pools after reforestation, soil samples were collected from within the Long-term Soil Experiment every 5-8 years from 16 permanent plots (half of them were cut in 2007 and replanted in 2009) that had pine seedlings planted in 1957. These samples have been archived at the Nicholas School of the Environment and Earth Sciences, Duke University, Durham, NC. Different P pools were measured in four soil layers up to a depth of 60 cm with two different methods (Mehlich III and a modified Hedley fractions) to investigate how forest development has changed the different P pools.

In Chapter 5, I apply the SWAT model to enhance our understanding of P movement to stream waters or vertically through soils over the sweep of land use changes. The model was calibrated and validated with observed discharge and stream water P concentrations data from two watersheds within the Calhoun CZO. Thereafter, I simulate six different land use scenarios that reflect land cover and use during different periods over the last 200 years. I also apply two rainfall rates to address how years of high rainfall or specific rainfall events (i.e., hurricanes) may have contributed to P movement.

In Chapter 6, I summarize and highlight key findings from this research.

CHAPTER 2

LITERATURE REVIEW

Phosphorus is a critical element for plant and animal life on Earth (Alt *et al.*, 2011). Thus, it is important to increase our knowledge about P sources and P distributions to secure the long-term availability of P for all life on Earth.

The main P pools are in the lithosphere and oceans with <1% of P being located in terrestrial ecosystems that includes: soil, plant biomass, water, and atmosphere (Stewart *et al.*, 2005). The major part of terrestrial P stores are in soil (100-3000 kg ha^{-1}); although more than 90% of soil P is unavailable for immediate uptake by plants (Condron *et al.*, 2005; Bünemann and Condron, 2007).

1.2 Phosphorus biogeochemistry in the environment

The primary P source on Earth is rock weathering processes during soil development. The primary minerals that contain substantial P content are calcium phosphate minerals, particularly, apatite [($Ca_5(PO_4)_3OH$); (Filippelli, 2002; Schlesinger and Bernhardt, 2013)]. Phosphorus is released from apatite due to reaction with dissolved carbon dioxide (CO_2):

$$Ca_5(PO_4)_3 + 4CO_2 + 3H_2O \longrightarrow 5Ca^{2+} + 3HPO_4^{2-} + 4HCO_3^{1-}$$

Several processes in soil contribute to the release of P from apatite such as: 1) reduction of soil pH in the rhizosphere due to respiration and production of CO_2 [e.g., (Schlesinger, 1997)]; 2) release of organic acids from plant root, decomposing organic matter, and microorganism metabolites (Deb and Datta, 1967; Antibus *et al.*, 1981; Jurinak *et al.*, 1986); and 3) reduction of iron III (Fe^{3+}) to iron II (Fe^{2+}) (Baldwin and Mitchell, 2000; Loeb *et al.*, 2008).

Plants are able to absorb inorganic P forms from soil and also microorganisms assist to mineralize organic P forms and release available inorganic P (McGill and Cole, 1981; Kroehler and Linkins, 1988). Plants recycle phosphorus and other nutrients to the soil through decomposition of dead plant parts including litterfall (Attiwill and Adams, 1993). A portion of available P moves from soil to stream with surface and lateral runoff. In addition, eroding soil plays a role in transporting soil P to streams and finally oceans (Filippelli, 2002). Phosphorus cycling and availability in soil are driven by both biological processes that govern organic P formation and geologic process that govern inorganic P release from primary minerals but also storage in secondary minerals (i.e., iron oxide adsorption). Soil order and stage of soil development are important factors for identifying the likely forms of P in soil, specially availability of P in soil (Sharpley *et al.*, 1985; Cross and Schlesinger, 1995).

1.3 Soil phosphorus availability over time

Walker and Syers (1976) presented a model that described a pattern of soil P pools and availability as soil P content changes during ecosystem development (Fig. 2.1). According to their model, young soils are dominated by primary mineral P, intermediate soils have P equally distributed among primary mineral, secondary mineral, bioavailable P (labile P), and soil organic P, and old soils have lower amounts of P in the system and much of the remaining P is linked to insoluble or physically protected, non-labile (i.e., not biologically available) forms.

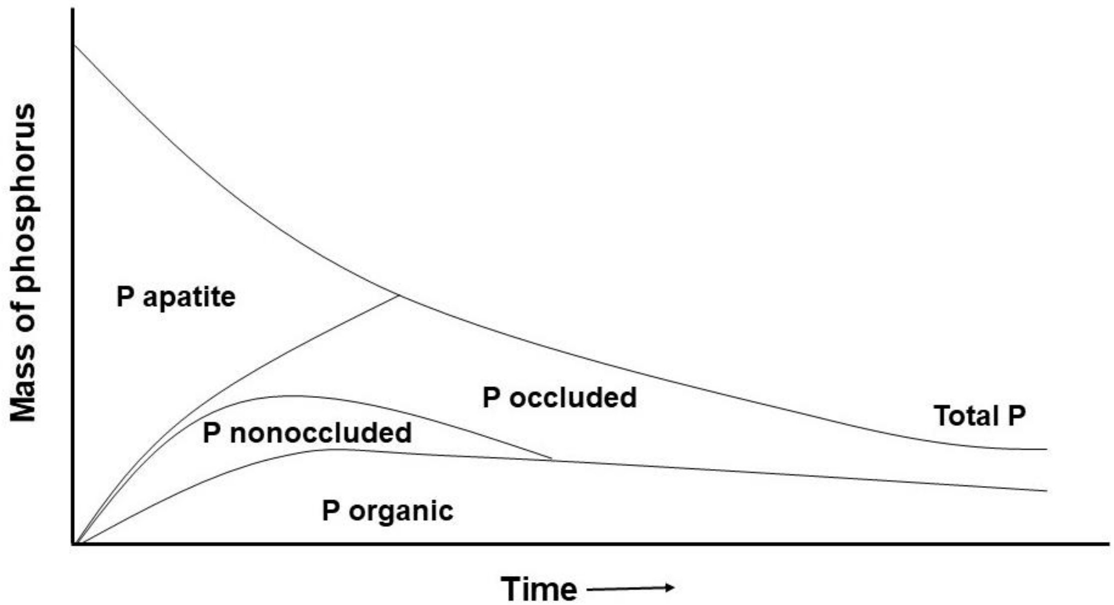

Figure 2.1. Changes in soil phosphorus (P) forms during soil development (Reproduced from Walker and Syers (1976)).

Walker and Syers (1976) predicted that ecosystems composed of old and highly weathered soils would eventually reach a "terminal steady state". In this case, little P would remain regularly available for biological uptake, ultimately leading to limited P for ecosystem development. A test of the Walker and Syers (1976) ecosystem development model over a four million year chronosequence in Hawaii showed that young soil had low P and nitrogen (N) but high available concentrations of cations like calcium (Ca^{2+}) and potassium (K^{+}). Intermediate developed soil had increased P and N availability, however, the available cations tended to decline. The oldest soil contained high N and low levels of P and cation availability (Chadwick *et al.*, 1999).

1.4 Soil phosphorus distribution

Phosphorus in soil includes different inorganic and organic forms. Generally, P pools can be allocated to three major pools which are: labile, moderately labile, and non-labile (Stevenson et al., 1999; Richter et al., 2006). The bioavailable P usually is a small pool (5-10 % of total P) in the soil, while the two other pools constitute a large part of total P in the soil. Bioavailable P pools are readily available for use by plants and microbes, or desorb to the soil compounds (Yang and Post, 2011). Moderately labile soil P buffers the bioavailable P because it can be changed to bioavailable P pools (Richter et al., 2006). The moderately labile P can also be adsorbed to soil particles and converted to non-labile forms. An example, based on the soil pH, would be how inorganic and organic P react with Ca^{2+}, aluminum (Al^{3+}), or Fe^{3+} forming insoluble oxides.

The quantification of bioavailable P can be consistent over time because moderately labile pools can buffer this more labile fraction, even though P bioavailability depends on changing pH (Stevenson, 1999) and on P release from bound-P in the soil (Frizano et al., 2003). At the lower (3-5) or higher (7-8) pH ranges, the amount of available P changes rapidly and is linked with Ca or Mg in higher pH and with Al or Fe in lower pH acidic soils (Vu *et al.*, 2008). The soil pH usually is around 6 in cultivated lands due to the addition of lime for agriculture. Therefore, P is more available in farmland (Stevenson, 1999).

The non-labile P forms can remain in the soil for years without converting to bioavailable P, because the non-labile organic P is resistant to mineralization while the inorganic forms of non-labile P are insoluble. (Stevenson, 1999). The transfer of P from primary minerals to the available forms for vegetation growth and soil biological cycling impacts the quantify of various P pools (Richter et al., 2006).

1.5 Land use impacts on P distribution

Land use induced gradients in nutrient availability may influence secondary succession, biomass production as well as response to emissions of pollutants such as N, acidifying substances, and greenhouse gases (Foster *et al.*, 2003). Land use changes impact biological and geological process and, in turn, soil composition (Franzluebbers *et al.*, 2000; Bormann *et al.*, 2007), soil nutrient cycling, and soil leaching losses (Celik, 2005; Liu *et al.*, 2010). These processes combined effect soil phosphorus distribution (Cherubin *et al.*, 2016; Maranguit *et al.*, 2017). Generally, in unfertilized cropping systems, the total P concentrations decrease with soil age and organic P fractions are the major source for plant-available P (Schoenau *et al.*, 1989; Beck and Sanchez, 1996). In fertilized systems, labile and moderately labile forms of inorganic P fractions increase and fertilizer-P is slowly transformed into more strongly bound P forms whereas organic P concentrations remain unchanged (Beck and Sanchez, 1996; Friesen *et al.*, 1997).

The southeastern Piedmont landscape of the USA underwent 150 years of deforestation and crop cultivation before reforestation. Long-term intensive farming activities in this area caused severe surface erosion (~ 17 cm of soil eroded) between 1750 and 1950 (Metz, 1958; Richter and Markewitz, 2001). In addition, some areas were fertilized with lime and P for crop production over during 150 year period (Ruffin, 1852; Gray and Thompson, 1933). The combination of land use changes and intensive erosion in the Calhoun Experimental Forest that later became the Calhoun Critical Zone Observatory affords an ideal opportunity to evaluate P redistribution in response to land use changes.

References

Alt, F., Oelmann, Y., Herold, N., Schrumpf, M., Wilcke, W., 2011. Phosphorus partitioning in grassland and forest soils of Germany as related to land-use type, management intensity, and land use–related pH. Journal of Plant Nutrition and Soil Science 174, 195-209.

Antibus, R., Croxdale, J., Miller, O., Linkins, A., 1981. Ectomycorrhizal fungi of Salix rotundifolia III. Resynthesized mycorrhizal complexes and their surface phosphatase activities. Canadian Journal of Botany 59, 2458-2465.

Attiwill, P.M., Adams, M.A., 1993. Nutrient cycling in forests. New phytologist 124, 561-582.

Baldwin, D.S., Mitchell, A., 2000. The effects of drying and re-flooding on the sediment and soil nutrient dynamics of lowland river–floodplain systems: a synthesis. Regulated Rivers: Research & Management 16, 457-467.

Beck, M.A., Sanchez, P.A., 1996. Soil phosphorus movement and budget after 13 years of fertilized cultivation in the Amazon basin. Plant and Soil 184, 23-31.

Bormann, H., Breuer, L., Gräff, T., Huisman, J.A., 2007. Analysing the effects of soil properties changes associated with land use changes on the simulated water balance: A comparison of three hydrological catchment models for scenario analysis. Ecological Modelling 209, 29-40.

Bünemann, E.K., Condron, L.M., 2007. Phosphorus and sulphur cycling in terrestrial ecosystems. Nutrient cycling in terrestrial ecosystems. Springer, pp. 65-92.

Celik, I., 2005. Land-use effects on organic matter and physical properties of soil in a southern Mediterranean highland of Turkey. Soil and Tillage Research 83, 270-277.

Chadwick, O.A., Derry, L.A., Vitousek, P.M., Huebert, B.J., Hedin, L.O., 1999. Changing sources of nutrients during four million years of ecosystem development. Nature 397, 491-497.

Cherubin, M.R., Franco, A.L., Cerri, C.E., Karlen, D.L., Pavinato, P.S., Rodrigues, M., Davies, C.A., Cerri, C.C., 2016. Phosphorus pools responses to land-use change for sugarcane expansion in weathered Brazilian soils. Geoderma 265, 27-38.

Condron, L.M., Turner, B.L., Cade-Menun, B.J., Sims, J., Sharpley, A., 2005. Chemistry and dynamics of soil organic phosphorus. Agronomy 46, 87.

Cross, A.F., Schlesinger, W.H., 1995. A literature review and evaluation of the. Hedley fractionation: Applications to the biogeochemical cycle of soil phosphorus in natural ecosystems. Geoderma 64, 197-214.

Deb, D., Datta, N., 1967. Effect of associating anions on phosphorus retention in soil. Plant and Soil 26, 303-316.

Filippelli, G.M., 2002. The global phosphorus cycle. Reviews in mineralogy and geochemistry 48, 391-425.

Foster, D., Swanson, F., Aber, J., Burke, I., Brokaw, N., Tilman, D., Knapp, A., 2003. The importance of land-use legacies to ecology and conservation. BioScience 53, 77-88.

Franzluebbers, A., Stuedemann, J., Schomberg, H., Wilkinson, S., 2000. Soil organic C and N pools under long-term pasture management in the Southern Piedmont USA. Soil Biology and Biochemistry 32, 469-478.

Friesen, D.K., Rao, I.M., Thomas, R.J., Oberson, A., Sanz, J., 1997. Phosphorus acquisition and cycling in crop and pasture systems in low fertility tropical soils. Plant and soil 196, 289-294.

Frizano, J., Vann, D.R., Johnson, A.H., Johnson, C.M., Vieira, I.C., Zarin, D.J., 2003. Labile phosphorus in soils of forest fallows and primary forest in the Bragantina region, Brazil. Biotropica 35, 2-11.

Gray, L.C., Thompson, E.K., 1933. History of agriculture in the southern United States to 1860.

Jurinak, J., Dudley, L., Allen, M., Knight, W., 1986. The role of calcium oxalate in the availability of phosphorus in soils of semiarid regions: a thermodynamic study. Soil Science 142, 255-261.

Kroehler, C.J., Linkins, A.E., 1988. The root surface phosphatases ofEriophorum vaginatum: Effects of temperature, pH, substrate concentration and inorganic phosphorus. Plant and Soil 105, 3-10.

Liu, X.-L., He, Y.-Q., Zhang, H.L., Schroder, J.K., Li, C.-L., Zhou, J., Zhang, Z.-Y., 2010. Impact of Land Use and Soil Fertility on Distributions of Soil Aggregate Fractions and Some Nutrients. Pedosphere 20, 666-673.

Loeb, R., Lamers, L.P., Roelofs, J.G., 2008. Prediction of phosphorus mobilisation in inundated floodplain soils. Environmental pollution 156, 325-331.

Maranguit, D., Guillaume, T., Kuzyakov, Y., 2017. Land-use change affects phosphorus fractions in highly weathered tropical soils. Catena 149, 385-393.

McGill, W., Cole, C., 1981. Comparative aspects of cycling of organic C, N, S and P through soil organic matter. Geoderma 26, 267-286.

Metz, L.J., 1958. The Calhoun experimental forest. unknown.

Richter, D.D., Allen, H.L., Li, J., Markewitz, D., Raikes, J., 2006. Bioavailability of slowly cycling soil phosphorus: major restructuring of soil P fractions over four decades in an aggrading forest. Oecologia 150, 259-271.

Richter, D.D., Markewitz, D., 2001. Understanding soil change : soil sustainability over millennia, centuries, and decades. Cambridge University Press, Cambridge.

Ruffin, E., 1852. An essay on calcareous manures. JW Randolph.

Schlesinger, W., 1997. Biogeochemistry: An analysis of global change. Academic Press, San Diego. Biogeochemistry: An analysis of global change. 2nd ed. Academic Press, San Diego.

Schlesinger, W.H., Bernhardt, E.S., 2013. Biogeochemistry: an analysis of global change. Academic press.

Schoenau, J., Stewart, J., Bettany, J., 1989. Forms and cycling of phosphorus in prairie and boreal forest soils. Biogeochemistry 8, 223-237.

Sharpley, A., Jones, C., Gray, C., Cole, C., Tiessen, H., Holzhey, C., 1985. A detailed phosphorus characterization of seventy-eight soils. ARS-United States Department of Agriculture, Agricultural Research Service (USA).

Stevenson, F.J., 1999. Cycles of soils: carbon, nitrogen, phosphorus, sulfur, micronutrients. John Wiley & Sons.

Stevenson, F.J., Stevenson, E., Cole, M., 1999. Cycles of soils: carbon, nitrogen, phosphorus, sulfur, micronutrients. John Wiley & Sons.

Stewart, W.M., Hammond, L.L., Van Kauwenbergh, S.J., 2005. Phosphorus as a natural resource. Phosphorus: agriculture and the environment, 3-22.

Vu, D., Tang, C., Armstrong, R., 2008. Changes and availability of P fractions following 65 years of P application to a calcareous soil in a Mediterranean climate. Plant and soil 304, 21-33.

Walker, T., Syers, J.K., 1976. The fate of phosphorus during pedogenesis. Geoderma 15, 1-19.

Yang, X., Post, W.M., 2011. Phosphorus transformations as a function of pedogenesis: A synthesis of soil phosphorus data using Hedley fractionation method. Biogeosciences 8, 2907-2916.

CHAPTER 3

THE ROLE OF HILSLOPE AND LAND USE HISTORY ON P DISTRIBUTION IN THE CRITICAL ZONE [1]

[1] M. Foroughi, L. A. Sutter, and D. Markewitz. Submitted to Biogeochemistry of the Critical Zone Book Volume.

Abstract

Soil phosphorus (P) chemistry and plant availability change during ecosystem development and soil formation, transforming from primary minerals to various secondary organic and inorganic forms. These P transformations occur through both time and space as P is cycled into secondary compounds, and translocated downslopes and through the soil profile by erosion and leaching. Over decades, the slow cycling of organic and occluded P fractions can modulate soil P availability as can human interactions with the critical zone (e.g. through land use changes). The Calhoun Critical Zone Observatory (Calhoun CZO) is an ancient landscape (>2 million yrs of soil development) that has a modern (1750-1950) history of forest clearing and burning for agriculture that included P fertilization. Severe surface erosion (~17 cm of soil), along with cultural (i.e., slavery, share cropping, and tenant farming), and biological (i.e., the boll weevil) stressors led to large-scale agricultural abandonment and reforestation by the 1920s and 30s. This combination of processes makes Calhoun an ideal location to consider the hillslope and pedon scale redistribution of P in responses to human interaction with the critical zone. This chapter investigates different organic and inorganic P pools in three topographic positions in the Calhoun CZO forests, both with and without a history of agricultural land use and traces the flow paths of P from the ridges to the stream waters. We expected to detect greater total, bioavailable, and soil solution P concentration in the historically farmed hillslopes relative to those hillslopes that were never farmed. Further, we hypothesized that P would be greater downslope compared to ridge tops due to erosion and that subsoil (>1m) would be elevated in farmed hillslopes due to P leaching through the soil profile overtime. Finally, we expected to find more organic P (P_o) in never cultivated forest. Results indicate that historically farmed hillslopes have increased Mehlich III extractable P relative to forests without farming and this increase (4.7 ± 4.0 µg g^{-1}) was evident through 2m on hillslope

ridges, suggesting some vertical leaching. In toe slope locations, HCO_3^- and NaOH extractable P_o are slightly elevated compared to ridges (15 vs. 20 µg g^{-1}) reflecting downslope erosion of organic matter, although reference toe slopes are slightly greater than historically farmed toe slopes. Surface soil solution concentrations in lysimeters (15 and 60 cm) and on ion exchange resins (15 cm) were both slightly higher in reference areas, counter to our hypothesis, and had increased concentrations in soils of toe slopes, perhaps reflecting enhanced cycling from P_o. In contrast, the volume weighted mean concentration of 15 cm solutions under both land uses was the same in ridge locations (0.09 µmol L^{-1}). Across the landscape, 1st to 3rd order streams were quite low in P (typically <1 µmol $PO_4^{3-}{}_i$ L^{-1}) with only local >5th order rivers in mixed use watersheds having higher average concentrations (~4 µmol $PO_4^{3-}{}_i$ L^{-1}). After 60+ years since agricultural abandonment, inorganic soil P is still elevated on farmed ridges and extends through the top 2 m of soil. In toe slopes, organic P concentrations are slightly elevated in both land uses but in the reference forests, organic P and solution concentrations are greater than historically farmed forest. The Calhoun CZO retains a legacy of both inorganic P inputs, but also organic P loses.

1. Introduction

Soils are a key component of ecosystems. Studying soils and the associated nutrient cycling processes at and below Earth's surface is a key purpose of the Critical Zone Observatory (CZO) network (Mao *et al.*, 2018). Soil cycling of the essential and often co-limiting element phosphorus (P) is a critical attribute governing ecosystem structure and function (Bünemann *et al.*, 2010). Phosphorus is the least available and least mobile of the plant macro-nutrients in most soil orders (Khan et al., 2007), and its form (e.g., organic or inorganic), and spatial distribution vertically and horizontally also affects ecosystem processes. The distribution and conversion of soil P is dynamic and driven by both biological and pedological pathways well suited to investigation under the CZO context. Here we present a framework for considering P distribution in the upper portion of the critical zone and then describe a case study in the Calhoun CZO in the Piedmont of the southeast USA.

1.1 Effect of ecosystem development on P distribution

An early soil P conceptual model described patterns of P pool transformations during ecosystem development (Walker and Syers, 1976). The model suggested that, early in soil development, the majority of P is found in primary minerals, such as apatite. Generally, P transforms from primary minerals to organic and occluded forms (e.g., adsorbed to clay surfaces or protected within aggregates) in late-weathering stage soils like Ultisols and Oxisols (Cross and Schlesinger, 1995). Over long time periods, P typically moves from mineral forms of P (i.e., apatite) towards organic (P_o) and inorganic (P_i) with much of the P being occluded and not readily plant available. During pedogenesis, chemical weathering can release some P to solution where it can be taken up by plants and microbes, but P that is not captured by plants or microbial communities may leach to surface or ground water, or it may be adsorbed to secondary minerals

(Smeck, 1985). Strong binding of P with iron (Fe) and aluminum (Al) oxides accounts for much of the P weathered from primary minerals. In low pH forest soils, the binding of P with Fe/Al hydroxylated surfaces is favored (Sample et al., 1980; Delgado and Torrent, 2000), but the stability of these secondary mineral complexes are sensitive to soil pH and redox (reduction-oxidation) state (Miller et al., 2001). Changing physiochemical conditions in soil due to hillslope position or land use change can release surface-bound P, thus leading to movement within the landscape and potential for leaching to groundwater or surface water (Kaňa and Kopáček, 2006). In general, these pathways of P transformation have been well correlated with the stage of soil development (Smeck, 1985) and are related to increasing plant P limitation (Chadwick *et al.*, 1999).

In recent critical zone (CZ) research at the Calhoun CZO (Holbrook et al., 2019), these time dependent declines in total soil P have been demonstrated with depth (i.e., depth-time). In analyzing 37 m of CZ substrate in a single boring from granitic bedrock to saprolite to soil, total P declined from 0.173 mass % as P_2O_5 at 37 m to <0.03 mass % above 5 m. Earlier work had reported similar declines from rock at 0.049 mass % of P that decreased to ˜ 0.02 mass % in 0.15-0.35 m surface soil (Richter and Markewitz, 2001; Austin and Schroeder, 2017). The mineral percentage of apatite in the boring declined from 0.358 % at 37 m to undetectable above 11 m. This regional example provides support of mineral-bound P loss during soil development from bedrock to surficial soil layer.

1.2 Effect of topography on P distribution

Phosphorus translocation through the soil profile and across the hillslope can occur on pedologic timeframes (Smeck and Runge, 1971; Walker and Syers, 1976; Parton *et al.*, 2005) and is reflected in different P concentrations in eluvial and illuvial soil horizons (Smeck and Runge, 1971). In sandy surface horizons, soil P concentrations can be quite low while in subsurface clay-rich (Bt) or organic-rich (Bh) horizons P can accumulate. In addition, P translocation down the hillslope can occur along with both surface and subsurface water flow (Smeck and Runge, 1973). Phosphorus dissolved in water moves in the soil solution both horizontally and vertically. Precipitation that does not infiltrate but remains on the soil surface can move dissolved soil P from the ridge to the toe slope and eventually to the drainage outlet (Fig. 3.1; Daniel *et al.* (1994)).

Along with vertical or horizontal P movement in solution, erosive forces can redistribute P in adsorbed forms. Topography is a critical factor that influences runoff, drainage, and soil erosion and ultimately impacts P distribution (Brubaker et al., 1993; Wang et al., 2001). In agricultural landscapes that are fertilized with P, downslope movement with sediment is commonly observed. Available P is affected by slope position, with the lowest P availability on the steepest slopes because of P removal by water flow and erosion (Dessalegn *et al.*, 2014). Under severe soil erosion, parent material may be exposed and can contribute to increasing rates of rock weathering, thus releasing P into the soil (Vitousek *et al.*, 2003; Bern *et al.*, 2005).

1.3 Effect of land use on P distribution

Pedological and hillslope processes affecting P dynamics are also impacted by how land has been used through its history. This has been evident in the long-term elevation of soil P in sites that have been fertilized, even many years previously (Falkengren-Grerup *et al.*, 2006; Richter *et al.*, 2006; Campbell and Morris, 2018), as well as the transformation of P pools after forest clearing (Garcia-Montiel *et al.*, 2000), and with continued management (Alt *et al.*, 2011). Total P has been shown to increase in fertilized lands with P_i becoming the predominant source for plant available P as opposed to unfertilized lands where P_o is often the major source of plant available P (Schoenau *et al.*, 1989).

Soil P fractions, both with soil depth and across the landscape, can be evaluated over time to determine the influence of changes in land use practices on the distribution of soil P (Bowman and Cole, 1978; Cross and Schlesinger, 1995; Callaham *et al.*, 2006; Negassa and Leinweber, 2009; Cherubin *et al.*, 2016). Forest clearing and farming in the Southeast US Piedmont, particularly on ridgetops, was a common practice from 1800-1950, but since that time much of the landscape has been reforested or converted to pasture. The conversion of vegetative cover and the change in land use has played a critical role in changing soil total phosphorus (Total P) as well as P forms (i.e., inorganic, organic, adsorbed) in these upland ecosystems (Richter and Markewitz, 2001); impacts that are common in many ecosystems globally (Liu *et al.*, 2006; Zhi-Yao *et al.*, 2006). For example, prior research across the Calhoun CZO (Richter and Markewitz, 2001), has compared soil P availability of unfarmed hardwood forest relative to regenerating but unmanaged pine in old agricultural fields, and managed pasture. This study demonstrated that acid extractable-P (Mehlich III; Mehlich (1978)) concentrations were 2, 6, and 7 mg kg^{-1} in surface soil of hardwood, pine, and pasture, respectively (Table 3.1; (Richter and Markewitz, 2001). As such, P was elevated in the land uses that have an agricultural history (pine and pasture) in comparison to the unfarmed hardwood forests.

A similar comparison of native forest vegetation, pasture, and a crop-livestock system (CPS) in Brazil found the soil P stock in the topsoil of native forest vegetation (11.3 kg ha^{-1}) to be significantly lower than in pasture soil (21.6 kg ha^{-1} ($p < 0.01$)) and CPS soil (30.06 kg ha^{-1} ($p < 0.01$)) (Groppo *et al.*, 2015). Phosphorus in other cropland surface soils studies have also increased relative to forests due to P fertilizer additions and the slow mobility of P (Costa *et al.*, 2007; Pavinato *et al.*, 2009; Messiga *et al.*, 2010).

After forest clearing, burning, and conversion to pasture, pasture soil P concentrations can become elevated from the residual forest ash (Garcia-Montiel *et al.*, 2000; Markewitz *et al.*, 2004; Hamer *et al.*, 2013), but without further inputs, P_i typically starts to decline after a few years. For example, in a pasture chronosequence in Brazil, HCO_3+NaOH extractable P_i in the top 10 cm of soil initially increased from ~2.5 g m^{-2} under forest to ~5 g m^{-2} under 3-yr-old pasture but by age 20, it had declined to ~3 g m^{-2}. In another pasture chronosequence on Oxisols in Costa Rica, after an increase in HCO_3+NaOH P_i from 54 µg g^{-1} under forest to 73 µg g^{-1} under 5-yr-old pasture, P_i declined to 59.4 µg g^{-1} by age 20 (Townsend *et al.*, 2002).

Finally, in a recent effort considering the length of time for P to re-equilibrate after agricultural inputs, Goyette *et al.* (2018) assessed 23 watersheds of the St. Lawrence Basin of Quebec, Canada. These watersheds accumulated P over a century of agriculture until peaking in 1980. Despite reductions in P inputs thereafter, the study estimated a recovery to a baseline level of P leaching might require 100 to 6000 yrs (Goyette et al., 2018). The rate of recovery will depend on P sorption capacity of the soil as historical P fertilization could be release from the soil over decades.

1.4 Topography and Land Use in the Calhoun CZO

In spite of the many studies highlighted above, few represent the long sweep of forest recovery after agricultural abandonment present at the Calhoun CZO. However, previous efforts at the Calhoun CZO have not considered the watershed scale processes described above, including both P movement downslope with surface erosion or deeply into the soil profile. Previous work investigating the ~200-year history of forest clearing, agricultural P fertilization, and forest regeneration in the Calhoun CZO focused on retention of P in surface soils and conversion of P fractions during forest regeneration (Richter and Markewitz, 2001; Richter *et al.*, 2006). The objective of this study is to evaluate P distribution in different hillslope positions of small watersheds that previously included agriculture and compare them with forested hillslopes that were never converted to farmland (i.e., reference hillslopes).

We were particularly interested in assessing if 1) soil profiles in lower slope positions in hillslopes with an agricultural history would have more soil total P than ridgetop profiles due to down slope erosion or overland flow of P, particularly when compared to those lower slope profiles from reference hillslopes; 2) soil profiles on ridgetops from historically farmed hillslopes would have higher extractable P through 2 m due to slow vertical P leaching over six decades; 3) current soil solution P in lysimeters or ion exchange resins would be elevated in all hillslope positions under agricultural watersheds compared to reference; and 4) organic P fractions would demonstrate greater concentrations in reference areas due to the maintenance of some trees historically and thus deep roots, although we expected levels of the residual P (recalcitrant organic and mineral) fraction to be consistent across the land uses and hillslopes.

2. Methods

2.1 Study Site

The Calhoun CZO is located in the Enoree Ranger District of the Sumter National Forest (34° 7' 55.36" N, 82°18' 36.17" W) in South Carolina (SC) managed by the US Department of Agriculture (USDA) Forest Service (Fig. 3.2). The mean annual temperature and precipitation of the Calhoun CZO is approximately 17°C and 1260 mm, respectively. Elevation is 120 to 180 m above sea level. The soils are mostly highly weathered, acidic Ultisols in ridge, mid, and toe hillslope positions. Inceptisols occur in relatively narrow floodplains in second or greater order streams (Richter et al., 2015). The Calhoun CZO area has a history of forest clearing and burning in the early 1800s, which initiated an era of soil degradation and increased erosion rates. Severe surface erosion (~17 cm) resulted from cotton, corn, wheat, and other crops that were cultivated from 1800 until the early twentieth century when many agricultural lands were abandoned (Metz, 1958; Richter and Markewitz, 2001). During cultivation some lands were fertilized with lime and P for crop production (Ruffin, 1852; Gray and Thompson, 1933). After abandonment, some lands were converted to pasture and many others regenerated to forest. Originally, much of the reforestation occurred naturally, while by the 1950s and 60s fields were being planted in pine (Richter and Markewitz, 2001; Richter et al., 2015). Based on the 1933 aerial photographs obtained from the Photographic Archive of the Calhoun Experimental Forest, the lands that were bare and clear-cut for agricultural activity can be readily identified (Fig. 3.3A). Areas of hardwood forests, which were likely never clear-cut for cultivation, are also visible in the same aerial photographs (Brecheisen, 2015). Further field investigation of these hardwood forests and use of high-resolution LIDAR images of these areas both demonstrate a lack of erosion features.

2.2 Sample collection

Soil samples were collected from three hillslope transects (ridge, mid, and toe) in three watersheds with a history of agricultural use (AGW; Fig. 3.3). These hillslopes were compared to a single hillslope transect collected in three reference parcels (REF; Fig. 3.3B). Given the extensive history of human occupation of this region, there are virtually no complete watersheds that have escaped some human activity, so the non-farmed hillslopes serve as our reference locations. Both the AGW and REF included samples at three hillslope positions: ridge, mid, and toe (Fig. 3.3). In both AGW and REF locations, the soil samples were collected at seven depths: 0-7.5, 7.5-15, 15-35, 35-60, 60-100, 100-150, and 150-200 cm with a 6.5-cm diameter open-bucket hand auger. The upper four depths were selected based on previous Calhoun CZO soil P research protocols (Richter et al., 2006).

To measure the existing movement of P through soils, ceramic cup lysimeters were installed at two different depths (15 and 60 cm) adjacent to the position where soils were collected (Fig. 3.3). Lysimeters were installed using the method suggested by Artiola *et al.* (2004) in both AGW and REF locations at the three hillslope positions (ridge, mid, and toe). In the AGW watersheds an additional lysimeter was installed in the stream bank margin (Str. bank) at the base of the hillslope. In reference area REF2, an ephemeral stream was present in this zero-order watershed and lysimeters were installed nearby. In reference area REF3 there was a drainage channel at the base of the hillslope where stream bank lysimeters were installed, but this channel never carried surface water during the sampling period. Finally, the hillslope in reference area REF1 did not fully extend to a stream or channel so no additional lysimeters were installed. Solutions were removed from lysimeters every 10 to 20 days between January 2017 and December 2018 for AGW while REF soil solutions were collected May 2017 to December 2018.

Anion exchange resin capsules (Unibest, Walla Walla, WA.) were installed beside lysimeters at 15 cm depth in December 2016 to integrate P movement within the soil solution. Soil was removed with a punch-tube and resin placed at the base of the prior to returning the soil to cover the resin. At the time of each lysimeter solution collection, a set of resin capsules were collected and replaced such that each resin integrated P from the prior sampling time. Soil solution and resin capsules were carried on ice to the laboratory after collection, and all soil particles were removed by a deionized water wash. Surface water was collected from streams monthly from July 2014 to July 2017 at seventeen different local creeks, streams, and large rivers (Figs. 3.3 and 3.4). Stream samples were kept on ice and transferred to the laboratory after collection.

2.3 Sample analyses

Soils were air-dried and sieved through a 2 mm mesh screen. A moisture correction factor was determined after oven drying a 1-2 g subsample at 105˚C for 24 hrs. Soil pH was measured using pH_{H_2O} and pH_{CaCl_2} (Peech, 1965; Gee and Or, 2002). Particle size distribution was determined through the hydrometer method (Gee and Or, 2002). Anion exchange capacity (AEC) and cation exchange capacity (CEC) were calculated from Cl and K content measured using ion chromatography (Thermo Dionex ICS-2100, Sunnyvale, CA) on soils extracted with 0.1 M KCl and 0.5 M $NaNO_3$ (Sumner and Miller, 1996; Zelazny *et al.*, 1996). Soils were extracted with Mehlich III solution to determine bioavailable soil P (Mehlich, 1978) via spectrophotometry (Spectronic Genesys 2, NY) and colorimetry (Murphy and Riley, 1962). Additionally, Mg, Ca, Al, and Fe were determined in the Mehlich III extraction by inductively coupled plasma-mass spectrometry (ICP-MS; Perkin Elmer ICPMS model Elan DRCII, Ontario, Canada). Total carbon (TC) and total nitrogen (TN) were measured using a Flash 2000 CN elemental analyzer (CE Elantech, Lakewood, NJ).

Phosphorus pools were evaluated using soils collected from samples along a moderately (0-30 %) sloped transect from the AGW sites and all of the REF transects. The first P pool (the readily soluble and exchangeable P_i) was determined by anion exchange resin strips. To evaluate additional soil P pools, we followed Richter *et al.* (2006), which is based on the Tiessen and Moir (1993) modified, sequential fractionation method (Hedley *et al.*, 1982). In summary, this method separated extractable P from 0.5M $NaHCO_3$, 1 M NaOH, and 1M HCl to P_i and P_o that are associated with surface charge, Fe/Al oxides, and Ca, respectively. Samples were then extracted with hot (80^{o}C) concentrated hydrochloric acid (con. HCl). Finally, residual P and an independent total P sample were determined after a nitric acid and hydrogen peroxide digestion (Kimbrough and Wakakuwa, 1989; Niederberger *et al.*, 2015). The independent total P was compared to the sum of all pools in the sequential fractionation method. All P concentrations were determined via spectrophotometry, as above, using molybdate blue chemistry (Murphy and Riley, 1962). We occasionally group fractions as labile P (resin-P, 0.5 M $NaHCO_3$-P_i and P_o), moderately labile P (0.1 M NaOH-P_i and P_o), and occluded P fractions (HCl-P and residual-P).

Unfiltered lysimeter and stream samples were used to measure conductivity (Rhoades *et al.*, 1996), pH (Page, 1982), and alkalinity to an end point pH of 4.2 with 0.01 N HCl (Jenkins, 1982) on an auto-titrator (Mettler-Toledo, Columbus, OH). Thereafter, soil solution and stream samples were filtered within 24 hours of collection using a 0.40 µm polycarbonate filter and frozen. Thawed samples were measured for dissolved organic carbon (DOC) and TN (Shimadzu TOC-TN analyzer; Shimadzu Corp., Kyoto, Japan); anions (Cl^-, NO_2^-, SO_4^{2-}, NO_3^-, and PO_4^{3-}) and cations (Na^+, K^+, Mg^{2+}, and Ca^{2+}) (Dionex ICS-2100 Ion Chromatograph); and Fe, Al, and Mn (Perkin Elmer Inductively Coupled Plasma-MS model Elan DRCII). Soil solution samples were digested using a persulfate oxidation reagent (Koroleff, 1983) to measure total P (reported as $PO_4^{3-}{}_T$). To evaluate $PO_4^{3-}{}_T$ and inorganic-phosphate ($PO_4^{3-}{}_i$), we again used standard Spectronic Genesys 2 spectrophotometric chemistry [molybdate blue chemistry; (Murphy and Riley, 1962)].

Rinsed resin capsules were placed into centrifuge tubes and slowly shaken with 40 ml of 2M HCl to extract P. Samples were pH adjusted to measured values of $PO_4^{3-}{}_T$ and $PO_4^{3-}{}_i$ were evaluated via spectrophotometry by using molybdate blue chemistry method (Murphy and Riley, 1962).

2.4 Data Analyses

The main effects in the experimental design were land use (AGW vs REF) and hillslope position (ridge, mid, toe, and str. bank). Prior to analysis, data were investigated for normality and equal variance. Data greater than three standard deviations from the mean (1-2% of total data) were considered outliers and removed. For soil profile data, depth was treated as a repeated measure in space to account for depth dependent autocorrelation. These data were analyzed using repeated measure ANOVA to determine how different soil P fractions varied with land use, hillslopes, and their interaction. For soil solutions and resins, samples were collected repeatedly in time, so a repeated measure ANOVA was used to account for temporal autocorrelation (AR1). Resins only had one depth for comparison, and lysimeters were evaluated by depth. In addition, correlation analyses between P pools with other elements in the soils were undertaken using all depths and profiles sampled. All statistical analysis for this project were implemented using R software v3.4.4 (R Development Team, 2018).

3. Results

3.1 Soil analyses

Mehlich-III P concentrations generally decreased throughout the soil profile compared to total P, which remained relatively constant with depth (Fig. 3.5). The mean Mehlich III-P concentration was significantly ($P<0.0001$) greater in the AGW (4.72 µg g^{-1}) than in the REF (3.56 µg g^{-1}) (Table 3.2). In contrast, total P was higher in the REF ($P<0.0001$; Table 3.2). Total P was significantly greater at the mid-slope ($P= 0.026$) with means of 193, 257, and 185 µg g^{-1} for the ridge, mid, and toe slope, respectively (Table 3.3). Analysis of land use by hillslope position showed Mehlich-III P concentrations across all hillslope positions under AGW were higher than the REF. The ridge in AGW was significantly higher than the ridge ($P=0.00008$) in REF with Mehlich III-P concentrations of 4.0 and 2.1 µg g^{-1}, respectively (Table 3.4). In both hillslopes, Mehlich-III P declined from ridge to toe (Table 3.3) but only the ridge of the REF was significant less than the toe of REF (P= 0.017).

All six P_i and P_o pools decreased with depth through the soil profile in both land uses and all hillslope positions (Fig. 3.6 and Table 3.5). The mean concentration of Resin-P_i in AGW was 3.63 ug g^{-1}, which was significantly higher (P<0.0001) than the 2.58 ug g^{-1} found in REF. In contrast, HCO_3-P_i and NaOH-P_i were higher in REF compared with AGW (p-value of 0.03 and <0.0001, respectively). The P_o extracted by NaOH was also higher in REF (P= 0.0198), while HCO_3-P_o did not differ between land use histories. The effect of land use on occluded-P (residual-P and P extracted by con. HCl) was significant (P< 0.0001) with the largest difference being con. HCl-P_i in REF greater than AGW. Con. HCl-P_o and residual-P were slightly greater in AGW. Fractions of P_i and P_o (except con. HCl-P_o) in the toe slope were generally greater than the ridge (Table 3.3). Hillslope position significantly affected the amounts of resin-P_i, HCO_3-P_o, NaOH-P_o, 1M HCl, and con. HCl-P_o (Table 3.3); although the mean of con. HCl-P_o decreased from ridge (2.27 µg g^{-1}) to toe (0.06 µg g^{1}). There was no significant interaction between land uses and hillslopes (Table 3.4).

The effect of land use on several other soil characteristics (CEC, AEC, TC, TN, clay (%), Fe, Al, Ca, and Mg, and pH in 0.01 M $CaCl_2$) was also significant (P<0.001; Table 3.6). TC, Mg, Al, clay percent, and CEC were greater in REF than AGW (Table 3.4A). AEC and Al tended to be lower in the toe slope; however, other response variables such as pH_{CaCl2}, Fe, Ca, and TC tended to be higher in toe slope (Table 3.7). Generally, the average difference between pH_{H2O} and pH_{CaCl2} was 1.0 in both land uses and all hillslope positions through 2 m soil profile. The interaction of land use and hillslope position had a significant effect on Al (P< 0.001), Fe (P < 0.001), and clay % (p = 0.03; Table 3.8), although the interactions were idiosyncratic for each attribute. Total carbon decreased throughout the soil profile within the three hillslope positions of both land uses as did TN, but other factors did not follow consistent patterns (Table 3.9).

3.2 Soil solution analyses

Soil solutions collected from both lysimeter depths contained greater concentration of $PO_4^{3-}{}_T$ in REF than AGW (Fig. 3.7). At a depth of 15 cm, the mean of the $PO_4^{3-}{}_T$ in REF soil solution (0.55 µmol L^{-1}) was significantly greater ($P < 0.0001$) than AGW (0.48 µmol L^{-1}; Fig. 3.7). In contrast, $PO_4^{3-}{}_i$ was the same concentration in AGW and REF (0.34 and 0.30 µmol L^{-1}, respectively) at the same depth. At 60 cm, mean $PO_4^{3-}{}_T$ and $PO_4^{3-}{}_i$ of REF (0.64 and 0.41 µmol L^{-1}, respectively) were both significantly greater ($P = 0.0002$) than AGW (0.2 and 0.1 µmol L^{-1}; Fig. 3.7B). In general, $PO_4^{3-}{}_T$ concentration in soil solutions tended to increase from ridge to str. bank in both REF and AGW with some differences being significant (e.g., REF str. bank exceeds ridge, mid, and toe at 60 cm; P=0.0145, <0.0001, and <0.001, respectively). In the AGW, approximately 43-51% of $PO_4^{3-}{}_T$ was $PO_4^{3-}{}_i$ with the remaining percentage (49-57%) present as organic-PO_4^{3-} ($PO_4^{3-}{}_o$) across the different hillslope positions at 15 and 60 cm (Fig. 3.8). In REF the proportion of $PO_4^{3-}{}_o$ was a bit more variable but exceeded 60% at the toe slopes at 15 cm and at ridge for 60 cm (Fig. 3.8).

Land use and hillslope both significantly affected DOC ($P<0.0001$) at 15 and 60 cm. The average DOC concentration at 15 cm in AGW and REF were 10.97 and 9.95 mg L^{-1}, respectively. At 60 cm, DOC in AGW and REF were 9.44 and 3.84 mg L^{-1}, respectively. The interaction between land use and hillslope indicated that DOC on the ridge of AGW was significantly less ($P<0.0001$) than REF at 15 cm; however, DOC in toe of AGW was significantly higher than toe for REF at 15 cm ($p < 0.0001$; Fig. 3.9A). In general, the concentration of DOC increased down the hillslope in both land uses at 60 cm (Fig. 3.9B); although, it did not follow the same pattern at

15 cm. The mean DOC concentration increased in the order 6.68, 6.61, 6.83, and 10.34 mg L^{-1} for ridge, mid, toe, and str. bank, respectively, at 60 cm. DOC concentrations were not significantly correlated to P_o.

3.2 Resin capsule phosphorus

The average concentration of $PO_4^{3-}{}_i$ recovered from ion exchange resins in the REF hillslopes (2.19 µmol L^{-1} or 8.32 µg g^{-1} of resin) was significantly greater ($P < 0.0001$) than AGW (1.33 µmol L^{-1} or 5.03 µg g^{-1} of resin) and increased from ridge to Str. bank in both REF and AGW with hillslope position being significant (P=0.0027; Fig. 3.10). Across both land uses, mean $PO_4^{3-}{}_i$ concentration significantly increased along the gradient - from ridge and mid to toe and str. bank (P= 0.0022, 0.0001, 0.0002, and <0.0001, respectively), while increases were only significant in REF from ridge to str. bank (3.48 µg g^{-1} of resin to 12.61 µg g^{-1} of resin).

3.3 Stream analyses

The average of $PO_4^{3-}{}_i$ in 1st order streams of AGW and one REF location (mid-elevation; based on the DEM map) increased from August to November of each year and then generally declined during the winter and spring seasons (Fig. 3.11). The concentration of $PO_4^{3-}{}_i$ in these 1st order streams did not differ by land use and averaged 0.68 µmol L^{-1} (Fig. 3.12). Streams in slightly higher landscape positions (high-elevation) that were also 1st order as well as those slightly lower (low-elevation) and larger (2-3rd order) both had similar concentrations 0.74 and 0.75 µmol L^{-1}, respectively (Fig. 3.12). For comparison, the largest local rivers (Enoree and Tyger, 5-6th order) had higher average $PO_4^{3-}{}_i$ concentrations of 1.97 µmol L^{-1} (Fig. 3.12).

4. Discussion

We investigated soil and soil solution P concentration to reveal how land use history and hillslope position have impacted P distribution in the Calhoun CZO six decades after agricultural abandonment. Historical agricultural activity has influenced soil P distribution in the Calhoun CZO through additions of lime and fertilizer as well as through the erosion associated with clearing, farming, and farm abandonment. We hypothesized that this would increase P concentrations in lower slopes of the AGW due to erosion and overland flow; that vertical leaching in ridge locations would result in higher P concentrations through 2 m in AGW vs REF; that P in surface soils (<60 cm) would still be more actively cycling (i.e., increased lysimeter and resin concentrations) under AGW; and that there is a historical legacy of farming evident through a decline in organic P fractions, potentially due to the loss of surface soil C and deep rooting.

4.1 Hillslope effects

According to the conventional hillslope model [Fig. 1; (Daniel *et al.*, 1994)], we hypothesized that soil P concentration in AGW toe slope positions would be greater than ridge top soils; and also the AGW toe slope would be higher than the REF toe slope. The comparison of bioavailable P in different hillslope positions (ridge, mid, and toe) did not reveal an increase in inorganic P_i (Mehlich III, HCO_3, NaOH) but did demonstrate that P_o fractions (HCO_3, NaOH) increased from ridge to toe slope (Fig. 3.6 and Table 3.3). Further, we did not find any significant difference in the toe slope soil P concentration between AGW and REF. Increasing P in the toe slope was expected to result from historical erosion of the land that moved the surface layer of the soil from ridge to lower slope, especially in AGW. A previous study within the same AGW and REF locations indicated the depth to clay in the toe slope of AGW was 40 cm greater than the toe of REF, presumably from this downslope erosion and deposition on top of the argillic horizon in

AGW (Ryland, 2017). The lack of an increase in P_i from eroded surface soil may reflect other factors such as clay content, pH, or Ca concentration. Lower clay percentages in toe slope positions may limit P bonding with Fe/Al (hydr)oxide (Table 3.8). The higher Ca concentration and higher pH in the toe slopes could favor P solubilization and leaching (Table 3.7 and 3.8) which could also impact on total P concentration in lower slope. Flood plain legacy sediment evaluated in a 3rd order stream in the same research area did not show any elevation from legacy P_i input (Wade *et al.*, in press).

The increasing P_o fractions (extracted with HCO_3 and NaOH) from the ridge to the toe slope position (Fig. 3.7 and Table 3.2B) have a strong positive correlation with TC ($R^2 > 0.67$) as TC content (Table 3.6 and 3.7) also generally increased from ridge to toe slope, which has been predicted in this erosive landscape (Dialynas *et al.*, 2016). The higher DOC in soil solution at the toe slope of AGW (18.4 mg L^{-1}; volumetric weighted mean) relative to the AGW ridge (4 mg L^{-1}; volumetric weighted mean) also could reflect the higher amount of surficial horizon accumulating downslope in AGW. Previous studies in other locations have also found that organic matter tends to accumulate in these middle and toe slope positions (Tiessen *et al.*, 1994; Araújo *et al.*, 2004), although in those studies both labile and moderately labile P (P_i and P_o) increased from ridge to the lower slope positions whereas here we see an increase only for P_o. A watershed scale biogeochemistry model for the Calhoun CZO indicated the long-term persistence of soil organic carbon (SOC) after erosion to lower slopes (Dialynas *et al.*, 2016), which is consistent with our finding of increased downslope P_o. As noted above, other soil factors such as Ca, clay content, and pH could reduce the persistence of P_i in the lower slope.

4.2 Land use history effects

Because of past agricultural activity in the Calhoun CZO, we expected that the extractable P in ridgetop soil profiles from AGW would have a higher amount of available P relative to REF where there was no farming activity. When summed over the top 2 m of the soil profile, using an average bulk density of ~1.4 g cm^{-3} (Richter and Markewitz, 2001; Richter *et al.*, 2006), bioavailable P was 34 kg ha^{-1} higher in AGW than REF even after seven decades (Fig. 3.5 and Table 3.2). This higher bioavailable P in AGW is presumed to be the result of agricultural amendments, although quantitative input rates are unknown for the 150 years of agricultural activity. Exchangeable Ca in the AGW also exceed REF by 1687 (±377) kg ha^{-1} over the top 2 m, suggesting some liming inputs persist despite not receiving any additional lime after reforestation in the 1950s (Table 3.2). Soil pH also remains elevated in AGW compared to REF, which may contribute to higher P availability [Table 3.2; (Stevenson *et al.*, 1999)]. Other researchers have similarly found P fertilization, particularly in highly weathered soils, increases P_i in labile and moderately labile fractions (Cross and Schlesinger, 1995; Lilienfein *et al.*, 2000; Tchienkoua and Zech, 2003).

In contrast to bioavailable P and fertilizer inputs, total P concentration in AGW (5268 ±1982 kg ha^{-1}) were significantly less than in REF [(6487 ±2168 kg ha^{-1}); Fig. 3.5 and Table 3.2] over the top 2m. The soil erosion that followed the forest clearing and agriculture activity in the AGW included loss of soil to stream drainages, which may account for some loss of total P in AGW as well as the decreased total P in the toe slope. Dialynas *et al.* (2016) estimates that approximately 32% of the native SOC eroded from the AGW to the river floodplains, in line with similar evidence of clay loss to streams and rivers (Jackson *et al.*, 2005). Both the loss of organic matter with its associated P_o and clay with its associated Fe and Al bound P_i or P_o could reduce total P in AGW relative to the REF.

Beyond the ecosystem loss of total P, reforestation might redistribute P from soil to plant biomass (Richter *et al.*, 2006). Tree regrowth on the farmed ridges of the Calhoun CZO may have removed more P from soil in comparison with trees of REF that never achieved a bare soil condition. A mass balance on P in revegetating old-fields in the Calhoun CZO found vegetation (i.e., loblolly pine (*Pinus taeda* L.)) removed 39.4 kg ha^{-1} of P from the 0-60 cm soil during 28 years of forest growth from seedlings while total P removed from soil to vegetation and re-accumulating forest floor accounted for 82.5 kg ha^{-1} over 28 years of forest growth (Richter *et al.*, 2006). As such, summing through the upper 60 cm (as opposed to 2 m), the total P in the AGW ridge was 124 ± 316 kg ha^{-1} less than the REF ridge , indicating forest regrowth (i.e., 82.5 kg ha^{-1}) plus some erosion losses could account for the depletion of total P in AGW, the ridge top locations.

4.2.1 Land Use on Vertical Leaching and P in Solution

Given the recognized increase in bioavailable P in former fertilized soils as measured previously in 0-60 cm soil (Richter *et al.*, 2006) and quantified again here, we were specifically interested in identifying P movement vertically in the soil profile. Phosphorus mobility in soil profiles is generally recognized as being slow (Cooke and Williams, 1973), but we hypothesized that due to P leaching slowly over seven decades the soil profile in the ridge position under AGW would have more extractable P through the entire top 2 m. We did find a greater concentration of extractable P (Mehlich III) throughout the 2 m profile (Figure 3.5) for the AGW relative to REF sites. The bioavailable P (i.e., resin + HCO_3-P_i) in ridge topsoil profiles under AGW was 111 (±61) kg ha^{-1} while the same extractable P at ridge top of REF was 58 (±58) kg ha^{-1} through 0-2 m (Fig.

3.6 and Table 3.4). These data suggest ridge top under AGW has experienced vertical leaching of P.

It is recognized that adding P fertilizer to the soil surface, particularly over long periods, causes gradual P leaching through the soil profile (Cooke and Williams, 1973). Previous studies on P fertilization to farmland or pasture over 20-100 years demonstrated movement of soluble P through 0.5-0.6 m of the soil profile. Movement through these deep well drained sandy and coarse loamy soils in Woburn, UK was in part dependent upon the specific soil structure and texture (Bolton and Coulter, 1965; Cooke and Williams, 1973). Another study in farm land of Nebraska, showed when land was fertilized with 80 kg P ha^{-1} y^{-1} over 40 years, around 6% of P inputs accumulated in the clay horizon (0.45 m) over time (Eghball *et al.*, 1996). In soils rich in iron-oxide coated clays, P fixation strongly limits P leaching (Fox and Kamprath, 1970), so in the clay-rich Ultisols of the Calhoun CZO it is unexpected to find the same amount of P leach through 2 m.

Our lysimeter data in the upper 15 and 60 cm of the profile indicates a present concentration of soil solution P of 0.16-0.7 μmol L^{-1} in AGW. These values are similar to forest soil solutions concentrations of P (0.21-0.4 μmol L^{-1}) measured at 60 cm in coniferous forests of Washington (Ugolini *et al.*, 1977). In contrast, when applying poultry litter for fertilization to pastures in the southeastern US Piedmont, soluble P concentrations can range up to 10.5 – 52.5 μmol L^{-1} in surface and subsurface runoff (Vervoort *et al.*, 1998). In other locations, P leaching under fertilized grass land of Devon, UK with sandy loam to silt loam surface textures had a range of total dissolved P of 1.7- 5.2 μmol L^{-1} (Turner and Haygarth, 1999). Models of P leaching in sandy soils of the Netherlands also suggest that phosphate leaching in agricultural soil could vary from 4-5 μmol L^{-1} when the water-soluble soil P concentration is 17-23 μg g^{-1} or up to 16-21 μmol L^{-1} if water-soluble soil P is 43-57 μg g^{-1} (Schoumans and Groenendijk, 2000). In the Calhoun CZO water extractable resin P in AGW ridge locations is <2 μg g^{-1} (Tables 3.3 and 3.4) so according to this framework mobile P should be ~0.4-0.5 μmol L^{-1} in solution. These leaching rates may be relevant to sandy A and E horizons for un-eroded ridge tops in the Calhoun region but are likely high for clay rich Bt horizons throughout the landscape. Overall, the current soil solution concentrations (and first order stream waters) in the Calhoun CZO suggest that limited P is leaching after 70 years of reforestation but is likely less compared to conditions during cultivation and amendment applications.

The historical agricultural legacy of elevated bioavailable P led us to expect that vertical leaching and biogeochemical cycling of P in solutions (lysimeters and resins) would result in elevated concentrations under AGW compared to REF. In contrast with our hypothesis, the volume weighted total P concentration in 15 and 60 cm lysimeters, when averaged across all hillslope positions, was less under AGW than REF (Figs. 3.7 and 3.9). On the other hand, $PO_4{}^{3-}{}_i$ was a greater percent of $PO_4{}^{3-}{}_T$ in the AGW ridge compared with REF that could be related to historical fertilization and higher bioavailable P_i. Multiple soil factors may influence concentrations of water-soluble P in soil during reforestation. For example, higher clay percentages at the soil surface after erosion, often observed in slopes under AGW, may increase the bonding of P with Fe/Al oxide and decrease the release of P to soil solution. Similarly, higher AEC, as observed in AGW, may facilitate greater P sorption on the soil surface removing P from solution (Table 3.4A). Finally, SOC can compete with P for surface absorption sites, which could release more P into soil solution. The mean TC concentration under AGW (~6400 ug g^{-1}) was slightly less than REF (~8000 ug g^{-1}) as was the total content of carbon (41020 ±55651 kg ha^{-1} greater in REF than AGW; Table 3.9). This lower SOM in AGW soil (0-60 cm) may also reduce current amounts of P in soil solution as observations have shown that higher organic acid concentrations increase P availability in soil by competing for clay surface charge (Redel *et al.*, 2007; Zamuner *et al.*, 2008). Soil solution and resin P are only one component of the P cycle (i.e., biomass and microbial uptake, decomposition) and alone cannot conclusively explain why the current soil P in solution in AGW is less than REF overall but this was not our expectation.

4.2.2 Effects of land use history on P fractions

We hypothesized that the organic P fractions in undisturbed land (REF) would be greater than under disturbed land (AGW) due to a legacy of agricultural activity that resulted in OM and deep root loss. The organic forms of P (NaOH P_o) in REF were 51 (±130) kg ha^{-1} greater than AGW (Table 3.2). Previous research has demonstrated a positive correlation between TC and P_o in the soil (Turner *et al.*, 2007), and here we find a strong correlation between P_o and TC ($R^2 >$ 0.67). The loss of OM during forest conversion to agriculture has been demonstrated in the Calhoun CZO (Richter *et al.*, 1994) and elsewhere to have losses of 20-50% in the upper 30 cm layer (Davidson and Ackerman, 1993; Bruce *et al.*, 1999; Celik, 2005). More recent results from the Calhoun CZO, however, indicate that impacts from these losses still persist after 70 years of reforestation. For example, extractable organic C quantity under undisturbed land (i.e., hardwood forests similar to REF) was 8.8 times greater than under reforesting disturbed lands (i.e., secondary forests similar to AGW) throughout the upper 0.5 m of soil (Billings *et al.*, 2018). Similarly, root density under the reference condition (e.g., similar to our REF) was around double that under the reforesting condition (e.g., AGW) at 70 cm (Billings *et al.*, 2018). The greater root density and organic carbon abundance in REF compared to AGW is consistent with our expectation and observation of higher P_o under lands never converted to agriculture.

5. Conclusions

At the Calhoun CZO, after a history of agricultural land clearing including P fertilization and erosion, and approximately seven decades of reforestation a legacy on P biogeochemistry is evident but nuanced. For example, despite strong evidence of historical downslope erosion we found limited accumulation of soil P in lower hillslope positions in watersheds with an agricultural history suggesting soil P was partially washed away and leached to streams. In contrast, in ridge tops that were farmed longest, higher extractable P through 2 m soil profiles was evident compared to reference ridges reflecting P inputs and vertical leaching of P over several decades. Despite this greater extractable P, however, soil solution P and ion exchange resin P in agricultural hillslopes was low compared to reference hillslopes. Greater P cycling in reference sites could reflect the slightly greater organic P in these undisturbed hillslopes that was expected given no loss of organic carbon due to clearing and a long history of deep rooting compared to agricultural sites. Overall, these biogeochemical P patterns show that in this critical zone depleted of P due to millennia of geological weathering that anthropogenic influences including P (and Ca) additions are still evident. These influences, however, are most apparent on ridge tops and despite these legacies overall P concentrations in soils, soil solutions, and streams are low. Thus, the Calhoun CZO continues to develop in response to past and current human actions, and understanding those responses is important to sustaining CZ functions.

References

Alt, F., Oelmann, Y., Herold, N., Schrumpf, M., Wilcke, W., 2011. Phosphorus partitioning in grassland and forest soils of Germany as related to land-use type, management intensity, and land use–related pH. Journal of Plant Nutrition and Soil Science 174, 195-209.

Araújo, M.S., Schaefer, C.E., Sampaio, E.V., 2004. Soil phosphorus fractions from toposequences of semi-arid Latosols and Luvisols in northeastern Brazil. Geoderma 119, 309-321.

Artiola, J., Pepper, I.L., Brusseau, M.L., 2004. Environmental monitoring and characterization. Elsevier.

Austin, J.C., Schroeder, P.A., 2017. "Big Dig" 2016 soil pits and Rose Hill, http://criticalzone.org/calhoun/data/dataset/5986/.

Bern, C.R., Townsend, A.R., Farmer, G.L., 2005. Unexpected dominance of parent-material strontium in a tropical forest on highly weathered soils. Ecology 86, 626-632.

Billings, S.A., Hirmas, D., Sullivan, P.L., Lehmeier, C.A., Bagchi, S., Min, K., Brecheisen, Z., Hauser, E., Stair, R., Flournoy, R., 2018. Loss of deep roots limits biogenic agents of soil development that are only partially restored by decades of forest regeneration. Elem Sci Anth 6.

Bolton, J., Coulter, J., 1965. Distribution of fertilizer residues in a forest nursery manuring experiment on a sandy podsol at Wareham, Dorset. Report on Forest Research for, 90-102.

Bowman, R., Cole, C., 1978. An exploratory method for fractionation of organic phosphorus from grassland soils. Soil Science 125, 95-101.

Brecheisen, Z., Cook, C., & Harmon, M., 2015. US Forest Service Photograph from the Photographic Archive of the Calhoun Experimental Forest, http://criticalzone.org/calhoun/data/dataset/4324/.

Brubaker, S., Jones, A., Lewis, D., Frank, K., 1993. Soil properties associated with landscape position. Soil Science Society of America Journal 57, 235-239.

Bruce, J.P., Frome, M., Haites, E., Janzen, H., Lal, R., Paustian, K., 1999. Carbon sequestration in soils. Journal of soil and water conservation 54, 382-389.

Bünemann, E.K., Oberson, A., Frossard, E., 2010. Phosphorus in action: biological processes in soil phosphorus cycling. Springer Science & Business Media.

Callaham, M., Richter, D., Coleman, D., Hofmockel, M., 2006. Long-term land-use effects on soil invertebrate communities in Southern Piedmont soils, USA. European Journal of Soil Biology 42, S150-S156.

Campbell, J., Morris, L., 2018. Land use and soil legacy in the Lower Coastal Plain: A case study of Wormsloe State Historic Site, Georgia. Journal of Soil and Water Conservation 73, 386-399.

Celik, I., 2005. Land-use effects on organic matter and physical properties of soil in a southern Mediterranean highland of Turkey. Soil and Tillage Research 83, 270-277.

Chadwick, O.A., Derry, L.A., Vitousek, P.M., Huebert, B.J., Hedin, L.O., 1999. Changing sources of nutrients during four million years of ecosystem development. Nature 397, 491-497.

Cherubin, M.R., Franco, A.L., Cerri, C.E., Karlen, D.L., Pavinato, P.S., Rodrigues, M., Davies, C.A., Cerri, C.C., 2016. Phosphorus pools responses to land-use change for sugarcane expansion in weathered Brazilian soils. Geoderma 265, 27-38.

Cooke, G., Williams, R., 1973. Significant of Man-made Sources of Phosphorus: Fertilizers and Farming: The phosphorus Involved in Agricultural System and Possibilities of Its Movement into Natural Water. Phosphorus in Fresh Water and the Marine Environment. Elsevier, pp. 19-33.

Costa, M.H., Yanagi, S.N., Souza, P.J., Ribeiro, A., Rocha, E.J., 2007. Climate change in Amazonia caused by soybean cropland expansion, as compared to caused by pastureland expansion. Geophysical Research Letters 34.

Cross, A.F., Schlesinger, W.H., 1995. A literature review and evaluation of the. Hedley fractionation: Applications to the biogeochemical cycle of soil phosphorus in natural ecosystems. Geoderma 64, 197-214.

Daniel, T., Sharpley, A., Edwards, D., Wedepohl, R., Lemunyon, J., 1994. Minimizing surface water eutrophication from agriculture by phosphorous management. Journal of Soil and Water conservation-USA- 49, 30-30.

Davidson, E.A., Ackerman, I.L., 1993. Changes in soil carbon inventories following cultivation of previously untilled soils. Biogeochemistry 20, 161-193.

Delgado, A., Torrent, J., 2000. Phosphorus forms and desorption patterns in heavily fertilized calcareous and limed acid soils. Soil Science Society of America Journal 64, 2031-2037.

Dessalegn, D., Beyene, S., Ram, N., Walley, F., Gala, T.S., 2014. Effects of topography and land use on soil characteristics along the toposequence of Ele watershed in southern Ethiopia. Catena 115, 47-54.

Dialynas, Y.G., Bastola, S., Bras, R.L., Billings, S.A., Markewitz, D., 2016. bTopographic variability and the influence of soil erosion on the carbon cycle. Global Biogeochemical Cycles 30, 644-660.

Eghball, B., Binford, G., Baltensperger, D.D., 1996. Phosphorus movement and adsorption in a soil receiving long-term manure and fertilizer application. Journal of environmental quality 25, 1339-1343.

Falkengren-Grerup, U., ten Brink, D.-J., Brunet, J., 2006. Land use effects on soil N, P, C and pH persist over 40–80 years of forest growth on agricultural soils. Forest Ecology and Management 225, 74-81.

Fox, R.L., Kamprath, E., 1970. Phosphate Sorption Isotherms for Evaluating the Phosphate Requirements of Soils 1. Soil Science Society of America Journal 34, 902-907.

Garcia-Montiel, D.C., Neill, C., Melillo, J., Thomas, S., Steudler, P.A., Cerri, C.C., 2000. Soil phosphorus transformations following forest clearing for pasture in the Brazilian Amazon.

Gee, G., Or, D., 2002. 2.4 Particle-size analysis. Methods of soil analysis. Part 4, 255-293.

Goyette, J.-O., Bennett, E., Maranger, R., 2018. Low buffering capacity and slow recovery of anthropogenic phosphorus pollution in watersheds. Nature Geoscience, 1.

Gray, L.C., Thompson, E.K., 1933. History of agriculture in the southern United States to 1860.

Groppo, J., Lins, S., Camargo, P., Assad, E., Pinto, H., Martins, S., Salgado, P., Evangelista, B., Vasconcellos, E., Sano, E., 2015. Changes in soil carbon, nitrogen and phosphorus due to land-use changes in Brazil. Biogeosciences Discussions 12, 2533-2571.

Hamer, U., Potthast, K., Burneo, J.I., Makeschin, F., 2013. Nutrient stocks and phosphorus fractions in mountain soils of Southern Ecuador after conversion of forest to pasture. Biogeochemistry 112, 495-510.

Hedley, M.J., Stewart, J., Chauhan, B., 1982. Changes in inorganic and organic soil phosphorus fractions induced by cultivation practices and by laboratory incubations 1. Soil Science Society of America Journal 46, 970-976.

Jackson, C., Martin, J., Leigh, D., West, L., 2005. A southeastern piedmont watershed sediment budget: Evidence for a multi-millennial agricultural legacy. Journal of Soil and Water Conservation 60, 298-310.

Jenkins, S., 1982. Standard Methods for the Examination of Water and Wastewater: Joint Editorial Board: AE Greenberg, JJ Connors and D. Jenkins. 1980. American Public Health Association, Washington, DC 1134 pp. Pergamon.

Kaňa, J., Kopáček, J., 2006. Impact of soil sorption characteristics and bedrock composition on phosphorus concentrations in two Bohemian Forest lakes. Water, air, and soil pollution 173, 243-259.

Khan, M.S., Zaidi, A., Wani, P.A., 2007. Role of phosphate-solubilizing microorganisms in sustainable agriculture—a review. Agronomy for sustainable development 27, 29-43.

Kimbrough, D.E., Wakakuwa, J.R., 1989. Acid digestion for sediments, sludges, soils, and solid wastes. A proposed alternative to EPA SW 846 Method 3050. Environmental science & technology 23, 898-900.

Koroleff, F., 1983. Simultaneous oxidation of nitrogen and phosphorus compounds by persulfate. Methods of seawater analysis 2, 205-206.

Lilienfein, J., Wilcke, W., Ayarza, M.A., Vilela, L., do Carmo Lima, S., Zech, W., 2000. Chemical fractionation of phosphorus, sulphur, and molybdenum in Brazilian savannah Oxisols under different land use. Geoderma 96, 31-46.

Liu, D., Wang, Z., Zhang, B., Song, K., Li, X., Li, J., Li, F., Duan, H., 2006. Spatial distribution of soil organic carbon and analysis of related factors in croplands of the black soil region, Northeast China. Agriculture, ecosystems & environment 113, 73-81.

Mao, H., Zhao, Z., Cui, L., Liu, C., 2018. The influence of climate and topography on chemical weathering of granitic regoliths in the monsoon region of China. Acta Geochimica 37, 758-768.

Markewitz, D., Davidson, E.A., Moutinho, P., Nepstad, D.C., 2004. Nutrient loss and redistribution after forest clearing on a highly weathered soil in Amazonia. Ecol Appl 14, 177-199.

Mehlich, A., 1978. New extractant for soil test evaluation of phosphorus, potassium, magnesium, calcium, sodium, manganese and zinc. Communications in Soil Science and Plant Analysis 9, 477-492.

Messiga, A.J., Ziadi, N., Morel, C., Parent, L.-E., 2010. Soil phosphorus availability in no-till versus conventional tillage following freezing and thawing cycles. Canadian journal of soil science 90, 419-428.

Metz, L.J., 1958. The Calhoun experimental forest. unknown.

Miller, A.J., Schuur, E.A., Chadwick, O.A., 2001. Redox control of phosphorus pools in Hawaiian montane forest soils. Geoderma 102, 219-237.

Murphy, J., Riley, J.P., 1962. A modified single solution method for the determination of phosphate in natural waters. Analytica chimica acta 27, 31-36.

Negassa, W., Leinweber, P., 2009. How does the Hedley sequential phosphorus fractionation reflect impacts of land use and management on soil phosphorus: a review. Journal of Plant Nutrition and Soil Science 172, 305-325.

Niederberger, J., Todt, B., Boča, A., Nitschke, R., Kohler, M., Kühn, P., Bauhus, J., 2015. Use of near-infrared spectroscopy to assess phosphorus fractions of different plant availability in forest soils. Biogeosciences 12, 3415-3428.

Page, A.L., 1982. Methods of soil analysis. Part 2. Chemical and microbiological properties. American Society of Agronomy, Soil Science Society of America.

Parton, W.J., Neff, J., Vitousek, P.M., Turner, B., Frossard, E., Baldwin, D., 2005. Modelling phosphorus, carbon and nitrogen dynamics in terrestrial ecosystems. Organic phosphorus in the environment, 325-347.

Pavinato, P.S., Merlin, A., Rosolem, C.A., 2009. Phosphorus fractions in Brazilian Cerrado soils as affected by tillage. Soil and Tillage Research 105, 149-155.

Peech, M., 1965. Methods of Soil Analysis. Chemical and Microbiological Properties. American Society of Agronomy Madison.

Redel, Y.D., Rubio, R., Rouanet, J.L., Borie, F., 2007. Phosphorus bioavailability affected by tillage and crop rotation on a Chilean volcanic derived Ultisol. Geoderma 139, 388-396.

Rhoades, J., Sparks, D., Page, A., Helmke, P., Loeppert, R., Soltanpour, P., Tabatabai, M., Johnston, C., Sumner, M., 1996. Salinity: Electrical conductivity and total dissolved solids. Methods of soil analysis. Part 3-chemical methods., 417-435.

Richter, D., Markewitz, D., Wells, C., Allen, H., April, R., Heine, P., Urrego, B., 1994. Soil chemical change during three decades in an old-field loblolly pine (Pinus taeda L.) ecosystem. Ecology 75, 1463-1473.

Richter, D.D., Allen, H.L., Li, J., Markewitz, D., Raikes, J., 2006. Bioavailability of slowly cycling soil phosphorus: major restructuring of soil P fractions over four decades in an aggrading forest. Oecologia 150, 259-271.

Richter, D.d., Bacon, A.R., Billings, S.A., Binkley, D., Buford, M., Callaham, M., Curry, A.E., Fimmen, R.L., Grandy, A.S., Heine, P.R., Hofmockel, M., Jackson, J.A., LeMaster, E., Li, J., Markewitz, D., Mobley, M.L., Morrison, M.W., Strickland, M.S., Waldrop, T., Wells, C.G., 2015. Evolution of soil, ecosystem, and critical zone research at the USDA FS Calhoun Experimental Forest.

Richter, D.D., Markewitz, D., 2001. Understanding soil change : soil sustainability over millennia, centuries, and decades. Cambridge University Press, Cambridge.

Ruffin, E., 1852. An essay on calcareous manures. JW Randolph.

Ryland, R.C., 2017. Depth to the argillic horizon on historically farmed soil in the southeastern USA piedmont. uga.

Sample, E., Soper, R., Racz, G., 1980. Reactions of phosphate fertilizers in soils. The role of phosphorus in agriculture, 263-310.

Schoenau, J., Stewart, J., Bettany, J., 1989. Forms and cycling of phosphorus in prairie and boreal forest soils. Biogeochemistry 8, 223-237.

Schoumans, O., Groenendijk, P., 2000. Modeling soil phosphorus levels and phosphorus leaching from agricultural land in the Netherlands. Journal of Environmental Quality 29, 111-116.

Smeck, N.E., 1985. Phosphorus dynamics in soils and landscapes. Geoderma 36, 185-199.

Smeck, N.E., Runge, E., 1971. Phosphorus availability and redistribution in relation to profile development in an Illinois landscape segment. Soil Science Society of America Journal 35, 952-959.

Smeck, N.E., Runge, E., 1973. Factors influencing profile development exhibited by some hy dromorphic soils in Illinois. Pseudogley & Gley Genesis and Use of Hydromorphic Soils.

Stevenson, F.J., Stevenson, E., Cole, M., 1999. Cycles of soils: carbon, nitrogen, phosphorus, sulfur, micronutrients. John Wiley & Sons.

Sumner, M., Miller, W., 1996. Cation exchange capacity and exchange coefficients. Methods of Soil Analysis Part 3—Chemical Methods, 1201-1229.

Tchienkoua, M., Zech, W., 2003. Chemical and spectral characterization of soil phosphorus under three land uses from an Andic Palehumult in West Cameroon. Agriculture, Ecosystems & Environment 100, 193-200.

Tiessen, H., Chacon, P., Cuevas, E., 1994. Phosphorus and nitrogen status in soils and vegetation along a toposequence of dystrophic rainforests on the upper Rio Negro. Oecologia 99, 145-150.

Tiessen, H., Moir, J., 1993. Characterization of available P by sequential extraction. Soil sampling and methods of analysis 7, 5-229.

Townsend, A.R., Asner, G.P., Cleveland, C.C., Lefer, M.E., Bustamante, M.M., 2002. Unexpected changes in soil phosphorus dynamics along pasture chronosequences in the humid tropics. Journal of Geophysical Research: Atmospheres 107, LBA 34-31-LBA 34-39.

Turner, B., Haygarth, P., 1999. Phosphorus leaching under cut grassland. Water science and technology 39, 63.

Turner, B.L., Condron, L.M., Richardson, S.J., Peltzer, D.A., Allison, V.J., 2007. Soil organic phosphorus transformations during pedogenesis. Ecosystems 10, 1166-1181.

Ugolini, F., Minden, R., Dawson, H., Zachara, J., 1977. hAn example of soil processes in the Abies amabilis zone of Central Cascades, Washington. Soil Science 124, 291-302.

Vervoort, R., Radcliffe, D., Cabrera, M., Latimore, M., 1998. Nutrient losses in surface and subsurface flow from pasture applied poultry litter and composted poultry litter. Nutrient Cycling in Agroecosystems 50, 287-290.

Vitousek, P., Chadwick, O., Matson, P., Allison, S., Derry, L., Kettley, L., Luers, A., Mecking, E., Monastra, V., Porder, S., 2003. Erosion and the rejuvenation of weathering-derived nutrient supply in an old tropical landscape. Ecosystems 6, 762-772.

Wade, A.W., Richter, D.D., Cherkinsky, A., Craft, C.B., Heine, P.R., in press. Limited carbon content of centuries old soils forming in legacy sediment. Geomorphology

Walker, T., Syers, J.K., 1976. The fate of phosphorus during pedogenesis. Geoderma 15, 1-19.

Wang, J., Fu, B., Qiu, Y., Chen, L., 2001. Soil nutrients in relation to land use and landscape position in the semi-arid small catchment on the loess plateau in China. Journal of Arid Environments 48, 537-550.

Zamuner, E., Picone, L., Echeverria, H., 2008. Organic and inorganic phosphorus in Mollisol soil under different tillage practices. Soil and Tillage Research 99, 131-138.

Zelazny, L.W., He, L., Vanwormhoudt, A., 1996. Charge analysis of soils and anion exchange. Methods of Soil Analysis Part 3—Chemical Methods, 1231-1253.

Zhi-Yao, S., XIONG, Y.-M., Jian-Yun, Z., Yong-Chang, Y., Mai, Y., 2006. Soil organic carbon content and distribution in a small landscape of Dongguan, South China. Pedosphere 16, 10-17.

Table 3.1. Soil extractable phosphorus concentration in the upper soil profile of three different land uses in the Calhoun Critical Zone Observatory (Richter and Markewitz, 2001).

	Hardwood		Pine		Pasture	
Depth (cm)	Mean (μg g^{-1})	SE	Mean (μg g^{-1})	SE	Mean (μg g^{-1})	SE
0-30	1.80	0.37	5.60	2.50	6.27	1.65
30-60	0.40	0.18	0.09	0.02	0.70	0.50
60-100	0.19	0.03	0.18	0.06	0.16	0.04

Table 3.2. The effect of land use on phosphorus (P) fraction concentrations across all depths and hillslope positions. (n= number of samples, SE= standard error, AGW= watersheds with a history of agricultural use, REF= reference hillslope with no agricultural history).

P-fractions	AGW			REF			p-value
	n	Mean	SE	n	Mean	SE	
		µg g^{-1}	µg g^{-1}		µg g^{-1}	µg g^{-1}	
Mehlich III-P	174	4.72	0.31	63	3.56	0.49	<0.0001
Resin-P_i	56	3.63	0.41	62	2.58	0.30	<0.0001
HCO_3-P_i	58	1.62	0.28	62	2.08	0.29	0.0300
HCO_3-P_o	58	3.03	0.52	62	3.04	0.53	0.1660
NaOH-P_i	58	9.70	0.96	62	13.9	1.15	<0.0001
NaOH-P_o	58	15.3	2.08	61	17.2	2.62	0.0198
1MHCl-P_i	57	2.00	0.29	61	2.54	0.35	0.0018
Con. HCl-P_i	58	46.8	5.40	61	71.4	5.02	<0.0001
Con-HCl-P_o	57	0.96	0.21	60	0.54	0.16	<0.0001
Residual-P	57	114	7.69	63	111	4.77	<0.0001
Total-P	56	188	9.46	63	232	9.75	<0.0001

Table 3.3. The effect of hillslope position on phosphorus (P) fraction concentrations across all depths and land uses, (n= number of samples, SE= standard error).

P-fractions	Ridge			Mid			Toe			p-value
	n	Mean	SE	n	Mean	SE	n	Mean	SE	
		μg g^{-1}	μg g^{-1}		μg g^{-1}	μg g^{-1}		μg g^{-1}	μg g^{-1}	
Mehlich III-P	80	3.47	0.26	76	4.53	0.50	81	5.23	0.55	0.9730
Resin-P_i	40	1.40	0.26	38	4.92	0.50	40	3.01	0.36	<0.0001
HCO_3-P_i	40	1.20	0.19	40	2.09	0.35	40	2.32	0.43	0.4705
HCO_3-P_o	40	3.40	0.63	39	2.09	0.51	41	3.59	0.75	<0.0001
NaOH-P_i	40	9.15	0.63	40	11.2	0.90	40	15.2	1.95	0.4214
NaOH-P_o	40	15.2	1.93	39	12.8	2.27	40	20.7	3.98	0.0014
1MHCl-P_i	40	0.90	0.11	38	2.57	0.39	40	3.35	0.48	<0.0001
Con-HCl-P_i	38	57.9	7.11	40	58.1	6.36	41	62.0	6.64	0.9685
Con-HCl-P_o	36	2.27	0.30	40	0.07	0.01	41	0.06	0.01	<0.0001
Residual-P	40	101	5.36	39	149	8.30	41	88.6	5.54	0.0006
Total-P	40	194	9.94	38	258	11.3	41	185	12.3	0.0258

Table 3.4. The phosphorus (P) fraction concentrations by land uses and hillslope position across all depths (n=number of samples, SE= standard error, AGW=watersheds with a history of agricultural use, REF=reference hillslope with no agricultural history).

Fractions	AGW: Ridge			AGW: Mid			AGW: Toe			REF: Ridge			REF: Mid			REF: Toe			p-value
	n	Mean	SE	n	Mean	SE	n	Mean	SE	n	Mean	SE	n	Mean	SE	n	Mean	SE	
	Mean and SE in μg g^{-1}																		
Mehlich III-P	59	3.97	0.29	55	4.80	0.62	60	5.37	0.63	21	2.06	0.45	21	3.77	0.76	21	4.84	1.12	0.005
Resin-Pi	19	1.65	0.43	17	5.61	0.80	20	3.84	0.61	21	1.19	0.31	21	4.37	0.61	20	2.18	0.30	0.573
HCO3-Pi	19	1.14	0.30	19	1.53	0.35	20	2.16	0.67	21	1.19	0.26	21	2.59	0.57	20	2.47	0.57	0.339
HCO3-Po	19	3.37	0.90	19	2.03	0.75	20	3.66	1.04	21	3.41	0.91	20	2.14	0.72	21	3.53	1.10	0.173
NaOH-Pi	19	7.94	0.64	19	8.39	0.96	20	12.6	2.48	21	10.2	1.02	21	13.7	1.26	20	17.9	2.95	0.482
NaOH-Po	19	17.9	3.10	19	10.7	3.09	20	17.3	4.33	21	12.7	2.33	20	14.7	3.32	20	24.2	6.72	0.146
1MHCl-Pi	19	0.88	0.17	19	1.96	0.34	19	3.15	0.71	21	0.98	0.16	19	3.18	0.69	21	3.52	0.68	0.430
Con-HCl-Pi	19	45.6	9.86	19	49.6	10.6	20	45.2	8.03	19	70.3	9.69	21	65.8	7.21	21	78.0	9.35	0.961
Con-HCl-Po	18	2.86	0.41	19	0.10	0.02	20	0.07	0.02	18	1.68	0.42	21	0.05	0.02	21	0.06	0.02	0.098
Residual-P	19	98.6	9.26	18	156	15.7	20	91.3	9.82	21	104	6.03	21	143	7.68	21	86.0	5.64	0.907
Total-P	19	171	12.7	17	225	18.5	20	174	15.8	21	214	13.8	21	284	11.1	21	197	18.9	0.613

Table 3.5. The concentrations of Phosphorus fractionations in two land uses ordered by soil depth and hillslopes. SE= standard error, AGW= watersheds with a history of agricultural use, REF= reference hillslope with no agricultural history.

Land-use	Hillslope	Depth (cm)	Resin-P_i($\mu g\ g^{-1}$)		HCO_3-P_i($\mu g\ g^{-1}$)		HCO_3-P_o($\mu g\ g^{-1}$)		NaOH-P_i($\mu g\ g^{-1}$)		NaOH-P_o($\mu g\ g^{-1}$)		1MHCl-P_i($\mu g\ g^{-1}$)		Con.HCl-P_i($\mu g\ g^{-1}$)		Con-HCl-P_o($\mu g\ g^{-1}$)		Residual-P($\mu g\ g^{-1}$)		Total-P($\mu g\ g^{-1}$)	
			Mean	SE	Mean	SE	Mean	SE	Mean	SE	Mean	SE	Mean	SE	Mean	SE	Mean	SE	Mean	SE	Mean	SE
AGW	Ridge	0-7.5	5.62	0.29	3.82	0.33	10.50	1.36	8.61	0.75	39.6	5.19	2.11	0.26	20.8	3.60	4.92	1.11	73.4	2.10	179	27.6
		7.5-15	1.79	0.18	1.51	0.24	5.33	0.78	7.05	0.69	18.5	3.20	0.77	0.10	20.9	3.07	2.44	0.01	90.4	12.6	155	13.8
		15-35	0.77	0.08	0.71	0.11	3.41	0.40	8.53	1.51	22.7	3.09	0.67	0.12	36.4	10.6	1.78	0.07	118	18.1	179	19.8
		35-60	0.96	0.07	0.55	0.13	0.48	0.15	8.11	1.50	5.73	0.95	0.56	0.22	49.4	19.3	1.37	0.79	107	14.7	162	18.2
		60-100	0.81	0.25	0.33	0.10	1.02	0.17	5.70	1.58	7.90	3.72	0.83	0.42	54.1	22.7	3.20	0.14	81.6	11.7	157	15.6
		100-150	0.23	0.00	0.23	0.00	0.26	0.10	9.80	1.12	16.4	6.63	0.58	0.05	84.9	30.6	2.48	0.35	109	30.3	211	27.9
		150-200	0.56	0.14	0.23	0.00	0.58	0.31	8.60	1.37	11.8	3.00	0.33	0.11	81.5	34.0	1.91	0.17	122	42.5	162	67.8
	Mid	0-7.5	5.67	0.71	4.28	0.61	8.35	1.33	8.62	1.40	32.4	8.52	2.65	0.57	23.9	6.30	0.23	0.07	157	15.8	258	19.6
		7.5-15	3.80	1.21	2.04	0.25	3.27	0.54	7.78	0.82	16.2	2.92	1.91	0.10	24.4	7.11	0.11	0.03	136	7.56	209	13.7
		15-35	9.32	1.59	0.74	0.35	0.99	0.38	8.28	0.78	11.1	1.50	1.35	0.41	39.2	13.2	0.09	0.03	157	42.2	230	37.3
		35-60	4.35	0.76	0.51	0.25	0.05	0.01	7.28	1.66	5.24	1.22	1.07	0.38	40.9	16.7	0.08	0.02	120	31.9	239	44.8
		60-100	4.84	1.08	1.05	0.51	0.08	0.02	7.26	1.75	3.52	0.94	1.75	0.87	48.6	23.7	0.09	0.03	132	40.0	150	37.0
		100-150	6.51	2.91	0.42	0.15	0.05	0.01	8.52	3.84	0.35	0.11	1.05	0.35	75.9	31.8	0.04	0.02	202	30.4	290	71.5
		150-200	3.93	0.06	1.22	0.30	0.11	0.04	12.4	3.63	0.14	0.05	4.51	0.75	130	9.43	0.01	0.00	237	39.6	329	79.3
	Toe	0-7.5	8.48	0.92	7.77	0.34	12.83	1.55	17.0	2.19	53.2	7.28	7.01	2.31	35.7	8.34	0.20	0.05	82.3	20.9	208	28.8
		7.5-15	3.78	0.38	2.16	0.14	5.48	0.43	13.3	4.14	25.4	3.14	3.15	0.74	37.4	14.7	0.07	0.02	83.1	17.5	155	27.2
		15-35	3.22	0.38	0.49	0.08	3.74	0.84	11.3	3.09	19.3	4.51	2.43	0.56	36.6	12.3	0.05	0.01	88.5	18.9	180	31.1
		35-60	1.72	0.22	0.33	0.04	1.64	0.51	7.07	1.37	10.0	3.33	1.67	0.12	35.2	13.1	0.03	0.01	82.9	19.4	159	25.8
		60-100	3.52	1.48	0.16	0.04	0.24	0.12	5.75	1.06	4.44	1.62	1.62	0.32	42.4	6.9	0.04	0.02	105	22.1	147	26.7
		100-150	3.98	0.71	0.83	0.31	0.30	0.11	12.8	4.12	2.42	0.36	3.63	1.63	61.4	17.0	0.03	0.01	105	23.4	163	16.5
		150-200	1.33	0.21	4.06	2.40	0.25	0.01	25.0	14.9	0.76	0.46	12.8	7.26	79.2	42.6	0.04	0.01	94.3	30.6	222	79.3
REF	Ridge	0-7.5	2.40	0.56	3.28	0.31	10.96	1.78	10.8	1.50	28.8	0.82	1.53	0.21	46.9	9.31	3.23	1.09	113	6.20	199	7.77
		7.5-15	0.56	0.05	2.48	0.11	6.55	0.65	10.8	1.52	25.3	2.14	1.50	0.30	51.9	9.65	1.38	0.77	71.2	2.69	209	1.79
		15-35	2.39	0.74	1.04	0.07	3.30	0.88	13.1	3.26	14.8	2.07	0.66	0.13	40.0	4.75	1.55	0.83	103	8.26	179	2.19
		35-60	0.42	0.21	0.47	0.09	1.07	0.57	11.4	1.82	7.80	1.83	0.45	0.15	60.0	8.61	1.11	0.63	87.0	14.4	205	31.8
		60-100	0.32	0.14	0.37	0.09	0.56	0.21	12.1	1.84	6.93	2.17	0.60	0.24	116	26.9	0.67	0.24	134	2.81	278	23.1
		100-150	1.90	1.00	0.20	0.02	0.09	0.00	6.85	1.26	3.81	1.88	1.19	0.55	87.0	21.3	2.41	0.90	97.1	12.0	166	10.7
		150-200	0.35	0.20	0.50	0.10	0.33	0.11	6.64	1.82	1.86	0.80	0.94	0.25	59.7	25.7	0.15	0.06	121	11.4	264	48.1
	Mid	0-7.5	4.09	1.32	7.50	1.13	14.59	4.05	20.7	2.54	61.6	16.5	4.61	1.58	52.1	5.26	0.17	0.08	178	21.3	283	19.1
		7.5-15	3.39	0.23	4.19	0.37	6.05	0.51	15.9	0.99	35.3	1.80	2.44	0.28	51.6	8.00	0.06	0.01	218	12.1	280	13.8
		15-35	3.35	0.16	1.77	0.07	0.80	0.10	14.1	0.74	21.7	1.65	1.70	0.47	66.3	8.67	0.03	0.01	234	12.3	305	3.92
		35-60	2.67	0.17	0.82	0.11	0.21	0.12	13.7	2.32	10.2	0.46	1.54	0.32	78.2	13.9	0.04	0.01	243	3.39	330	22.9
		60-100	4.26	1.12	0.70	0.32	0.21	0.06	12.3	3.27	4.29	0.58	1.81	0.39	77.6	16.2	0.02	0.00	233	12.7	282	12.2
		100-150	5.63	1.10	0.43	0.05	0.07	0.01	10.4	2.47	0.64	0.39	3.08	1.23	80.6	28.0	0.03	0.01	184	6.66	266	40.7
		150-200	3.87	0.48	1.77	0.45	0.98	0.67	8.51	1.29	0.67	0.20	9.39	3.99	54.4	12.5	0.02	0.00	194	9.62	243	16.7
	Toe	0-7.5	4.09	0.96	6.57	1.08	11.06	1.91	29.7	6.54	84.1	17.8	7.63	1.95	38.3	4.02	0.19	0.07	80.7	14.2	198	33.4
		7.5-15	2.31	0.39	2.37	0.14	8.72	2.52	25.7	8.18	61.4	13.7	3.68	1.06	58.4	17.3	0.07	0.02	98.7	8.60	148	14.1
		15-35	2.16	0.60	1.28	0.39	3.40	1.23	25.6	11.1	34.2	8.54	2.67	0.97	39.9	1.17	0.05	0.02	81.5	3.40	223	46.5
		35-60	1.37	0.03	1.21	0.40	0.62	0.39	15.5	4.54	13.4	3.44	1.48	0.27	72.7	12.7	0.03	0.01	84.3	17.5	141	13.6
		60-100	1.38	0.15	0.66	0.21	0.52	0.26	11.3	2.50	5.29	1.28	1.15	0.12	83.7	19.1	0.03	0.01	102	10.0	166	24.8
		100-150	1.51	0.14	0.50	0.14	0.13	0.04	12.3	3.44	2.30	0.54	1.45	0.15	88.1	25.9	0.02	0.01	67.1	6.98	165	26.9
		150-200	2.14	0.24	2.66	0.37	0.24	0.07	18.1	6.63	1.36	0.11	3.55	0.58	110.0	17.6	0.00	0.00	88.0	12.7	192	16.8

Table 3.6. The effect of land use on soil chemical and physical attributes across all depths and hillslope positions. Total Carbon (TC) and Nitrogen (TN), Ca, Mg, Fe, Al concentration (μg g^{-1}), pH, Clay percentage, Anion Exchange Capacity (AEC), and Cation Exchange Capacity (CEC) (cmolc kg^{-1}), (n= number of samples, SE= standard error, AGW=watersheds with a history of agricultural use, REF=reference hillslope with no agricultural history).

Factors	AGW			REF			p-value
	n	Mean	SE	n	Mean	SE	
TC	179	6400	690	63	7900	1410	<0.0010
TN	177	3364	857	62	1146	625	<0.0001
MIII-Ca	178	193	13.0	63	132	20.7	<0.0010
MIII-Mg	181	149	6.80	62	183	14.3	<0.0010
MIII-Fe	180	110	4.50	63	75.0	5.65	<0.0010
MIII-Al	181	807	20.0	63	852	27.4	<0.0010
Clay-pct	176	18	0.9	63	23	2.0	<0.0010
pH_{CaCl2}	179	4.2	0.0	63	3.9	0.0	<0.0010
AEC	176	0.6	0.1	63	0.5	0.1	<0.0001
CEC	178	4.6	0.2	60	5.0	0.3	<0.0010

Table 3.7. The effect of hillslope positions on soil chemical and physical attributes across land uses over all depths. Total Carbon (TC) and Nitrogen (TN), Ca, Mg, Fe, Al concentration (μg g^{-1}), pH, Clay percentage, Anion Exchange Capacity (AEC), and Cation Exchange Capacity (CEC) (cmolc kg^{-1}), (n= number of samples, SE= standard error).

Factors	Ridge			Mid			Toe			p-value
	n	Mean	SE	n	Mean	SE	n	Mean	SE	
TC	82	6822	1054	78	6063	1059.6	82	7356	1140	0.0176
TN	79	5170	1670	79	2276	952.7	81	966	412	0.4281
MIII-Ca	80	176	18.0	79	175	22.9	82	180	18.2	0.9105
MIII-Mg	81	169	11	80	162	12.5	82	141	9.10	0.1942
MIII-Fe	82	94.3	6.60	80	94.2	5.80	81	115	6.90	0.0092
MIII-Al	82	835	27	80	846	34.5	82	776	21.9	0.0150
Clay-pct	82	22	1.7	75	19	1.6	82	18	1.0	0.3887
pH_{CaCl2}	80	4.2	0.1	80	4.1	0.0	82	4.2	0.0	0.0014
AEC	79	0.8	0.2	82	0.7	0.1	80	0.2	0.0	0.0034
CEC	81	5.1	0.3	77	4.9	0.3	80	4.2	0.2	0.0758

* Clay data are from Ryland (2017)

Table 3.8. Soil chemical and physical attributes by land use and hillslope position over all depths: Total Carbon (TC) and Nitrogen (TN), Ca, Mg, Fe, Al concentration (μg g^{-1}), pH, Clay percentage, Anion Exchange Capacity (AEC), and Cation Exchange Capacity (CEC) (cmolc kg^{-1}), (n=number of samples, SE= standard error, AGW=watersheds with a history of agricultural use, REF=reference hillslope with no agricultural history).

Factors	AGW: Ridge			AGW: Mid			AGW: Toe			REF: Ridge			REF: Mid			REF: Toe			
	n	Mean	SE	n	Mean	SE	n	Mean	SE	n	Mean	SE	n	Mean	SE	n	Mean	SE	p-value
TC	61	6389	1187	57	5468	1108	61	7215	1262	21	8082	2279	21	7677	2558	21	7767	2583	0.137
TN	58	6225	2167	59	2865	1268	60	1089	554	21	2258	1838	20	537	140	21	614	166	0.827
MIII-Ca	59	207	21.8	58	186	26.0	61	185	22.0	21	88.9	20.8	21	144	47.0	21	164	35.0	0.342
MIII-Mg	61	168	11.0	59	149	13.0	61	129	9.00	20	171	24.6	21	201	29.0	21	176	21.0	0.824
MIII-Fe	61	101	8.00	59	101	6.00	60	128	8.00	21	75.2	10.0	21	74.2	12.0	21	76.6	7.75	<0.001
MIII-Al	61	824	35.0	59	824	42.5	61	775	24.0	21	869	36.0	21	910	52.0	21	776	51.0	<0.001
Clay-pct	61	21	1.9	54	16	1.3	61	17	1.1	21	26	3.7	21	25	4.0	21	20	2.3	0.030
pH_{CaCl2}	59	4.4	0.1	59	4.2	0.1	61	4.2	0.0	21	3.6	0.1	21	3.9	0.1	21	4.2	0.1	0.376
AEC	61	0.9	0.2	56	0.7	0.2	59	0.2	0.0	21	0.3	0.1	21	0.7	0.3	21	0.3	0.1	0.085
CEC	61	5.0	0.4	57	4.9	0.4	60	4.0	0.2	20	5.3	0.6	20	4.8	0.6	20	4.8	0.5	0.529

Table 3.9. General Chemical and physical soil information in two land use with three hillslopes in seven depth. Total Carbon (TC) and Nitrogen (TN), Ca, Mg, Fe, Al concentration (μg g^{-1}), pH, Clay percentage, Anion Exchange Capacity (AEC), and Cation Exchange Capacity (CEC) (cmol kg^{-1}). SE= standard error. AGW= watersheds with a history of agricultural use, REF= reference hillslope with no agricultural history.

Land-use	Hillslope	Depth (cm)	TC(μg g^{-1})		TN(μg g^{-1})		MIII-Ca (μg g^{-1})		MIII-Mg (μg g^{-1})		MIII-Fe (μg g^{-1})		MIII-Al(μg g^{-1})		Clay-pct		pH_{CaCL2}		AEC (Cmolkg^{-1})		CEC (Cmolkg^{-1})	
			Mean	SE	Mean	SE	Mean	SE	Mean	SE	Mean	SE	Mean	SE	Mean	SE	Mean	SE	Mean	SE	Mean	SE
AGW	Ridge	0-7.5	26181	3171	1275	219	588	241	141	25.2	167	29.3	687	120	9.0	1.2	4.6	0.3	0.2	0.1	6.7	1.1
		7.5-15	8154	770	468	22.9	279	83.7	97.4	14.3	159	21.8	717	50.5	10	1.5	4.5	0.2	0.6	0.3	2.8	0.4
		15-35	3833	679	302	35.0	138	27.5	112	21.8	96.4	15.7	877	65.2	27	5.4	4.2	0.1	0.4	0.2	2.6	0.3
		35-60	2701	486	12241	7605	160	41.8	182	26.9	60.0	4.70	866	64.4	35	5.9	4.3	0.1	0.5	0.1	6.0	1.4
		60-100	1364	270	8019	5229	226	51.1	226	33.9	72.5	8.94	1023	35.5	31	4.3	4.2	0.1	1.0	0.5	4.9	0.7
		100-150	731	155	105	24.0	128	27.0	208	30.3	69.5	10.9	854	116	20	2.6	4.2	0.1	1.3	1.0	5.7	1.0
		150-200	470	150	358	265	148	56.6	223	43.0	74.8	12.2	822	93.4	16	3.2	4.4	0.2	0.5	0.2	5.6	0.9
	Mid	0-7.5	33077	6072	1629	292	413	188	148	26.3	148	24.7	864	112	9.0	1.8	4.2	0.2	0.4	0.2	8.4	1.9
		7.5-15	7983	1505	488	76	268	87.9	72.4	8.87	126	13.4	956	165	12	2.1	4.3	0.2	0.5	0.3	3.3	0.4
		15-35	3026	268	270	15.0	103	21.6	79.2	16.9	95.7	12.5	845	77.5	20	3.5	4.1	0.1	0.1	0.0	2.6	0.3
		35-60	2120	314	234	27.0	123	27.2	134	29.6	87.1	9.35	933	125	21	4.9	4.0	0.1	1.1	0.4	4.3	0.9
		60-100	1037	165	1611	1294	136	41.0	152	24.6	76.6	11.1	831	83.8	17	2.6	4.1	0.1	0.5	0.2	5.1	0.8
		100-150	749	239	1354	740	180	58.2	248	30.9	84.3	13.4	717	53.1	18	2.4	4.1	0.1	0.4	0.2	6.9	0.8
		150-200	588	245	69.4	23.0	203	77.4	188	41.8	85.6	14.8	503	69.4	16	3.0	4.3	0.1	1.1	0.3	5.3	0.9
	Toe	0-7.5	8417	4896	1370	132	397	81.3	174	30.8	158	29.4	841	57.6	11	2.2	4.3	0.1	0.1	0.1	6.3	1.2
		7.5-15	22369	4031	1086	552	209	52.9	104	23.9	124	20.7	753	48.5	10	2.4	4.3	0.1	0.2	0.1	2.8	0.4
		15-35	6733	757	473	82.0	98.2	11.4	89.1	21.0	121	15.6	792	65.1	15	3.6	4.1	0.1	0.2	0.1	2.7	0.4
		35-60	4853	1006	282	40.0	67.5	13.6	73.3	10.9	117	11.4	729	63.6	16	2.7	4.0	0.1	0.1	0.0	3.1	0.5
		60-100	2732	800	222	24.0	113	33.4	142	13.7	123	14.7	833	54.0	22	2.8	4.1	0.1	0.3	0.1	4.3	0.6
		100-150	1434	343	257	69.0	191	37.0	172	24.7	113	21.2	809	80.9	23	1.9	4.2	0.1	0.1	0.1	4.2	0.4
		150-200	1838	319	195	36.0	231	52.2	156	22.0	96.6	15.2	642	58.2	20	0.8	4.4	0.1	0.2	0.1	5.5	0.7
REF	Ridge	0-7.5	24015	2695	888	61	75.8	20.0	83.5	6.26	147	15.0	846	58.5	8.8	0.0	3.2	0.1	0.0	0.0	5.2	0.7
		7.5-15	17853	5322	711	141	122	23.3	51.6	6.99	126	13.4	888	81.4	8.8	0.3	3.4	0.1	0.0	0.0	3.1	0.6
		15-35	6051	1071	382	35.0	59.0	3.73	94.7	23.4	62.8	3.06	819	69.3	27	5.0	3.7	0.1	0.5	0.3	4.8	0.3
		35-60	4317	866	320	35.0	49.5	8.21	199	24.8	50.5	0.37	877	48.2	43	5.5	3.8	0.1	0.3	0.2	4.4	1.1
		60-100	2531	110	241	5.00	153	50.1	292	25.7	42.4	2.62	928	15.8	47	3.5	3.8	0.1	0.6	0.2	4.6	0.9
		100-150	1214	157	184	3.00	65.4	8.45	218	35.8	51.7	7.68	954	91.6	29	3.1	3.8	0.1	0.2	0.1	7.1	1.7
		150-200	593	71.0	121	15.0	137	67.9	274	32.1	46.1	4.40	771	25.3	16	0.9	3.8	0.0	0.6	0.2	8.5	0.8
	Mid	0-7.5	30955	5536	1650	339	330	142	206	66.1	170	19.0	1168	93.9	8.6	0.4	3.6	0.1	0.2	0.1	5.6	1.6
		7.5-15	10852	1419	665	72.0	97.9	27.6	122	24.5	114	13.6	773	23.3	5.5	0.5	3.9	0.1	1.7	0.9	3.3	0.1
		15-35	5775	654	391	49.2	171	55.2	128	4.95	52.0	3.79	1120	50.2	21	1.3	3.9	0.1	0.1	0.0	3.9	0.5
		35-60	3973	585	484	92.0	77.4	8.31	262	38.7	61.5	11.6	939	32.3	44	3.0	3.9	0.1	0.2	0.1	5.2	1.2
		60-100	1189	327	190	30.4	44.7	3.72	186	36.1	42.3	1.31	975	82.3	43	9.3	4.0	0.1	0.6	0.2	4.7	1.0
		100-150	651	194	155	27.0	42.4	8.72	165	33.9	43.3	0.45	698	60.8	31	7.5	3.9	0.1	0.7	0.3	6.2	1.3
		150-200	343	100	95.0	24.0	37.2	9.80	145	10.8	36.0	2.99	696	33.1	20	3.9	3.8	0.1	1.2	0.4	4.0	0.5
	Toe	0-7.5	32849	4214	2146	344	401	101	184	53.3	126	13.0	780	79.7	5.9	0.6	4.0	0.1	0.0	0.0	9.2	2.4
		7.5-15	10828	1631	812	127	84.3	2.80	126	7.58	105	2.62	795	109	8.0	0.6	4.2	0.0	0.0	0.0	3.4	0.6
		15-35	5049	479	430	34.0	129	33.8	102	7.20	75.1	4.53	820	84.9	18	0.7	4.1	0.0	0.3	0.2	3.4	0.6
		35-60	2571	72.0	329	6.00	97.9	3.95	163	18.7	61.8	7.67	839	59.9	34	2.9	4.1	0.0	0.3	0.1	3.6	0.4
		60-100	1545	156	209	24.0	112	11.4	219	22.7	42.0	1.20	909	40.7	29	0.0	4.2	0.1	0.5	0.1	4.1	0.2
		100-150	741	75.0	180	10.0	143	30.4	226	53.4	48.4	8.14	623	98.4	23	0.8	4.0	0.0	0.5	0.1	4.8	0.8
		150-200	787	45.0	189	22.0	183	63.4	212	38.3	77.9	13.1	666	97.7	18	2.2	4.0	0.0	0.8	0.2	6.7	0.9

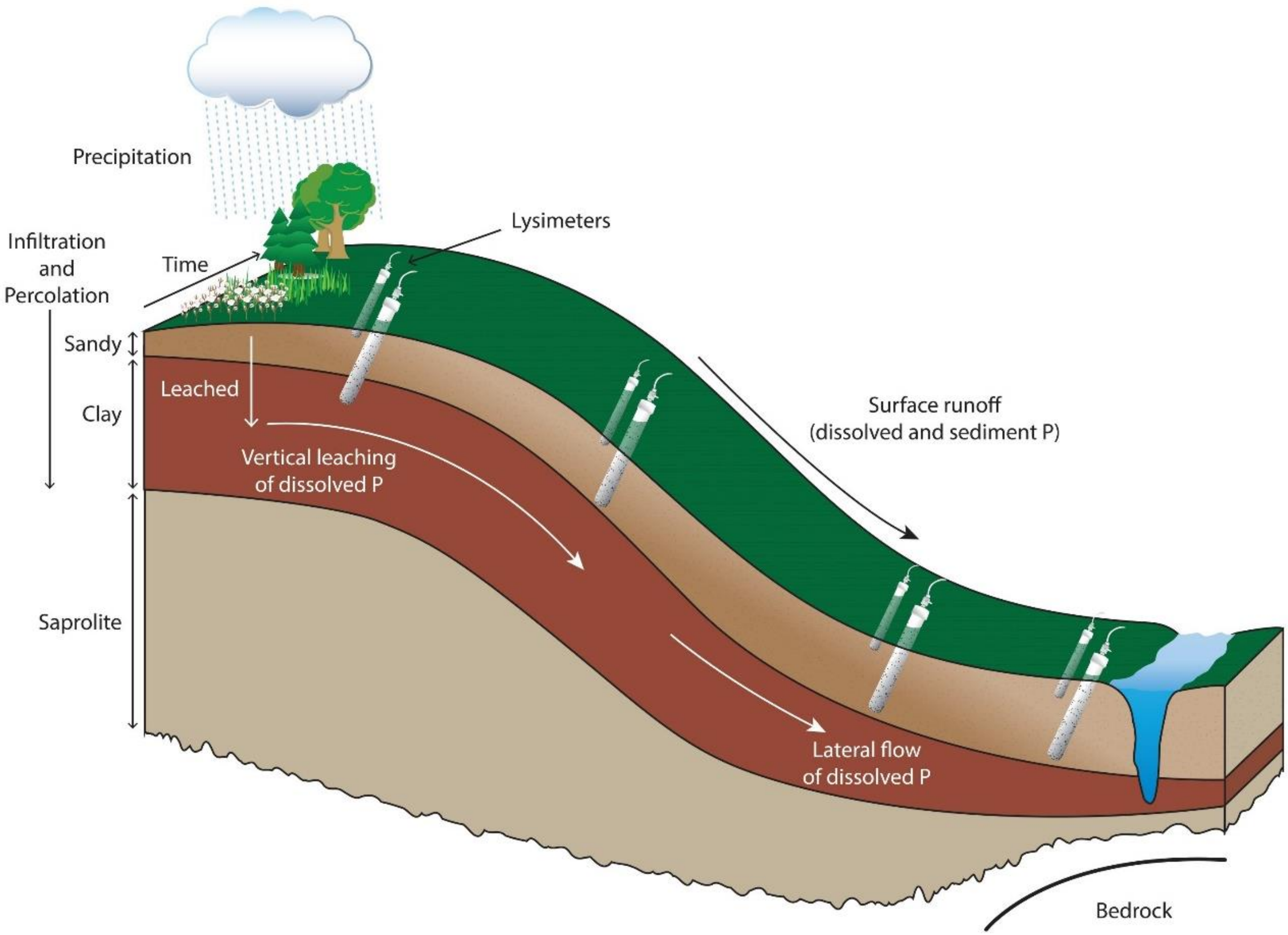

Figure 3.1. Conceptual framework for transport of dissolved and particle phosphorus (P) through an idealized hillslope in the Calhoun CZO (Image courtesy of Wade Newbury).

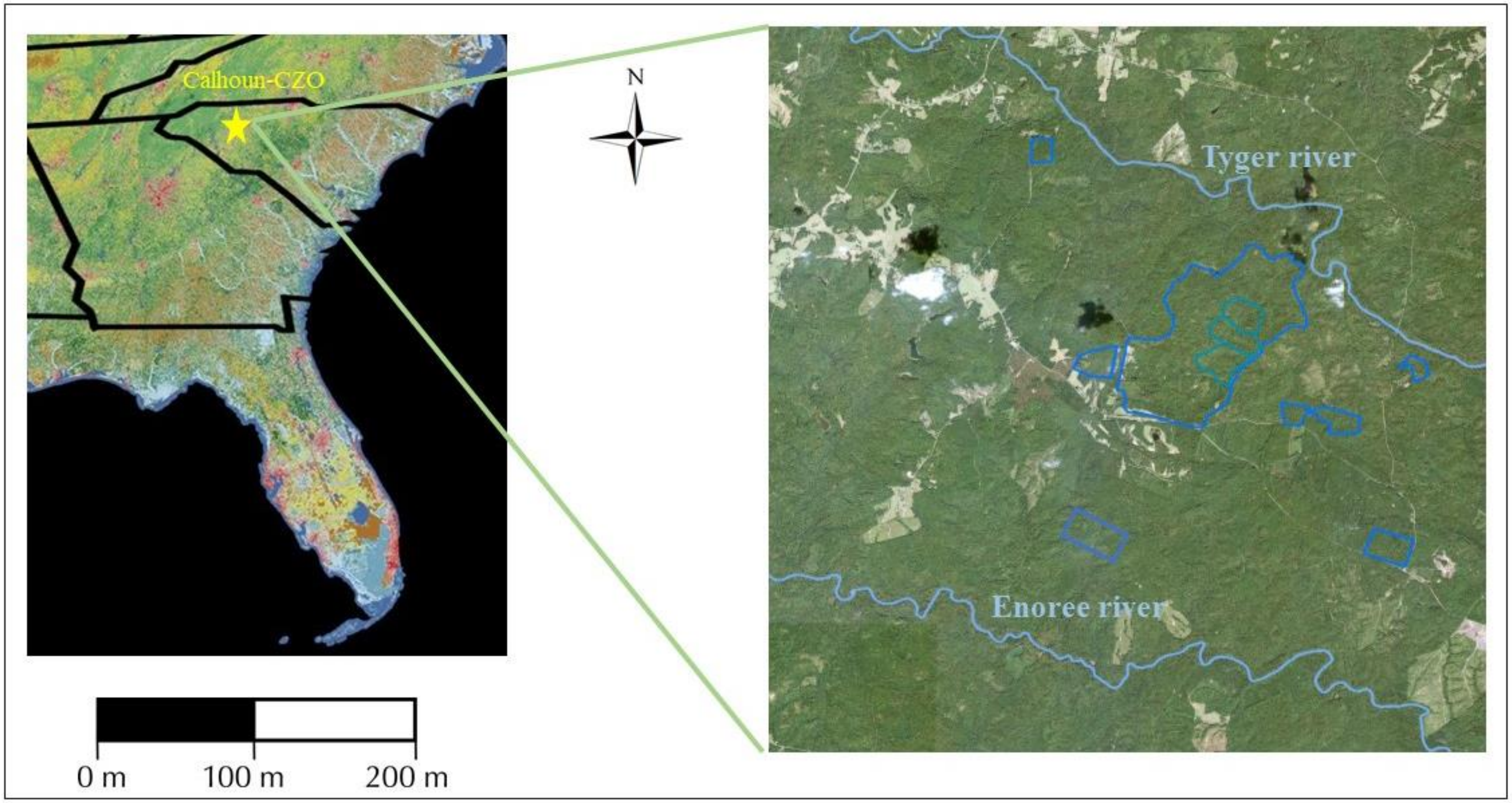

Figure 3.2. Calhoun Critical Zone Observatory, Sumter National Forest, South Carolina USA. The inset depicts watershed and hillslope areas of study in blue polygons.

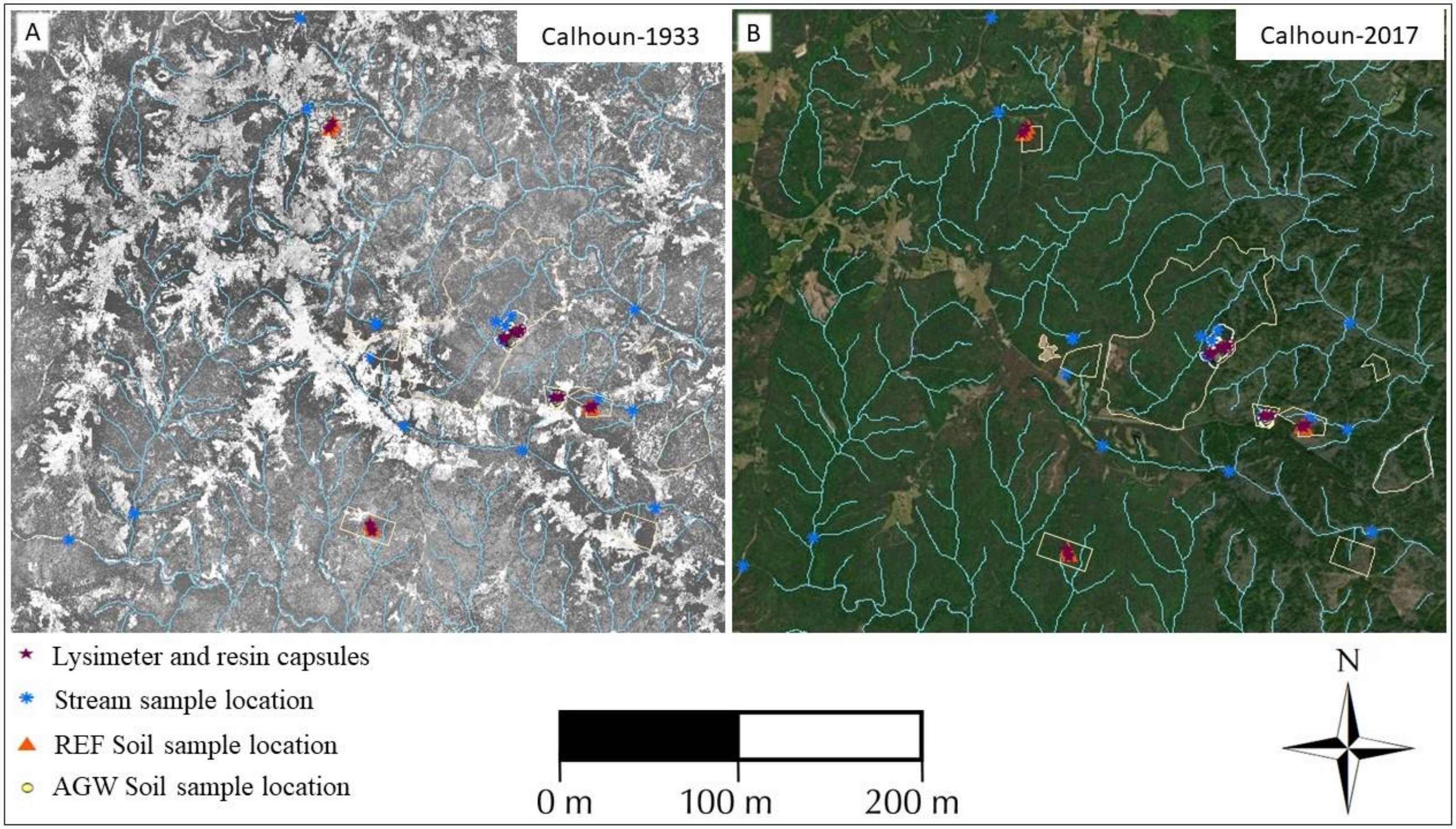

Figure 3.3. Time comparison of the Calhoun Critical Zone Observatory (SC) land cover. US Forest Service 1933 photograph obtained from the Photographic Archive of the Calhoun Experimental Forest (A) and current land cover (B). (*http://criticalzone.org/calhoun/data/dataset/4324/*). AGW= watersheds with a history of agricultural use, REF= reference hillslope with no agricultural history.

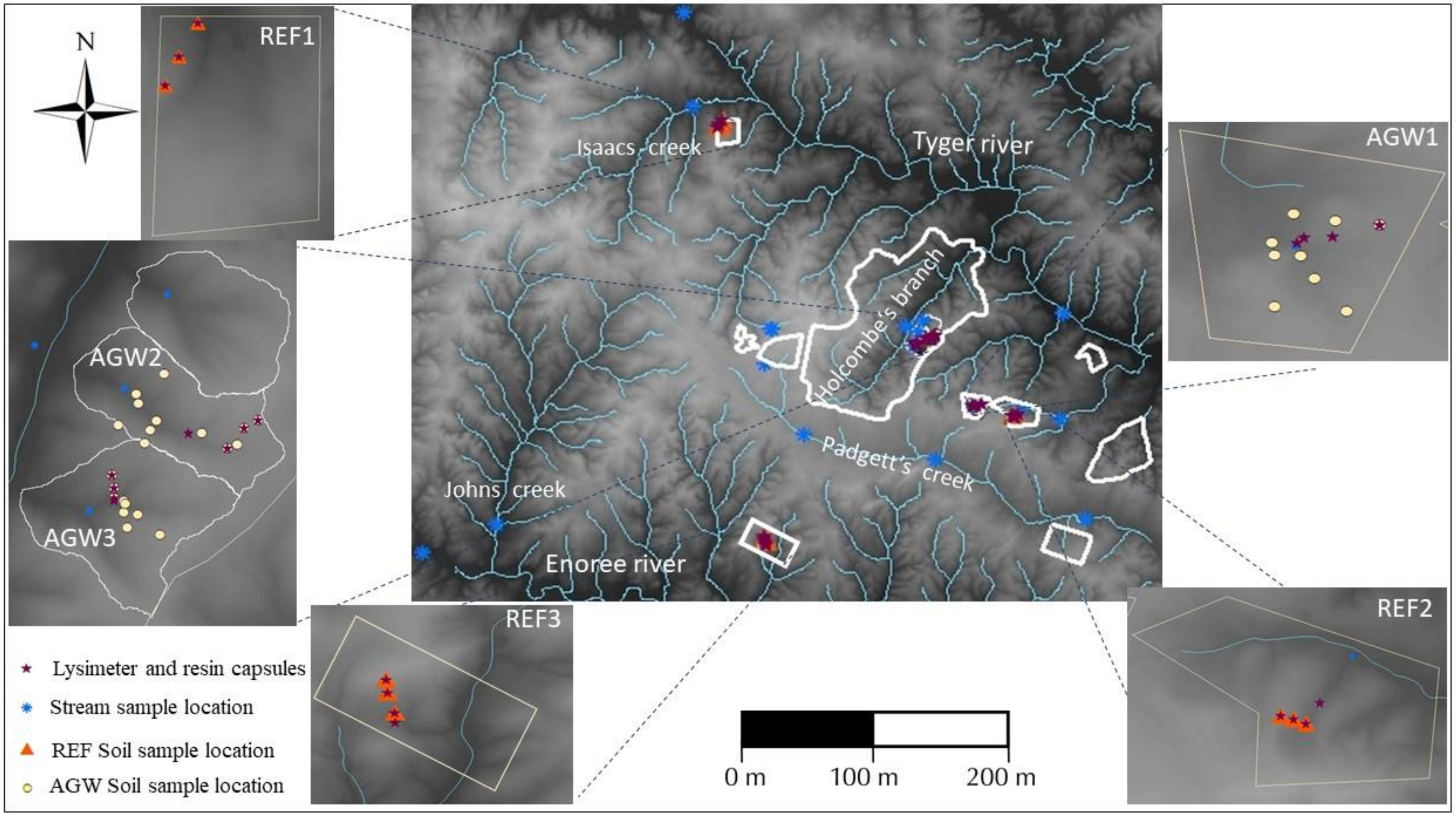

Figure 3.4. Digital elevation map (DEM) with stream sample locations and insets of soil and lysimeter sample locations in watersheds or hillslopes in the Calhoun Critical Zone Observatory. AGW= watersheds with a history of agricultural use, REF= reference hillslope with no agricultural history.

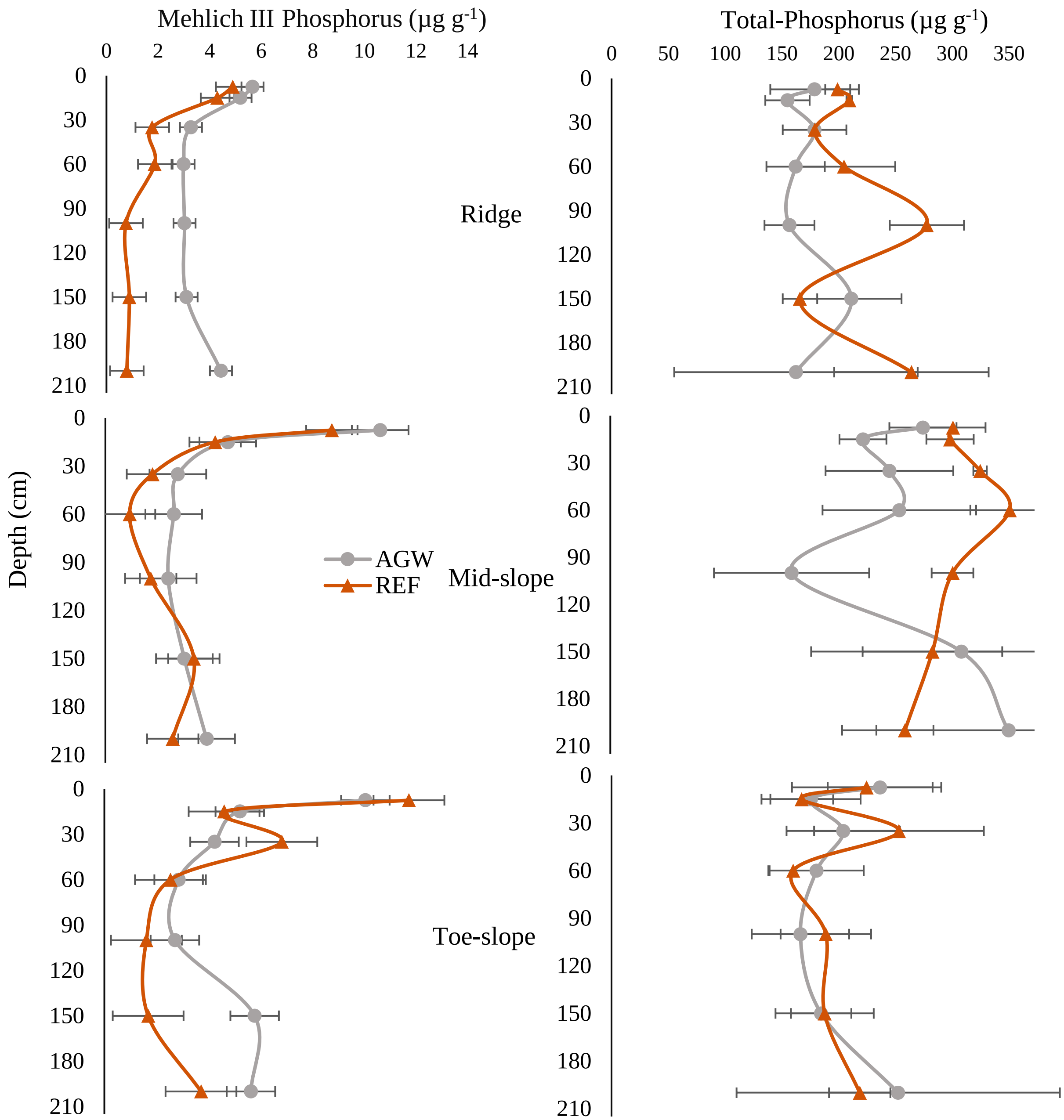

Figure 3.5. Total phosphorus (Total P) and Mehlich-III P in two land uses (AGW and REF) within three hillslope positions (ridge, mid, and toe) in the Calhoun Critical Observatory, SC. Sample size of AGW-Mehlich III: 174; AGW-total P: 57; REF-Mehlich III and total P: 63. AGW= watersheds with a history of agricultural use, REF= reference hillslope with no agricultural history.

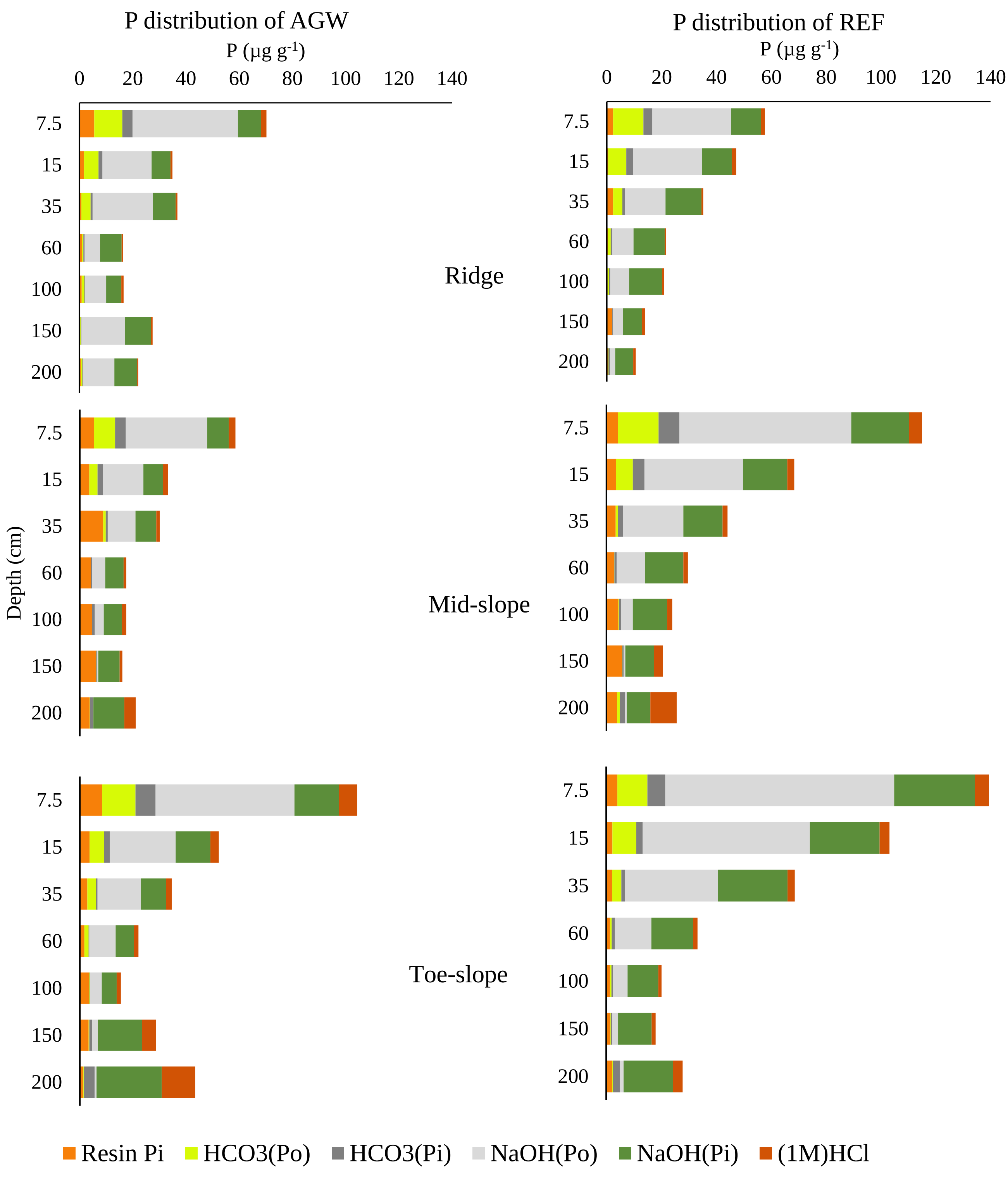

Figure 3.6. Phosphorus fractions across depths and hillslopes in two land uses (AGW and REF) of the Calhoun Critical Observatory, SC. AGW= watersheds with a history of agricultural use, REF= reference hillslope with no agricultural history.

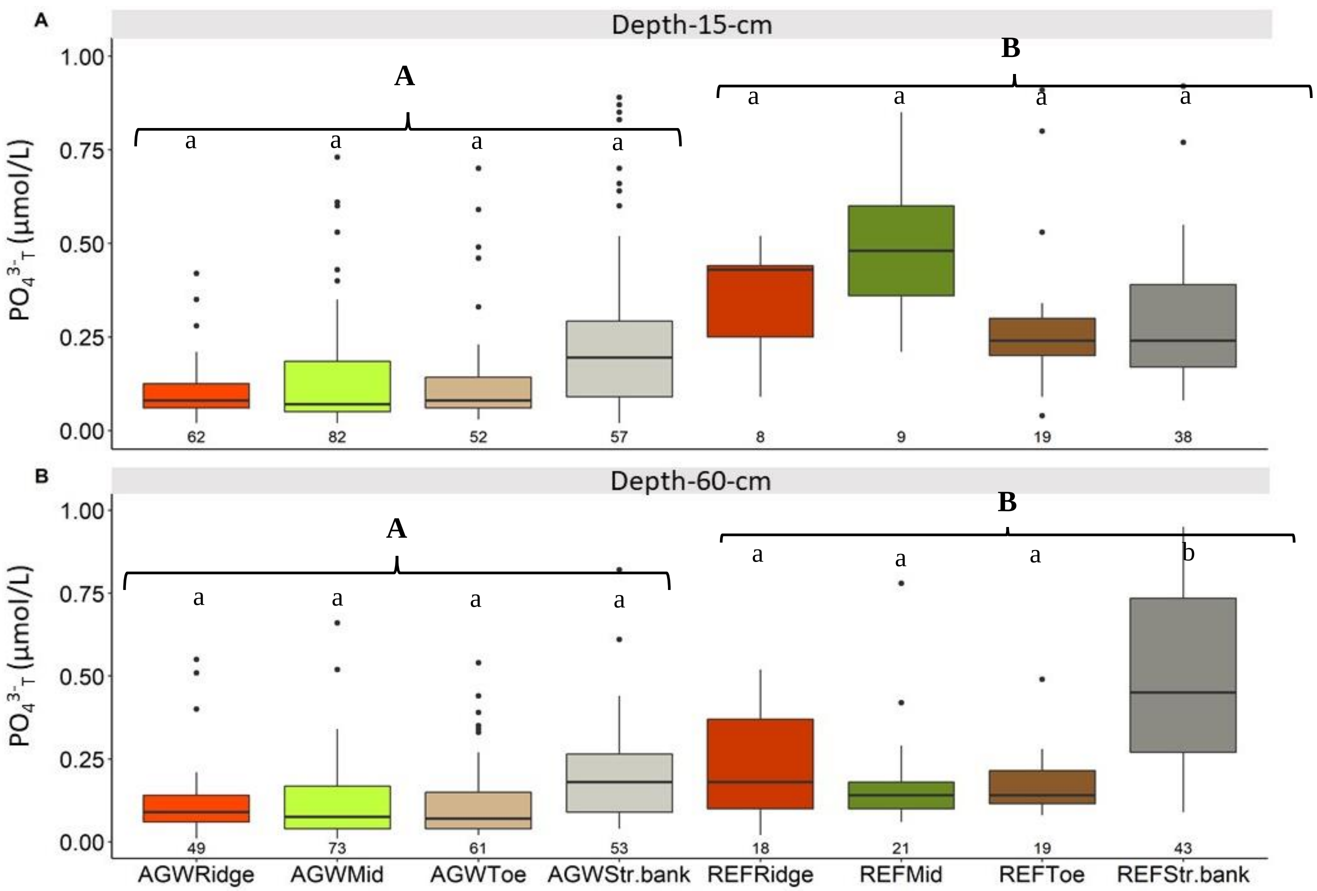

Figure 3.7. Total phosphorus ($PO_4^{3-}{}_T$) collected from ceramic cup lysimeters at 15 and 60 cm soil depths across two land uses (AGW and REF) and four different hillslope positions (ridge, mid, toe, and stream bank (str.bank)). AGW= watersheds with a history of agricultural use, REF=reference hillslope with an agricultural history. Numbers under bar are sample size collected between January 2017 to December 2018. There are three lysimeters at all locations and depths except REF str.bank that has two.

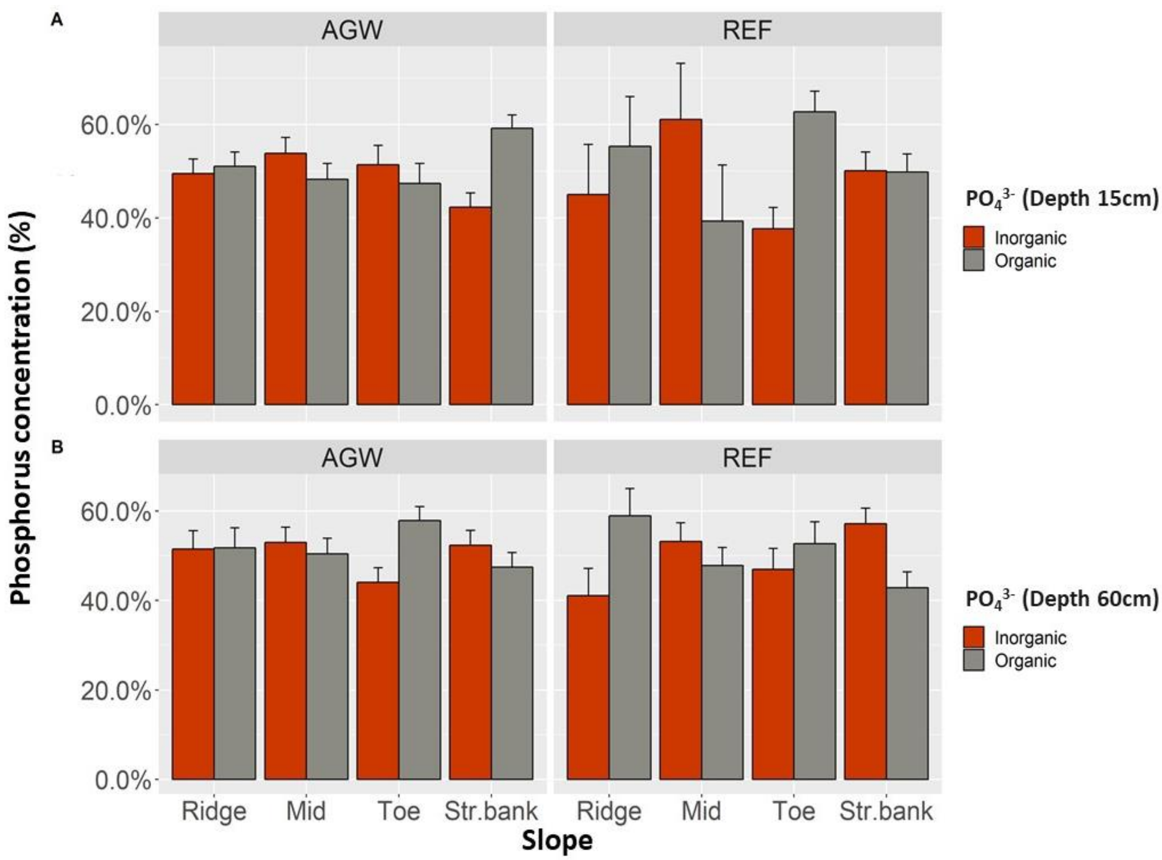

Figure 3.8. The percentage of inorganic and organic phosphate in soil solutions from ceramic cup lysimeter across two land uses (AGW and REF) within four hillslope positions (ridge, mid, toe, and stream bank (str.bank)) at 15 and 60 cm in the Calhoun Critical Zone Observatory. AGW= watersheds with a history of agricultural use, REF= reference hillslope with no agricultural history. Samples collected between January 2017 to December 2018. There are three lysimeters at all locations and depths except REF str.bank that has two.

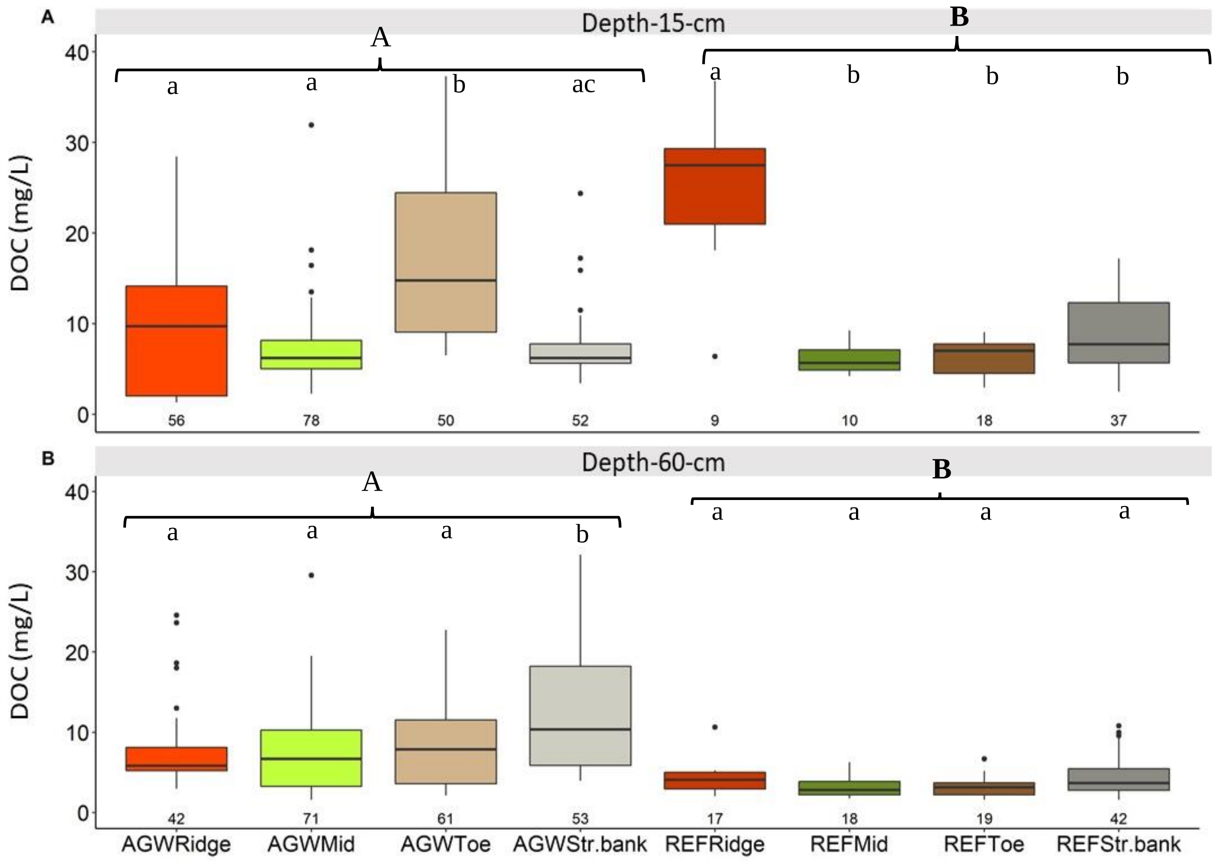

Figure 3.9. Dissolved organic carbon (DOC) from ceramic cup lysimeter across two land uses (AGW and REF) within four hillslope positions (ridge, mid, toe, and stream bank (str. bank)) at 15 (A) and 60 (B) cm. AGW= watersheds with a history of agricultural use, REF= reference hillslope with no agricultural history. Numbers under bar are sample size collected between January2017 to December 2018. There are three lysimeters at all locations and depths except REF str.bank that has two.

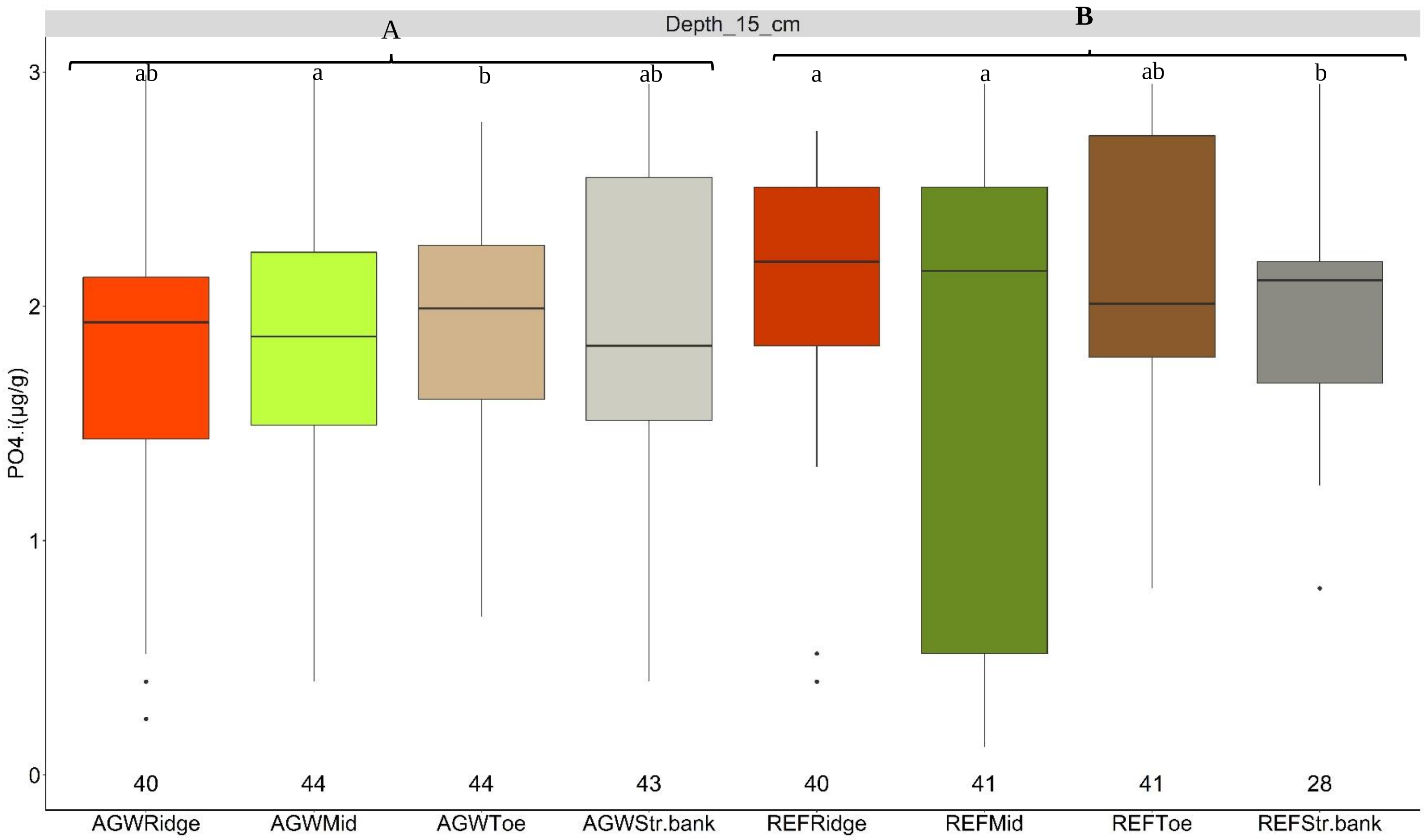

Figure 3.10. Inorganic phosphorus ($PO_4{}^{3-}{}_i$) collected from resin capsules at 15 cm soil depth across two land uses (AGW and REF) and four different hillslope positions. AGW= watersheds with a history of agricultural use, REF= reference hillslope with no agricultural history. Numbers under bar are sample sizes collected between January 2017 to December 2018. There are three lysimeters at all locations and depths except REF str.bank that has two.

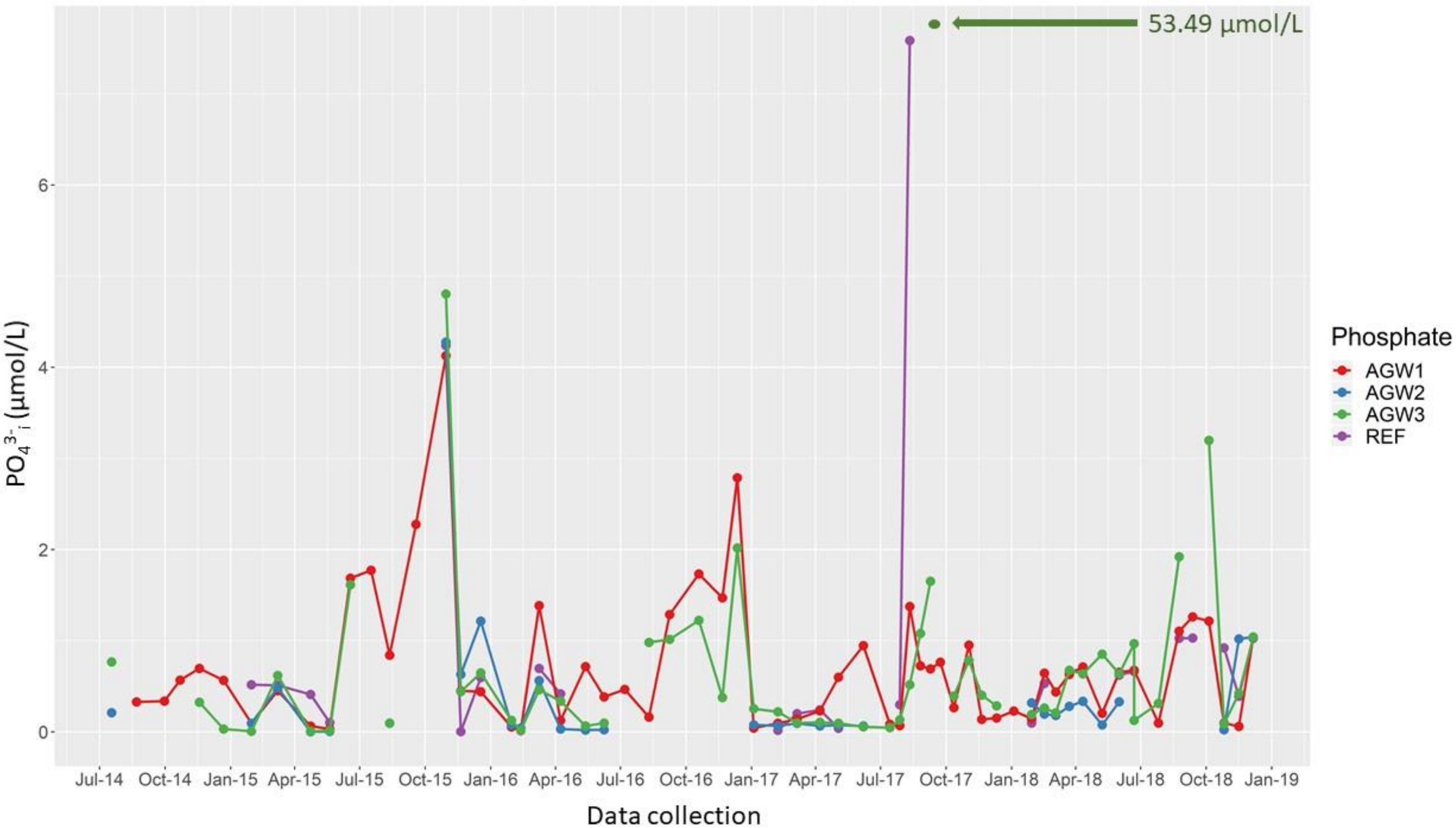

Figure 3.11. Time series of inorganic phosphorus ($PO_4^{3-}{}_i$) concentration (µmol L^{-1}) of first order streams in three AGW and one REF site over five years. AGW= watersheds with a history of agricultural use, REF= reference hillslope with no agricultural history.

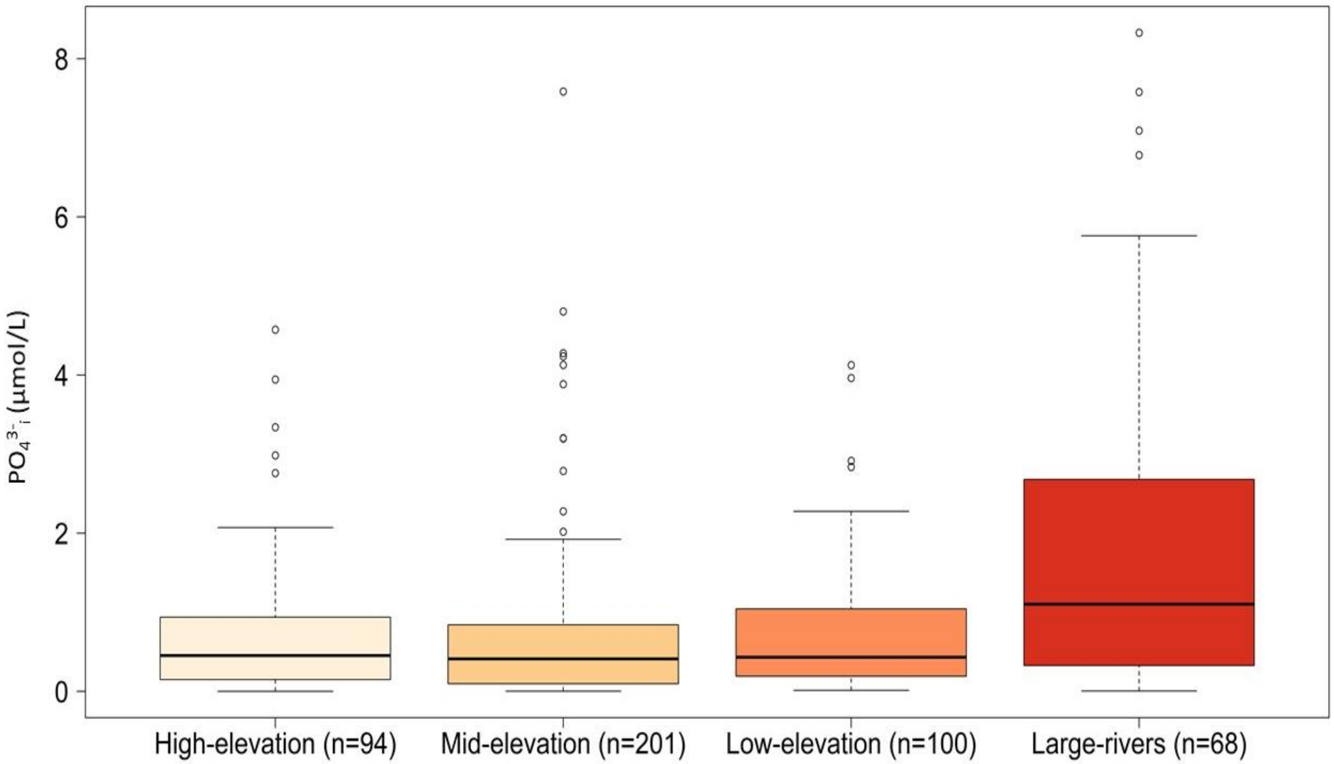

Figure 3.12. Inorganic phosphorus ($PO_4^{3-}{}_i$) concentration in streams of different landscape elevations and sample size collected from July 2014 to July 2018. The concentration of $PO_4^{3-}{}_i$ which was below 10 µmol L^{-1} showed in the figure. (Two points not included here have concentrations of 11.07 and 53.49 µmol L^{-1} from large-river and low-elevation, respectively).

CHAPTER 4

SOIL PHOSPHORUS DYNAMICS OVER SIXTY YEARS OF FOREST DEVELOPMENT IN THE CALHOUN CRITICAL ZONE OBSERVATORY IN THE SOUTHEASTERN US PIEDMONT [1]

[1] M. Foroughi, L. A. Sutter, D.D. Richter, A. Thompson, and D. Markewitz. To be submitted to Soil Science Society of American Journal.

Abstract

Agricultural land use and reforestation have altered soil phosphorus distributions and have demonstrated that slowly cycling P fractions play a significant role in soil P bioavailability on time scales longer than a growing season. The objective of this study was to determine P distribution and bioavailability in a Southeastern Piedmont Ultisol during forest development from 1957 to 2017. This research at the Calhoun Critical Zone Observatory, South Carolina, USA catalogs changes in 0-60 cm mineral soil P fractions through six repeated samplings in eight plots uncut since planting and eight plots that were cut in 2007. We hypothesized that in uncut plots soil organic P (P_o) would increase over time at the expense of HCl extractable Ca-HPO_3 pools. In cut plots we expected a loss of organic P, but an increase in the bioavailable Mehlich III, resin, and HCO_3 extractable pools. Results indicated that between 2005 to 2017 the slowly cycling NaOH P_o did not increase in the uncut plots but increased ~4 μg g^{-1} in the 0-7.5 cm soil layer of cut plots. Whereas, the Mehlich III extractable P in 0-7.5 cm decreased in uncut (from 38.7 to 15.7μg g^{-1}) and cut plots (from 25.2 to 17.7 μg g^{-1}). Changes in soil P fractions relative to tree demand for P suggest HCl extractable pools that were likely elevated from a legacy of P fertilization continue to decline and that organic P pools that are likely increasing due to recycling of P from debris decomposition have the main roles in supplying soil P to plants.

1. Introduction

The distribution of soil P fractions changes with land use and the dynamic soil chemical environment (Grieve, 2001; Alt *et al.*, 2011; Aguiar *et al.*, 2013). Soil P fractions have specifically been evaluated over time under changing land use from agriculture to reforestation as there is interest in the fate of historic P applications (MacDonald *et al.*, 2012). A legacy of P fertilization in the form of higher soil extractable P has been found after reforestation on previous agricultural land over several decades to centuries (Koerner *et al.*, 1997; Falkengren-Grerup *et al.*, 2006; Richter *et al.*, 2006; Dambrine *et al.*, 2007; Goyette *et al.*, 2018).

The retention of this fertilizer P and the relationship between available (labile) and slowly cycling (recalcitrant) P fractions has a significant impact on P availability to plants because the majority of soil P is held in pools unavailable for immediate use by plant roots and soil microbes (Chang and Jackson, 1957). Most of our knowledge about bioavailable P in soils has focused on the correlation between inputs of P fertilizer, measures of bioavailable P, and agricultural production within a given crop year (Bray and Kurtz, 1945; Olsen, 1954; Mehlich, 1978). The associated soil measurement methods and management implications only relate to short-term soil bioavailable P dynamics (Schmidt *et al.*, 1997); however, slowly cycling P fractions can have a significant role in soil P bioavailability in time scales longer than a growing season (Johnson *et al.*, 2003; Richter *et al.*, 2006).

Over multiple growing seasons, total P concentrations generally decrease over time, and in unfertilized cropping systems organic P fractions are the major source for plant-available P (Schoenau *et al.*, 1989; Beck and Sanchez, 1996; Solomon *et al.*, 2002). In fertilized systems, P fertilization enriches the bioavailable P pools, but may also increase slowly cycling P fractions depending on soil attributes such as presence of clays or Fe and Al (oxy)hydroxides (Beck and

Sanchez, 1996; Friesen *et al.*, 1997). For example, labile P concentrations in Inceptisols increased 2.6-6.3 mg kg^{-1} with continued application of 26-42 kg ha^{-1} P fertilizer for 8 years (Zheng *et al.*, 2002). Similarly, on an Oxisol annual application of P fertilizer (50-100 kg ha^{-1}) increased total P 28-64% (108-248 kg ha^{-1}) relative to unfertilized crop lands and in this case all of slowly cycling P fractions (Hedley *et al.*, 1982) were also enriched compared to the reference sites by 40-92 mg kg^{-1} (Lilienfein *et al.*, 2000).

If agriculture is abandoned and fertilization discontinued, reforestation over decades can potentially alter readily available P pools and shift P demand to the slower cycling fractions (Compton and Boone, 2000; Wall and Hytönen, 2005). Most studies on forest development on agricultural land have focused on general physical and chemical soil characteristics (changes in soil acidity, carbon, nitrogen) (Richter *et al.*, 1994; Vesterdal *et al.*, 2002; Ritter *et al.*, 2003) with fewer measuring specific impacts of forest development on different P pools. De Schrijver *et al.* (2012) working on Haplic Luvisols with a sandy loam texture measured P pools with increasing forest age and found labile P_i declined by 10-20% while P_o increased 3-8% of total P. A meta-analysis of afforestation on previous farmland indicated that over multiple years bioavailable and total P on average had significant decreases of 19.6 and 10.5%, respectively (Deng *et al.*, 2017).

One study of forest regrowth on long-term agricultural land in the Southeastern US Piedmont is of specific interest as it is the location of the current study. This research that was initiated on an old cotton (*Gossypium sp.)* field in 1957 as a loblolly pine (*Pinus taeda*) spacing study is unique in not being a chronosequence study like those above but rather having repeated soil measurements on permanent plots. A comparison of soil from 1962 to 1990 indicated that labile P had only minor changes as 5-year-old trees matured over the next 28 years (Richter *et al.*, 2006). In contrast, to the labile fraction the slowly cycling P fractions, especially P_i associated with

Ca, were depleted through the upper 60 cm and were presumed to be buffering concentrations of labile P. Soil resampling has continued in this experiment such that currently we were specifically interested in evaluating the P distribution over the whole 65 years of forest growth on this previous agricultural land situated in the Calhoun Critical Zone Observatory in South Carolina, USA.

The specific objectives of this study are to investigate 1) bioavailable P, 2) slowly cycling P, and 3) organic P fractions in mineral soil over the last 27 years since 1990. In addition, since the original publication (Richter et al., 2006) half of the permanent plots were harvested such that we are interested in evaluating the effect of cutting on the P pools. We hypothesized that 1) in the uncut plots bioavailable P would continue to decline but only gradually due to continued buffering by slowly cycling P fractions, 2) slowly cycling HCl extractable P fractions related to Ca-phosphates will continue to decline but other NaOH or HCl fractions related to Fe and Al amorphous minerals in the Bt horizon will remain unchanged, and 3) P_o fractions, especially labile P_o pools will increase due to a buildup of organic matter (OM) on the surface and in the mineral A horizon. Finally, in relation to harvesting we hypothesized that 4) bioavailable and organic P fractions will increase compared to uncut plots as a result of decomposing residual debris.

2. Methods

2.1 Study Site

The Calhoun Critical Zone Observatory (34° 7' 55.36'' N, 82°18' 36.17'' W), Union County, South Carolina (SC) is home to this Long-Term Soil Experiment (LTSE). This research area was original designated as the Calhoun Experimental Forest within the Sumter National Forest by the US Department of Agriculture (USDA) Forest Service (Metz, 1958). The Calhoun had an average annual precipitation of approximately 1247 mm and mean annual temperature of 17°C, between

1979-2018 (Clinton, SC; https://www.ncdc.noaa.gov/cdo-web/). Cecil and Appling (fine, kaolinitic, thermic Typic Kanhapludults), and Cataula (fine, kaolinitic, thermic Oxyaquic Kanhapludults) soil series are predominant above the granitic bedrock of the region on slopes < 3% (Richter *et al.*, 1994; Markewitz *et al.*, 1998). Previous LTSE work (Richter *et al.*, 2006) reported the general soil characteristics from 0-3 meters, including bulk density (1.4-1.5 g cm^{-3}), pH_{CaCl2} (3.8-4.4), and clay (10-48%).

The Calhoun experimental forest supported a mixed deciduous forest that included southern and northern red oaks, hickories, and other hardwood species before 1800 (Metz, 1958; Richter and Markewitz, 2001). After European settlers migrated to the Southeast, the upland hardwood forests were converted to farmland (Metz, 1958). Much of the forest was cleared and burned to be managed for corn, wheat, tobacco, and mostly cotton after 1800 (Ruffin, 1852; Gray and Thompson, 1933). After the Civil War, intense deforestation along with a substantial use of lime and P fertilizer occurred (Taylor, 1953; Sheridan, 1979). LTSE lands were originally replanted with loblolly pine seedlings (winter 1957) after having been cultivated in cotton for about 150 years (Richter *et al.*, 1994; Markewitz *et al.*, 1998). The 60-yr-old plots are still dominated by pine in the overstory with mixed hardwoods in the understory.

2.2 Sample collection

LTSE soils collected in 1962, 1968, 1978, 1982, 1990, 1997, 2005, 2010, and 2017 have been archived at the Nicholas School of the Environment and Earth Sciences, Duke University, Durham, NC. Soil were collected as twenty 2-cm diameter punch-tube samples per plot (Richter *et al.*, 2006) divided into four different depths (0-7.5, 7.5-15, 15-35, and 35-60 cm) at 16 permanent plots (Fig. 4.1). Eight of these plots were clear-cut in 2007 and replanted prior to the 2009 growing season. Approximately every five years between 1962-2017, soil and forest floor samples were collected from the uncut plots. Samples of the cut plots were collected from 2005 to 2017. The 16 permanent plots include 4 blocks and 4 spacings (6x6, 8x8, 10x10, and 12x12). The spacings 6x6 and 12x12 ft were cut (i.e., cut plots) and the others are uncut plots (Fig. 4.1).

2.3 Sample analyses

Collected soils were air-dried and sieved through a 2 mm screen. A moisture correction factor was determined after oven drying a 1-2 g subsample at 105˚C to a constant weight. The labile P was determined in Mehlich-III extractions (Mehlich, 1978) via colorimetry (Murphy and Riley, 1962). To be consistent with previous P fractions measurement (Richter *et al.*, 2006), we corrected the fractions data based on the linear regression between the 9 randomly selected soils samples from 1990, 1997, and 2005 that were originally measured in 2005 (Richter *et al.*, 2006) and re-measured by us in 2017 (Supplementary Fig. 4.1).

Fractions were determined in soils sampled in 2005, 2010, and 2017 from all 16 permanent plots. In addition, six randomly selected soil samples from 1990 were analyzed to compare with previous research results for analytical consistency. The readily soluble and exchangeable P_i was extracted by anion exchange resin strips. To determine other soil P pools, we followed the sequential fractionation method (Hedley *et al.*, 1982) as modified by Tiessen and Moir (1993). In summary, this method separated extractable P_i and P_o with 0.5M $NaHCO_3$ (pH=8.5), 1 M NaOH, and 1 M HCl that showed P associated with surface charge, Fe/Al oxides, and Ca, respectively. Then, occluded P in crystalline Fe phases (Lilienfein *et al.*, 2000; Crews and Brookes, 2014) was estimated by extracted with hot (80^{o}C) concentrated HCl. In the final step, the residual P and an independent total P of samples were extracted with a nitric acid and hydrogen peroxide digestion (Kimbrough and Wakakuwa, 1989; Niederberger *et al.*, 2015). All P fractionation concentrations were measured via spectrophotometry, as above, using molybdate blue chemistry (Murphy and Riley, 1962) after neutralization to a phenol thalene endpoint.

To be consistent with previous P fractions measurement (Richter *et al.*, 2006), we corrected the fractions data based on the linear regression between the 6 randomly selected soils samples from 1990 that were originally measured in 2005 (Richter *et al.*, 2006) and re-measured by us in 2017 (Supplementary Fig. 4.2).

To evaluate the Short Range Ordered (SRO) Fe and Al, soils of uncut plots from 1997, 2005, and 2017 were extracted with acid ammonium oxalate (AAO) solution (Carter, 1993; Loeppert and Inskeep, 1996) and then extracted Fe, Al , and P in the AAO solution were measured by inductively coupled plasma-mass spectrometry (ICP-MS; Perkin Elmer ICPMS model Elan DRCII, Ontario, Canada).

2.4 Data Analyses

Earlier work at this location (Richter *et al.*, 2006), reported bulk density for 0-15 and 35-60 cm depths of 1.52 and 1.44 g cm^{-3}, respectively. We used these bulk densities to estimate the change in P content for the current study.

We employed a repeated measure, linear mixed-effects model on the longitudinal data to evaluate which soil P fractions changed with time and spacing. All statistical analyses were conducted in R using the “lme” function for mixed-effects models in the “nlme” package (Pinheiro *et al.*, 2013). Across these analyses, the year and spacings were set as fixed effects and the block was treated as a random effect. Furthermore, the covariance structure used for the repeated measure design was found to be corAR1 based on the Akaike information criteria (AIC) and the restricted maximum likelihood (REML) method used to fit all the linear mixed-effect models. Post-hoc tests for significant fixed effects ($P < 0.05$) in the ANOVA followed by Tukey's HSD comparison. Each

P fraction was statistically analyzed for each soil layer separately. Also, cut and uncut plots analyzed separately as well.

3. Results

3.1 P fractions in uncut plots

The Mehlich III extractable P (Mehlich III-P) decreased in the 0-7.5 and 7.5-15 cm depth incremented from 1962 to 2017 (Fig. 4.2). Average Mehlich III-P significantly declined (p <0.0001) from 38.7 to 15.7 µg g^{-1} in the surface layer (0-7.5 cm). Although the Mehlich III-P pool increased at 7.5-15 cm until 1997, it showed a decreasing trend afterwards. The change at 7.5-15 cm between 1962 and 2017 indicated a significant decrease of 4.5 µg g^{-1} (p-value = 2.18 e^{-9}). In contrast, at 35-60 cm depth between 1962 and 2010 the Mehlich III-P pool significantly increased (p <0.0001) from 0.2 to 1.3 µg g^{-1}.

The labile P (resin P_i, HCO_3 P_i, and HCO_3 P_o) fractions slightly decreased in the 7.5 cm depth increment over the years; however, HCO_3 P did not change statistically. In contrast, the same P pools tended to increase in the deeper soil layers (Fig. 4.3 and Table 4.2). For example, extracted resin P_i significantly declined at 0-7.5 and 7.5-15 cm (p <0.01) from 12.6 and 10.7 µg g^{-1} to 5.31 and 7.04, respectively. Contrary to resin P_i, the HCO_3 P_i significantly increased (p <0.003) in most subsoil layers (15-60 cm). In general, across the labile P pools, the extracted NaOH P_i was significantly greater in 1962 (p <0.001) than 2017 at 0-7.5 and 35-60 cm layers. In addition, the NaOH P_o concentration in 2017 was significantly (p <0.0001) less than 1962 through 15 cm soil depth (Fig. 4.3, Tables 4.1 and 4.2).

The 1M HCl P_i significantly decreased (p =<0.01) in 0-15 cm over time (Table 4.2). In contrast, HCl P_i (1M HCl P_i + Concentrated HCl P_i) increased significantly (p =0.01) from 16.8 to

25.6 μg g^{-1} in 15-35 cm through 2017 (Fig. 4.3). Generally, residual and total P did not follow a consistent pattern in the four different soil layers over 55 years (Table 4.2). Only in the 7.5-15 cm depth increment was the total P concentration decline significant ($p < 0.05$; Table 4.2).

3.2 Labile to slowly cycling P ratios in uncut plots

The ratio of readily and slowly cycling organic P (HCO_3P_o/NaOH P_o) indicated a significant increase (p =<0.01) from 1962 to 2017 in most soil layers (Fig. 4.4A). The HCO_3 P_o/NaOH P_o ration increased from 0.31 in 1962 to 0.51 in 2017. The inorganic pool ratio (resin+HCO_3P_i/NaOH P_i) also slightly increased for all different soil depths and was significant in the deepest layer (p =<0.01; Fig. 4.4B).

One component of the slowly cycling P fraction is associated with Fe and Al. Oxalate extractable Fe, Al, and P (AAO-Fe, -Al, and -P) were measured in three years (1997, 2005, and 2017; Fig. 4.5). The average AAO-Fe and -Al slowly increased during forest regeneration throughout 60 cm; however, the changes of AAO-Fe and -Al over the years of investigation were significant ($p < 0.01$ and < 0.05, respectively) only at 7.5-15 cm. AAO-Fe and -Al showed a negative relation and strong correlation with Mehlich III-P for all sample through 60 cm (r= -0.35 and -0.49 between P_i with Fe and Al, respectively); however, NaOH P_i and Concentrated HCl P_i had a positive relationship with AAO-Fe and -Al (Supplementary Fig. 4.3).

3.3 P fractions in cut plots

Mehlich III-P for the permanent plots harvested in 2007 (i.e., cut plots, n=8) decreased significantly ($p < 0.01$) from 2005 to 2017 in the 0-7.5 cm (25.2 to 17.7 μg g^{-1}) and 7.5-15 cm (33.1 to 22.8 μg g^{-1}) soil layers (Fig. 4.6). In contrast, the deeper layers between 2005 and 2017 showed no difference, although the Mehlich III-P concentration in 35-60 cm declined significantly ($p<0.05$) from 1.127 μg g^{-1} in 2010 to 0.727 μg g^{-1} in 2017.

Labile P (resin P_i, HCO_3 P_i and P_o) showed no significant changes from 2005 to 2017 (Fig. 4.7 and Supplementary Table 4.2). The concentration of slowly cycling P_o (NaOH P_o) significantly increased by 3.8 μg g^{-1} ($p <0.001$) in 0-7.5 cm over 12 years (Table 4.4 and Fig 4.7). In the subsurface 7.5-15 cm layer, most P fractions (highly and moderately available pools) remained constant except for concentrated HCl that increased around 3 μg g^{-1} (Fig. 4.7 and Table 4.3). Residual and total P decreased after harvesting, replanting, and growth of trees over the 12 years studied (Table 4.3 and 4.4). Furthermore, residual P significantly declined ($p<0.01$) from 2005 (66.9 μg g^{-1}) to 2017 (33.3 μg g^{-1}) in the 7.5-15 cm layer (Table 4.4 and Supplementary Table 4.2).

3.4 Labile to slowly cycling P ratios in cut plots

The ratio of readily cycling P_o relative to slowly cycling of P_o (HCO_3P_o/NaOH P_o) in cut plots significantly decreased ($p <0.01$) from 0.58 to 0.45 at the surface layer (0-7.5 cm) between 2005-2017 (Fig. 4.8A). In addition, readily available P_i relative to slowly cycling P_i also declined significantly ($p <0.05$) in the upper 15 cm soil depth. The ratio of (resin P_i+HCO_3 P_i)/NaOH P_i significantly decreased ($p <0.01$) in 0.22 at 0-7.5 cm depth over 12 years (Fig. 4.8B).

4. Discussion

After 60 years of pine trees regenerating (1957-2017) on former cropland, soil P redistribution occurred between labile, slowly cycling, and occluded soil P fractions. Overall, the Mehlich III, labile, and slowly cycling P fractions decreased with forest age, although patterns were specific with P fraction and soil layer. Below we address our hypotheses relating to bioavailable P, slowly cycling P, and organic P fractions in the cut and uncut plots.

4.1 Bioavailable P in uncut plots

The Mehlich III-P content decreased 23 µg g^{-1} (26 kg ha^{-1}) throughout the 0-60 cm soil profile as the forest aged from 1962 to 2017 (Fig. 4.2). During early forest regeneration (1962-1990), the accumulation of P in biomass of 82.5 kg ha^{-1} was six times greater than the reduction of Mehlich III-P in soils (13 kg ha^{-1}), suggesting that the tree demand extracts P from more stable pools (Richter *et al.*, 2006). The additional 13 kg ha^{-1} decline in Mehlich III-P from 1990 to 2017 was also likely below tree demand. A linear extrapolation of annual tree (1.4 kg-P ha^{-1} yr^{-1} tree biomass) and forest floor (1.6 kg-P ha^{-1} yr^{-1}) accumulations estimated through 1990 results in forest floor (43.2 kg ha^{-1}) and tree biomass (37.8 kg ha^{-1}) P contents above Mehlich III declines. These linear extrapolations are certainly high given known patterns of pine plantation growth, particularly through age 60 (Switzer *et al.*, 1966), but even rates half as high would still exceed MIII declines by three-fold suggesting that the biological P demand had to be met from other sources such as the more stable pools.

The labile P pool (resin P_i, HCO_3 P_i and P_o), which includes available P beyond Mehlich remained fairly constant from 1962-2017 and 1990-2017 in the 0-7.5 cm soil layer (Supplementary Table 4.1 and Fig. 4.3) and actually increased over the 0-60 cm layer (Table 4.1). As such, this fraction does not appear to have contributed to plant demand. The slowly cycling P fractions (predominantly HCl extractable Ca-P) were shown to be enriched by cultivation with fertilization at this site and soil P enrichment after agriculture is a common response as noted above (Koerner *et al.*, 1997; Lilienfein *et al.*, 2000; Zheng *et al.*, 2002; Falkengren-Grerup *et al.*, 2006; Dambrine *et al.*, 2007; Goyette *et al.*, 2018). For example, in one study on a similar soil (Typic Hapludult) undergoing 12 years of fertilization, all Hedley P fractions were enriched 3-36 times relative to unfertilized pastureland and the largest increases were in Ca-P (Sharpley *et al.*, 2004). In the current soil, increase in these Ca-P pools may have resupplied the available P fractions during several decades of forest growth (Richter *et al.*, 2006). The slowly cycling and occluded P fractions in the present study declined about 81 kg ha^{-1} through the 60 cm soil profile over 55 years of forest development (Table 4.1), which is still less than the estimated accumulated biomass P (120 to 165 kg ha^{-1} yr^{-1}). This Ca-P supports an interpretation that the slowly cycling P fractions have supplied part of the required labile P accumulated in tree biomass and forest floor.

On the other hand, the labile pools (resin P_i, HCO_3 P_i and P_o) may have been renewed by organic sources. Boreal and temperate coniferous forest floor deposition and decomposition has been demonstrated to provide dissolved P_o to fine roots or as leachate to the mineral soil (Berg, 2018). In 70-year-old temperate hardwood forests as much as 60% of the annual P uptake (6 of 10 kg ha^{-1} yr^{-1}) was ascribed to forest floor P recycling (Yanai, 1992). Similarly, HCO_3 extracted-P_o in an oak forest in Belgium increased from 3 to more than 8% (90 to 120 kg ha^{-1}) of total P (~3000 kg ha^{-1})in the surficial soil layer over 36 years (De Schrijver *et al.*, 2012). The available P_o fractions in tropical forests also increase with increasing forest age: available and slowly cycling P_o increased to 50% of total P in the soil in one study (Frizano *et al.*, 2002). In the current location, in the uncut plots soil organic carbon (SOC) content also increased from 1962 to 2005 in the topsoil layers (0-35 cm) due to litterfall and dead biomass decomposition (Richter *et al.*, 1999; Mobley *et al.*, 2019), which may also increase P_o and buffer Mehlich III or other bioavailable P pools. In short, it does appear the bioavailable P pools have been buffered from declines during this period of continued forest growth, although both Ca-P and organic P may play a role.

4.2 Slowly cycling and occluded P in uncut plots

The total slowly cycling P fractions (both P_i and P_o extracted with NaOH) decreased throughout the 60 cm soil profile from 1962 to 2017 as did the NaOH-P_i from 1990 to 2017. In

2017, the content of NaOH-extracted P was approximately 93 kg ha^{-1} less than 1962 (Table 4.1, Supplementary table 4.1, and Fig. 4.3). Our hypothesis was that the slowly cycling P would continue to buffer the available P fractions providing P to meet requirements for biological growth. The NaOH-P_o did not show any significant changes between 1990 to 2017 while NaOH-P_i was depleted by 10.7 kg ha^{-1} in the surficial soil layer (Supplementary table 4.1 and Fig. 4.3). This depletion could account for 25% of the estimated amount of P uptake during the 27 yr period of forest growth (39 kg ha^{-1} P).

The lack of a decline in NaOH-P_o from 1990 to 2017 may also relate to an increasing role of organic matter cycling as suggested for bioavailable P above. In fact, the increase in P_o percentage over time may reflect an important stage in forest development for maintaining available P over the long-term, (Wells and Jorgensen, 1975; Walker and Syers, 1976; Roberts *et al.*, 2015). In a steady-state forest, soil mineral P proportion is estimated to be less than 20% of total P uptake with most forest P demand being supplied by OM recycling, whether through surface litter or subsurface root litter (Wells and Jorgensen, 1975; Attiwill and Adams, 1993; Roberts *et al.*, 2015). Our estimation showed the total P_o pools (HCO_3+NaOH) as a percentage of total soil P increased from ~25% to ~30% over the 1962 to 2017 period. Overall, the depletion of slowly cycling P between 1990 to 2017 was lower than that during 1962 to 1990 suggested here to reflect SOC accumulation and increased P_o recycling.

The concentrated HCl pool reflects another slowly cycling P fraction. HCl extracted-P_i (1M HCl+ Concentrated HCl) in 15-35 cm between 1962-2017 actually increased by 9.5 µg g^{-1} (29 kg ha^{-1}) while the other three soil layers did not show any significant changes (Fig. 4.3). Previous research in pastureland also found an 11µg g^{-1} increase in concentrated HCl-P_i in the 24-46 cm soil layer between 1876 to 2009 (Crews and Brookes, 2014). P extracted with concentrated

HCl is associated with Fe and Al (Lilienfein *et al.*, 2000; Crews and Brookes, 2014). As such, changes in soil clay content, especially Fe and Al (oxy)hydroxides contents might be associated with changing P contents in this fraction. In the case of Fe and Al (oxy)hydroxides, a changing soil environment after agricultural abandonment might also influence the crystallinity of these minerals and the surface adsorption potential for P (McLaughlin *et al.*, 1981). Following this reasoning, we measured SRO Fe and Al with AAO and found a gradual increase from 1990 to 2017 in all soil layers (Fig. 4.5). SRO Fe and Al had a negative relationship with Mehlich III-P (r <=-0.35) in the 0-60 cm (Supplementary Fig. 4.3A). Besides the correlation between SRO Fe and Al with Mehlich III-P, the concentrated HCl-P_i pool and NaOH P_i showed a strong correlation with AAO-Fe and -Al (r= >0.69 and => 0.45, respectively) in 2005 and 2017 (Supplementary Fig. 4.3B and C). Our measurement of Fe and Al with concentrated HCl extracts for P indicated that there are high correlations between Fe and Al with P (r=0.91 and 0.93, respectively; Supplementary Fig. 4.4); correlation between the P and Ca in the same extraction were quite low (r=0.14). Changes in P fractions under an unfertilized perennial hay field showed a strong association between P and Fe, in which this correlation tended to increase with soil age (Selmants and Hart, 2010). In the current case, HCl-P_i content increase in the 15-35 cm layer may reflect some accumulation of clay in this upper portion of the Bt after agricultural abandonment or it may relate to changes in the crystallinity of the Fe and Al (oxy)hydroxides as the chemical environment changes with reforestation.

4.3 P_o and P_i in uncut plots

According to the depletion of slowly cycling P_o (NaOH extracted-P_o) relative to no change or increase of HCO_3 extracted-P_o in the 0-60 cm soil layer from 1962 to 2017, the ratio of readily cycling P_o/slowly cycling P_o increased after 60 years of forest development (Fig. 4.4A). In contrast, the more available P_i tends to significantly increase in only 35-60 cm depth over time. We hypothesized that increasing the content of SOC in surficial soil and transforming slowly cycling P_o to highly available P_o fractions (HCO_3-P_o) would cause the available P_o to increase in upper 60 cm over time. Enhancing OM in the surficial soil layer caused a decrease in soil pH over long time. Similarly, the SRO Fe and Al (AAO Fe and Al) content increased with forest development (Fig. 4.5), but a negative correlation was shown between Fe and Al with Mehlich III-P ($r \le -0.35$) (Supplementary Fig. 4.3). Although, the SRO Fe and Al have higher surface area to react with P in low pH, accumulated organic matter in the surficial soil layer may saturate the Fe and Al surface inhibiting P adsorption and facilitating P leaching to deeper soil layers (Guppy *et al.*, 2005). A similar process of organic acid displacement of NaOH P_i from SRO Fe and Al oxide in the first soil layer (0-7.5 cm) leading to increasing P_i associated with Fe and Al in 7.5-35 cm layer during 1962-1990 observation was proposed (Richter *et al.*, 2006).

4.4 Bioavailable P fractions in cut plots

The Mehlich III and labile P fractions slowly declined between 2005 to 2017 in the soils of the cut plot (Fig. 4.6). The rates of decline were similar to those in the uncut plots (Fig. 4.2). We hypothesized that the available P would increase in the soil after harvesting the 50-year-old loblolly pine stand due to release of P from the harvest debris and leaching into the mineral soil, which was not what was observed. It is possible that part of the mineralized P could be lost to the surface water in runoff prior to replanting. Previous research in the northeast of the US indicated that the loss of dissolved P in streamflow is small (0.03 kg ha^{-1} yr^{-1}) in clear-cut forest watersheds even though this amount of P loss is three times more than undisturbed watersheds in the same area (Yanai, 1998). Retaining harvest debris on site is expected to reduce loss of nutrients and increase nutrition availability (Jurgensen *et al.*, 1992; Blumfield and Xu, 2003). Although increases in bioavailable P were not measured, a short-term increase in the ratio of labile to slowly cycling inorganic be pools (i.e., Resin+HCO_3-P_i/NaOH-P_i) after harvesting may reflect rapid OM decomposition that increased available P pools, which decreased again after forest regrowth was initiated (Fig. 4.8B). Again, in the northeastern US the rate of P leaching after harvest increased from forest floor to the mineral soil to 1 kg ha^{-1} yr^{-1} (Yanai, 1998). This input is still below the annual uptake of 2.9 kg ha^{-1} P estimated for young pine at this site previously (Richter *et al.*, 2006). The difference between Mehlich III decline and tree demand could be supplied with additional mineral soil organic matter mineralization (as opposed to surface organic matter) but overall, the observed changes in bioavailable P after harvesting did not decline as hypothesized.

4.5 Slowly cycling and occluded P fractions in cut plots

In addition to increases in bioavailable P after cutting we expected to see increases in slowly cycling P_o fractions. The content of slowly cycling P_o in surficial soil (0-7.5 cm) in the cut plots from 2005 to 2017 increased 4.3 kg ha^{-1} (Table 4.3). The same pool did not change in the uncut plots over the same time and soil layer. This slowly cycling P_o pool in the 0-60 cm layer of the uncut plots did decline significantly between 1957-1990 by 22.8 kg ha^{-1} (Richter *et al.*, 2006). Our expectation, as above, was that decomposition of harvest residue would enrich soil P_o fractions. In southeastern loblolly pine ~80% of organic matter and P may be lost from litterfall in 10 years (Binkley, 2002). After clear-cut harvest, decomposition may be accelerated, for example, in a mixed boreal forest in Finland 49% of stored P in harvest residue was released in three years (Palviainen *et al.*, 2004). As such, high rates of decomposition in the cut plots is expected and may influence a buildup of soil P_o pools.

In contrast with P_o fractions, the Ca-associated with P (1M HCl) significantly declined by 4.9 kg ha^{-1} in the 15-35 cm layer (Table 4.3). We expected the Ca-associated P_i to decline. The 1M

HCl P_i is presumed to increase with fertilization and Ca leaching with reforestation and soil re-acidification is also expected. In fact, Ca leaching with re-acidification was observed in the upper 60 cm during forest growth in the uncut plots from 1962 to 1990 (Richter *et al.*, 1994) as was depletion of this HCl P_i fraction by 7.6 kg ha^{-1} (Richter *et al.*, 2006). In the O horizon in the uncut permanent plots Ca continued to increase between 1990-2010 (Bacon, 2014). Based on the previous research and data from the cut plots, the Ca associated P fraction continued to decline after harvest.

Unlike the Ca-associated P fraction, the occluded P content (concentrated HCl extracted-P_i) increased 3.3 kg ha^{-1} in 7.5-15 cm after 2005 (Fig. 4.7 and Supplementary Table 4.2). A similar increase was seen in the uncut plots between 1990-2017 but at 15-35 cm (Table 4.3). This occluded P fraction also increased in the surficial soil layer of an Oxisols during 15 years of forest growth from 149 to 190 µg g^{-1} (Townsend *et al.*, 2002). As noted above, this P fraction is related to strong bonding with Fe and Al (Lilienfein *et al.*, 2000; Crews and Brookes, 2014), although some researchers suggest this pool is related to P associated with Ca from primary minerals (Tiessen and Moir, 1993; Richter *et al.*, 2006) . Correlation between Fe, Al, and Ca with P in the concentrated HCl extracts of this study demonstrate a much stronger association with Fe and Al (Supplementary Fig. 4.4). Further, this study suggests over decades slowly cycling P bound to Fe and Al (oxy)hydroxides may respond to changing soil environments.

Overall, the more available P_i and P_o after regrowth of the forest increased in soil compared to the slowly cycling P_i and P_o due to higher SOC and lower soil pH over time. The pattern of P changes for more than 60 years forest development, from seedling to mature trees, on previous agricultural land showed the available P fractions had minor declined, especially in the first decades. The Ca associated with P fraction had the highest depletion during the several first decades; however, the P associated with Fe and Al declined more in the last few years. After the establishment of forest growth and forest floor, the biological cycle has been supplied forest tree. The total soil P declined was 34 kg ha $^{-1}$ in the last 27 years which is less than the amount of P required from trees and accumulated in OM.

5. Conclusion

Quantifying the legacy effect of agricultural P fertilization on P distributions during afforestation requires quantification of slowly cycling P over decades. Phosphorus fractionation indicated that slowly cycling P, enriched through P fertilization, contributed to the resupply of available P for more than 60 years of forest growth. The growing forest built an O horizon and increased P_o fractions relative to the total P in the surficial soil over time. Harvesting and replanting of the 50-year-old forest also demonstrated increased P_o fractions in the surficial soil layer. The long-term soil experiment continues to inform our understanding of the role of slowly cycling P fractions in maintaining the balance between available soil P and forest demand and the effect of harvesting and replanting forest on soil P fractions.

References

Aguiar, A.d.C.F., Cândido, C.S., Carvalho, C.S., Monroe, P.H.M., de Moura, E.G., 2013. Organic matter fraction and pools of phosphorus as indicators of the impact of land use in the Amazonian periphery. Ecological indicators 30, 158-164.

Alt, F., Oelmann, Y., Herold, N., Schrumpf, M., Wilcke, W., 2011. Phosphorus partitioning in grassland and forest soils of Germany as related to land-use type, management intensity, and land use–related pH. Journal of Plant Nutrition and Soil Science 174, 195-209.

Attiwill, P.M., Adams, M.A., 1993. Nutrient cycling in forests. New phytologist 124, 561-582.

Bacon, A.R., 2014. Pedo-genesis and anthropedo-genesis on the Southern Piedmont. Doctor of Philosophy PhD thesis. Duke University, Durham, NC. Bacon_duke_0066D_12361. pdf.

Beck, M.A., Sanchez, P.A., 1996. Soil phosphorus movement and budget after 13 years of fertilized cultivation in the Amazon basin. Plant and Soil 184, 23-31.

Berg, B., 2018. Decomposing litter; limit values; humus accumulation, locally and regionally. Applied Soil Ecology 123, 494-508.

Binkley, D., 2002. Ten-year decomposition in a loblolly pine forest. Canadian Journal of Forest Research 32, 2231-2235.

Blumfield, T., Xu, Z., 2003. Impact of harvest residues on soil mineral nitrogen dynamics following clearfall harvesting of a hoop pine plantation in subtropical Australia. Forest Ecology and Management 179, 55-67.

Carter, M.R., 1993. Soil sampling and methods of analysis. CRC Press.

Compton, J.E., Boone, R.D., 2000. Long-term impacts of agriculture on soil carbon and nitrogen in New England forests. Ecology 81, 2314-2330.

Crews, T.E., Brookes, P.C., 2014. Changes in soil phosphorus forms through time in perennial versus annual agroecosystems. Agriculture, Ecosystems & Environment 184, 168-181.

Dambrine, E., Dupouey, J.-L., Laüt, L., Humbert, L., Thinon, M., Beaufils, T., Richard, H., 2007. Present forest biodiversity patterns in France related to former Roman agriculture. Ecology 88, 1430-1439.

De Schrijver, A., Vesterdal, L., Hansen, K., De Frenne, P., Augusto, L., Achat, D.L., Staelens, J., Baeten, L., De Keersmaeker, L., De Neve, S., 2012. Four decades of post-agricultural forest development have caused major redistributions of soil phosphorus fractions. Oecologia 169, 221-234.

Deng, Q., McMahon, D.E., Xiang, Y., Yu, C.L., Jackson, R.B., Hui, D., 2017. A global meta-analysis of soil phosphorus dynamics after afforestation. New Phytologist 213, 181-192.

Falkengren-Grerup, U., ten Brink, D.-J., Brunet, J., 2006. Land use effects on soil N, P, C and pH persist over 40–80 years of forest growth on agricultural soils. Forest Ecology and Management 225, 74-81.

Friesen, D.K., Rao, I.M., Thomas, R.J., Oberson, A., Sanz, J., 1997. Phosphorus acquisition and cycling in crop and pasture systems in low fertility tropical soils. Plant and soil 196, 289-294.

Frizano, J., Johnson, A.H., Vann, D.R., Scatena, F.N., 2002. Soil Phosphorus Fractionation during Forest Development on Landslide Scars in the Luquillo Mountains, Puerto Rico 1. Biotropica 34, 17-26.

Goyette, J.-O., Bennett, E., Maranger, R., 2018. Low buffering capacity and slow recovery of anthropogenic phosphorus pollution in watersheds. Nature Geoscience, 1.

Gray, L.C., Thompson, E.K., 1933. History of agriculture in the southern United States to 1860.

Grieve, I.C., 2001. Human impacts on soil properties and their implications for the sensitivity of soil systems in Scotland. Catena 42, 361-374.

Guppy, C.N., Menzies, N.W., Blamey, F., Moody, P.W., 2005. Do decomposing organic matter residues reduce phosphorus sorption in highly weathered soils? Soil Science Society of America Journal 69, 1405-1411.

Hedley, M.J., Stewart, J., Chauhan, B., 1982. Changes in inorganic and organic soil phosphorus fractions induced by cultivation practices and by laboratory incubations 1. Soil Science Society of America Journal 46, 970-976.

Johnson, A., Frizano, J., Vann, D., 2003. Biogeochemical implications of labile phosphorus in forest soils determined by the Hedley fractionation procedure. Oecologia 135, 487-499.

Jurgensen, M., Graham, R., Larsen, M., Harvey, A., 1992. Clear-cutting, woody residue removal, and nonsymbiotic nitrogen fixation in forest soils of the Inland Pacific Northwest. Canadian Journal of Forest Research 22, 1172-1178.

Kimbrough, D.E., Wakakuwa, J.R., 1989. Acid digestion for sediments, sludges, soils, and solid wastes. A proposed alternative to EPA SW 846 Method 3050. Environmental science & technology 23, 898-900.

Koerner, W., Dupouey, J., Dambrine, E., Benoit, M., 1997. Influence of past land use on the vegetation and soils of present day forest in the Vosges mountains, France. Journal of ecology, 351-358.

Lilienfein, J., Wilcke, W., Ayarza, M.A., Vilela, L., do Carmo Lima, S., Zech, W., 2000. Chemical fractionation of phosphorus, sulphur, and molybdenum in Brazilian savannah Oxisols under different land use. Geoderma 96, 31-46.

Loeppert, R., Inskeep, W., 1996. Iron.In:Sparks,D.L.(Ed.), Method of Soil Analysis. Part 3. Chemical Methods. Soil Science Society of America, Madison Wisconsin, USA, 639-664.

MacDonald, G.K., Bennett, E.M., Taranu, Z.E., 2012. The influence of time, soil characteristics, and land-use history on soil phosphorus legacies: a global meta-analysis. Global Change Biology 18, 1904-1917.

Markewitz, D., Richter, D.D., Allen, H.L., Urrego, J.B., 1998. Three decades of observed soil acidification in the Calhoun Experimental Forest: Has acid rain made a difference? Soil Science Society of America Journal 62, 1428-1439.

McLaughlin, J., Ryden, J., Syers, J., 1981. Sorption of inorganic phosphate by iron-and aluminium-containing components. Journal of Soil Science 32, 365-378.

Metz, L.J., 1958. The Calhoun experimental forest. unknown.

Mobley, M., Yang, Y., Yanai, R., Nelson, K., Bacon, A., Heine, P., Richter, D., 2019. How to Estimate Statistically Detectable Trends in a Time Series: A Study of Soil Carbon and Nutrient Concentrations at the Calhoun LTSE. Soil Science Society of America Journal.

Murphy, J., Riley, J.P., 1962. A modified single solution method for the determination of phosphate in natural waters. Analytica chimica acta 27, 31-36.

Niederberger, J., Todt, B., Boča, A., Nitschke, R., Kohler, M., Kühn, P., Bauhus, J., 2015. Use of near-infrared spectroscopy to assess phosphorus fractions of different plant availability in forest soils. Biogeosciences 12, 3415-3428.

Palviainen, M., Finér, L., Kurka, A.-M., Mannerkoski, H., Piirainen, S., Starr, M., 2004. Decomposition and nutrient release from logging residues after clear-cutting of mixed boreal forest. Plant and soil 263, 53-67.

Pinheiro, J., Bates, D., DebRoy, S., Sarkar, D., Team, R.C., 2013. nlme: Linear and nonlinear mixed effects models. R Package Version 3.1–111. Computer manual.

Richter, D., Markewitz, D., Wells, C., Allen, H., April, R., Heine, P., Urrego, B., 1994. Soil chemical change during three decades in an old-field loblolly pine (Pinus taeda L.) ecosystem. Ecology 75, 1463-1473.

Richter, D.D., Allen, H.L., Li, J., Markewitz, D., Raikes, J., 2006. Bioavailability of slowly cycling soil phosphorus: major restructuring of soil P fractions over four decades in an aggrading forest. Oecologia 150, 259-271.

Richter, D.D., Markewitz, D., 2001. Understanding soil change : soil sustainability over millennia, centuries, and decades. Cambridge University Press, Cambridge.

Richter, D.D., Markewitz, D., Trumbore, S.E., Wells, C.G., 1999. Rapid accumulation and turnover of soil carbon in a re-establishing forest. Nature 400, 56.

Ritter, E., Vesterdal, L., Gundersen, P., 2003. Changes in soil properties after afforestation of former intensively managed soils with oak and Norway spruce. Plant and soil 249, 319-330.

Roberts, K., Defforey, D., Turner, B.L., Condron, L.M., Peek, S., Silva, S., Kendall, C., Paytan, A., 2015. Oxygen isotopes of phosphate and soil phosphorus cycling across a 6500 year chronosequence under lowland temperate rainforest. Geoderma 257, 14-21.

Ruffin, E., 1852. An essay on calcareous manures. JW Randolph.

Schmidt, J., Buol, S., Kamprath, E., 1997. Soil phosphorus dynamics during 17 years of continuous cultivation: a method to estimate long-term P availability. Geoderma 78, 59-70.

Schoenau, J., Stewart, J., Bettany, J., 1989. Forms and cycling of phosphorus in prairie and boreal forest soils. Biogeochemistry 8, 223-237.

Selmants, P.C., Hart, S.C., 2010. Phosphorus and soil development: does the Walker and Syers model apply to semiarid ecosystems? Ecology 91, 474-484.

Sharpley, A.N., McDowell, R.W., Kleinman, P.J., 2004. Amounts, forms, and solubility of phosphorus in soils receiving manure. Soil science society of America journal 68, 2048-2057.

Sheridan, R.C., 1979. Chemical fertilizers in southern agriculture. Agricultural History 53, 308-318.

Solomon, D., Lehmann, J., Mamo, T., Fritzsche, F., Zech, W., 2002. Phosphorus forms and dynamics as influenced by land use changes in the sub-humid Ethiopian highlands. Geoderma 105, 21-48.

Switzer, G., Nelson, L., Smith, W., 1966. The Characterization of Dry Matter and Nitrogen Accumulation by Loblolly Pine (Pinus taeda L.) 1. Soil Science Society of America Journal 30, 114-119.

Taylor, R.H., 1953. Fertilizers and Farming in the Southeast, 1840-1950: Part I: 1840-1900. The North Carolina Historical Review 30, 305-328.

Tiessen, H., Moir, J., 1993. Characterization of available P by sequential extraction. Soil sampling and methods of analysis 7, 5-229.

Townsend, A.R., Asner, G.P., Cleveland, C.C., Lefer, M.E., Bustamante, M.M., 2002. Unexpected changes in soil phosphorus dynamics along pasture chronosequences in the humid tropics. Journal of Geophysical Research: Atmospheres 107, LBA 34-31-LBA 34-39.

Vesterdal, L., Ritter, E., Gundersen, P., 2002. Change in soil organic carbon following afforestation of former arable land. Forest ecology and management 169, 137-147.

Walker, T., Syers, J.K., 1976. The fate of phosphorus during pedogenesis. Geoderma 15, 1-19.

Wall, A., Hytönen, J., 2005. Soil fertility of afforested arable land compared to continuously. Plant and Soil 275, 247-260.

Wells, C.G., Jorgensen, J.R., 1975. Nutrient cycling in loblolly pine plantations. Proc North Am For Soils Conf.

Yanai, R.D., 1992. Phosphorus budget of a 70-year-old northern hardwood forest. Biogeochemistry 17, 1-22.

Yanai, R.D., 1998. The effect of whole-tree harvest on phosphorus cycling in a northern hardwood forest. Forest Ecology and Management 104, 281-295.

Zheng, Z., Simard, R.R., Lafond, J., Parent, L.E., 2002. Pathways of soil phosphorus transformations after 8 years of cultivation under contrasting cropping practices. Soil Science Society of America Journal 66, 999-1007.

Table 4.1. Soil phosphorus transfers and translocations over 55 years (1962-2017) of forest development for eight permanent uncut plots based on Hedley fractions. Only statistically significant gains or losses in 0-60 cm depth are included. Calhoun Experimental Forest, South Carolina.

Soil P fractions		1962-1990 (t-test)* soil P (kg ha^{-1})	1962-1990 (ANOVA) soil P (kg ha^{-1})	1990-2017 (27 year) soil P (kg ha^{-1})	1962-2017 (55 year) soil P (kg ha^{-1})
Resin P_i	Labile, exchangeable	0.0	0.0	-12.8	-11.7
HCO_3 P_i	Labile, adsorbed	+22.0	+22.0	-5.4	+18.8
HCO_3 P_o	Readily mineralizable	0.0	0.0	+10.7	+15.9
NaOH P_i	P_i associated with Fe and Al	-3.4 (0-7.5, 15-35 cm)	-14.8 (0-7.5 cm)	-10.7	-66.7
NaOH P_o	Slowly mineralizable	-22.8	-22.8	+2.7	-26.6
1 M HCl	P_i associate with Ca	-7.6 (0-15 cm)	-5.5 (0-7.5 cm)	0.0	-8.0
Concentrated HCl P_i	Stable P_i associate with crystalline Fe	-52.2 (0-15, 35-60 cm)	0.0	+29.8	+20.1
Residual P	Recalcitrant organic and mineral	0.0	0.0	0.0	0.0
Total P	Sum of statistically significant change	-63.0	-21.2	+14.3	-58.2

*1962-1990 data reported in previous published paper Richter *et al.* (2006)

Table 4.2. Soil phosphorus changes from 1962 to 2017 in eight permanent uncut plots at the Calhoun Experimental Forest, South Carolina. The post hoc P-value was obtained following ANOVA results in Supplementary Table 4.1 using Tukey test.

	1962		2017		
	Mean	SE	Mean	SE	P-value
	µg g^{-1}	µg g^{-1}	µg g^{-1}	µg g^{-1}	
Resin.P$_i$					
0-7.5	12.6	1.09	5.31	1.10	7.25e^{-8}
7.5-15	10.7	1.47	7.04	1.48	0.0096
15-35	3.97	0.42	2.39	0.42	0.0963
35-60	1.86	0.79	2.07	0.84	1.0000
HCO$_3$.P$_i$					
0-7.5	9.23	1.06	7.26	1.07	0.2652
7.5-15	6.92	2.30	11.1	2.31	0.2956
15-35	1.05	0.79	5.04	0.80	0.0013
35-60	1.60	0.22	3.46	0.23	0.0001
HCO$_3$.P$_o$					
0-7.5	8.35	0.92	8.23	0.92	0.9999
7.5-15	7.39	0.92	7.44	0.92	1.0000
15-35	3.39	0.40	5.59	0.40	0.0037
35-60	2.03	0.31	4.60	0.31	8.69e^{-6}
NaOH.P$_i$					
0-7.5	39.0	3.10	16.6	3.10	1.14e^{-8}
7.5-15	35.6	4.22	31.7	4.23	0.9665
15-35	20.9	3.09	29.7	3.09	0.2482
35-60	46.8	4.09	35.4	4.12	0.0024
NaOH.P$_o$					
0-7.5	25.9	2.08	16.2	2.08	0.0007
7.5-15	29.1	1.70	17.7	1.70	4.95e^{-8}
15-35	18.6	1.23	16.9	1.24	0.7899
35-60	13.5	1.39	14.1	1.40	0.9947
1MHCl.P$_i$					
0-7.5	7.48	0.70	2.19	0.70	5.82e^{-5}
7.5-15	4.94	0.52	2.43	0.52	0.0140
15-35	1.25	0.17	1.20	0.17	0.9995
35-60	0.48	0.31	0.81	0.31	0.9867
Concentrated HCl.P$_i$					
0-7.5	11.8	1.71	12.0	1.72	0.9999
7.5-15	14.4	1.76	13.2	1.77	0.9896
15-35	16.8	2.27	25.6	2.31	0.0105

35-60	58.1	5.97	56.3	6.03	0.9925
Concentrated HCl.P_o					
0-7.5	1.22	1.44	1.03	1.55	0.9999
7.5-15	1.22	0.60	1.31	0.60	0.9990
15-35	1.20	1.55	1.91	1.56	0.8960
35-60	1.84	1.29	4.83	1.30	0.0969
Residual					
0-7.5	19.8	5.16	24.2	5.19	0.8155
7.5-15	20.0	5.45	22.7	5.45	0.9966
15-35	30.9	7.04	44.9	7.13	0.3070
35-60	74.6	10.9	103	10.9	0.4357
Total Recovery (Sum)					
0-7.5	135	10.4	93.0	10.4	$4.58e^{-5}$
7.5-15	130	8.00	113	8.00	0.3563
15-35	97.6	7.66	132	7.66	0.0043
35-60	200	19.5	220	18.9	0.8282
Total					
0-7.5	143	13.3	108	13.4	0.1139
7.5-15	152	12.0	121	12.0	0.0348
15-35	124	8.68	129	8.80	0.9639
35-60	258	17.5	239	17.6	0.6940

Table 4.3. Soil phosphorus transfer and translocations over 12 years of forest development in eight permanent cut plots based on Hedley fractions. Only statistically significant gains (+) or losses (-) in 0-60 cm depth are included. Calhoun Experimental Forest, South Carolina.

Soil P fractions		2005-2017 (12 year) soil P (kg ha^{-1})
Resin P_i	Labile, exchangeable	0.0
HCO_3 P_i	Labile, adsorbed	-1.8
HCO_3 P_o	Readily mineralizable	0.0
NaOH P_i	P_i associated with Fe and Al	0.0
NaOH P_o	Slowly mineralizable	+4.3
1 M HCl	P_i associate with Ca	-4.9
Concentrated HCl P_i	Stable P_i associate with crystalline Fe	+3.4
Residual P	Recalcitrant organic and mineral	-38.3
Total P	Sum of statistically significant change	-37.3

Table 4.4. Soil phosphorus changes from 2005 to 2017 in eight permanent cut plots at the Calhoun Experimental Forest, South Carolina. The post hoc P-value was obtained following ANOVA results in Supplementary Table 4.2 using Tukey test.

	2005		**2017**		
	Mean	SE	Mean	SE	P-value
	μg g^{-1}	μg g^{-1}	μg g^{-1}	μg g^{-1}	
Resin.P_i					
0-7.5	7.86	1.46	5.48	1.46	0.072
7.5-15	9.11	2.00	7.42	1.98	0.271
15-35	1.51	0.79	1.52	0.78	0.999
35-60	0.73	0.39	0.85	0.38	0.853
HCO_3.P_i					
0-7.5	8.35	1.79	7.60	1.78	0.495
7.5-15	11.0	2.45	9.70	2.45	0.169
15-35	4.99	0.91	4.87	0.91	0.976
35-60	3.68	0.16	3.18	0.16	0.035
HCO_3.P_o					
0-7.5	8.95	0.81	8.23	0.81	0.803
7.5-15	7.90	0.71	7.93	0.71	0.999
15-35	7.22	1.17	5.66	1.17	0.592
35-60	4.71	0.61	5.00	0.61	0.939
NaOH.P_i					
0-7.5	20.9	7.18	23.8	7.18	0.456
7.5-15	31.6	8.69	34.7	8.69	0.447
15-35	27.6	3.55	25.3	3.55	0.739
35-60	42.1	4.83	39.8	4.83	0.861
NaOH.P_o					
0-7.5	15.6	1.65	19.4	1.65	$6.4e^{-6}$
7.5-15	16.2	1.65	19.6	1.65	0.323
15-35	17.9	1.19	18.6	1.19	0.709
35-60	14.3	1.59	14.2	1.59	0.995
1MHCl.P_i					
0-7.5	1.88	0.32	2.17	0.32	0.795
7.5-15	1.99	0.29	1.84	0.29	0.926
15-35	2.82	0.37	1.21	0.37	0.017
35-60	2.61	0.57	1.77	0.57	0.557
Concentrated HCl.P_i					
0-7.5	9.39	1.51	9.90	1.51	0.925
7.5-15	10.8	1.87	13.7	1.87	0.027
15-35	23.9	4.88	24.6	4.88	0.984
35-60	44.9	6.91	50.6	6.91	0.130

Concentrated HCl.P_o					
0-7.5	2.93	0.59	2.40	0.59	0.867
7.5-15	2.79	0.51	3.01	0.51	0.649
15-35	3.53	0.88	3.72	0.88	0.996
35-60	4.57	1.18	5.27	1.18	0.772
Residual					
0-7.5	60.2	8.24	29.5	8.24	0.073
7.5-15	66.9	9.52	33.3	9.52	0.003
15-35	75.6	15.7	61.1	15.7	0.678
35-60	97.7	10.6	78.4	10.6	0.051
Total Recovery (Sum)					
0-7.5	133	10.7	106	10.7	0.047
7.5-15	158	20.4	129	20.4	0.057
15-35	163	13.0	142	13.1	0.283
35-60	211	19.1	194	19.1	0.005
Total					
0-7.5	162	15.2	123	15.2	0.089
7.5-15	186	23.3	149	23.3	0.471
15-35	189	18.0	153	18.0	0.612
35-60	228	20.9	221	20.9	0.936

Supplementary Table 4.1. Soil phosphorus changes from 1962 to 2017 in eight permanent uncut plots at the Calhoun Experimental Forest, South Carolina.

	1962		1990		2005		2010		2017		
	Mean	SE	Mean	SE	Mean	SE	Mean	SE	Mean	SE	P-value
	µg g^{-1}	µg g^{-1}	µg g^{-1}	µg g^{-1}	µg g^{-1}	µg g^{-1}	µg g^{-1}	µg g^{-1}	µg g^{-1}	µg g^{-1}	
Resin.P_i											
0-7.5	12.6	1.09	12.9	1.09	7.98	1.09	7.17	1.09	5.31	1.10	$5.76e^{-10}$
7.5-15	10.7	1.47	10.9	1.51	11.1	1.47	10.8	1.47	7.04	1.48	0.0006
15-35	3.97	0.42	3.75	0.42	0.62	0.42	1.59	0.42	2.39	0.42	$4.8e^{-6}$
35-60	1.86	0.79	1.58	0.79	0.33	0.78	1.00	0.79	2.07	0.84	0.4709
HCO_3.P_i											
0-7.5	9.23	1.06	10.4	1.06	8.91	1.06	7.49	1.06	7.26	1.07	0.0029
7.5-15	6.92	2.30	16.6	2.39	11.6	2.30	14.0	2.30	11.1	2.31	0.0035
15-35	1.05	0.79	4.57	0.79	4.19	0.79	4.65	0.79	5.04	0.80	0.0010
35-60	1.60	0.22	2.23	0.24	3.22	0.22	3.48	0.22	3.46	0.23	$6.83e^{-6}$
HCO_3.P_o											
0-7.5	8.35	0.92	6.68	0.92	9.26	0.92	8.96	0.92	8.23	0.92	0.1708
7.5-15	7.39	0.92	5.89	0.92	8.41	0.92	7.93	0.92	7.44	0.92	0.2791
15-35	3.39	0.40	3.25	0.40	6.63	0.40	6.02	0.40	5.59	0.40	$4.78e^{-07}$
35-60	2.03	0.31	1.64	0.33	5.75	0.31	5.09	0.31	4.60	0.31	$1.6e^{-11}$
NaOH.P_i											
0-7.5	39.0	3.10	25.9	3.10	19.0	3.10	13.6	3.10	16.6	3.10	$1.88e^{-10}$
7.5-15	35.6	4.22	37.4	4.22	35.7	4.22	35.9	4.22	31.7	4.23	0.9072
15-35	20.9	3.09	24.5	3.09	26.5	3.09	22.7	3.09	29.7	3.09	0.2951
35-60	46.8	4.09	41.2	4.09	43.5	4.08	44.8	4.09	35.4	4.12	0.0021
NaOH.P_o											
0-7.5	25.9	2.08	16.44	2.08	14.8	2.08	15.9	2.08	16.2	2.08	$5.78e^{-5}$
7.5-15	29.1	1.70	18.58	1.70	16.1	1.70	16.8	1.70	17.7	1.70	$3.23e^{-9}$

15-35	18.6	1.23	16.22	1.23	16.6	1.23	17.6	1.23	16.9	1.24	0.5262
35-60	13.5	1.39	14.66	1.39	13.12	1.39	14.0	1.39	14.1	1.40	0.1571
1MHCl.P_i											
0-7.5	7.48	0.70	2.63	0.70	2.25	0.70	2.35	0.70	2.19	0.70	$9.55e^{-6}$
7.5-15	4.94	0.52	3.09	0.52	2.76	0.52	2.59	0.52	2.43	0.52	0.0116
15-35	1.25	0.17	1.02	0.17	1.29	0.17	1.28	0.17	1.20	0.17	0.7268
35-60	0.48	0.31	0.59	0.31	1.04	0.31	1.57	0.31	0.81	0.31	0.1571
Concentrated HCl.P_i											
0-7.5	11.8	1.72	8.52	1.71	7.59	1.71	9.44	1.71	12.0	1.72	0.2382
7.5-15	14.4	1.77	10.0	1.76	8.92	1.76	18.5	1.76	13.2	1.77	0.0047
15-35	16.8	2.31	15.2	2.27	23.8	2.27	24.3	2.27	25.6	2.31	0.0002
35-60	58.1	6.18	46.0	5.98	52.2	5.97	55.7	5.97	56.3	6.03	0.2466
Concentrated HCl.P_o											
0-7.5	1.22	1.44	1.22	1.44	2.18	1.44	0.80	1.44	1.03	1.55	0.4711
7.5-15	1.22	0.60	1.22	0.60	3.01	0.60	0.43	0.60	1.31	0.60	0.2520
15-35	1.20	1.55	1.20	1.55	3.34	1.55	5.70	1.55	1.91	1.56	0.6785
35-60	1.84	1.29	1.84	1.29	8.16	1.29	3.51	1.29	4.83	1.30	0.0018
Residual											
0-7.5	19.8	5.16	19.8	5.16	35.9	5.16	11.2	5.16	24.2	5.19	$6.21e^{-5}$
7.5-15	20.0	5.45	20.0	5.45	43.4	5.45	20.8	5.45	22.7	5.45	0.0261
15-35	30.9	7.04	30.9	7.04	46.4	7.04	47.4	7.04	44.9	7.13	0.0601
35-60	74.6	10.9	74.6	10.9	89.1	10.9	79.6	10.94	103	10.9	0.4479
Total											
0-7.5	143	13.3	118	13.3	118	13.3	102	13.3	108	13.4	0.0661
7.5-15	152	12.0	131	12.0	146	12.0	142	12.0	121	12.0	0.0382
15-35	124	8.68	120	8.68	143	8.68	152	8.68	129	8.80	0.0026
35-60	258	17.5	228	17.5	243	17.5	223	17.5	239	17.6	0.2427

Supplementary Table 4.2. Soil phosphorus changes from 2005 to 2017 in eight permanent cut plots at the Calhoun Experimental Forest, South Carolina.

	2005		**2010**		**2017**		
	Mean	SE	Mean	SE	Mean	SE	P-value
	μg g^{-1}	μg g^{-1}	μg g^{-1}	μg g^{-1}	μg g^{-1}	μg g^{-1}	
Resin.P_i							
0-7.5	7.86	1.46	7.35	1.46	7.35	1.46	0.071
7.5-15	9.11	2.00	7.10	1.98	7.10	1.98	0.168
15-35	1.51	0.79	2.10	0.78	2.10	0.78	0.721
35-60	0.73	0.39	0.35	0.38	0.35	0.38	0.151
HCO_3.P_i							
0-7.5	8.35	1.79	8.58	1.78	7.60	1.78	0.337
7.5-15	11.0	2.45	11.6	2.45	9.70	2.45	0.041
15-35	4.99	0.91	5.62	0.91	4.87	0.91	0.466
35-60	3.68	0.16	3.62	0.16	3.18	0.16	0.029
HCO_3.P_o							
0-7.5	8.95	0.81	9.29	0.81	8.23	0.81	0.644
7.5-15	7.90	0.71	7.98	0.71	7.93	0.71	0.997
15-35	7.22	1.17	5.12	1.14	5.66	1.17	0.329
35-60	4.71	0.61	4.89	0.60	5.00	0.61	0.943
NaOH.P_i							
0-7.5	20.9	7.18	18.6	7.17	23.8	7.18	0.038
7.5-15	31.6	8.69	29.1	8.67	34.7	8.69	0.139
15-35	27.6	3.55	25.0	3.54	25.3	3.55	0.672
35-60	42.1	4.83	36.3	4.81	39.8	4.83	0.403
NaOH.P_o							
0-7.5	15.6	1.65	17.3	1.65	19.4	1.65	$0.10e^{-5}$
7.5-15	16.2	1.65	17.3	1.65	19.6	1.65	0.339
15-35	17.9	1.19	17.9	1.19	18.6	1.19	0.683
35-60	14.33	1.59	14.9	1.59	14.2	1.59	0.774

1MHCl.P_i							
0-7.5	1.88	0.32	2.28	0.32	2.17	0.32	0.644
7.5-15	1.99	0.29	2.91	0.29	1.84	0.29	0.037
15-35	2.82	0.37	2.37	0.37	1.21	0.37	0.017
35-60	2.61	0.57	2.07	0.57	1.77	0.57	0.579
Concentrated HCl.P_i							
0-7.5	9.39	1.51	11.7	1.48	9.94	1.51	0.345
7.5-15	10.8	1.87	15.4	1.85	13.7	1.87	0.002
15-35	23.9	4.88	29.1	4.86	24.6	4.88	0.429
35-60	44.9	6.91	57.1	6.89	50.6	6.91	0.003
Concentrated HCl.P_o							
0-7.5	2.93	0.59	0.88	0.59	0.59	29.5	0.018
7.5-15	2.79	0.51	1.04	0.51	0.51	33.3	0.009
15-35	3.53	0.88	3.34	0.88	0.88	61.0	0.062
35-60	4.57	1.18	4.55	1.17	1.18	78.0	0.076
Residual							
0-7.5	60.2	8.24	26.7	8.10	29.5	8.24	0.043
7.5-15	66.9	9.52	35.9	9.36	33.3	9.52	0.002
15-35	75.6	15.7	43.7	15.7	61.1	15.7	0.231
35-60	97.7	10.6	69.3	10.5	78.4	10.6	0.004
Total Recovery (Sum)							
0-7.5	134	10.7	104	10.5	107	10.7	0.026
7.5-15	158	20.4	128	20.3	129	20.4	0.034
15-35	163	13.1	134	12.8	142	13.1	0.121
35-60	211	19.1	190	19.1	194	19.1	0.001
Total							
0-7.5	162	15.2	119	15.0	123	15.2	0.049
7.5-15	186	23.3	131	22.5	149	23.3	0.130
15-35	189	18.0	166	18.0	153	18.0	0.284
35-60	228	20.9	223	20.8	221	20.9	0.938

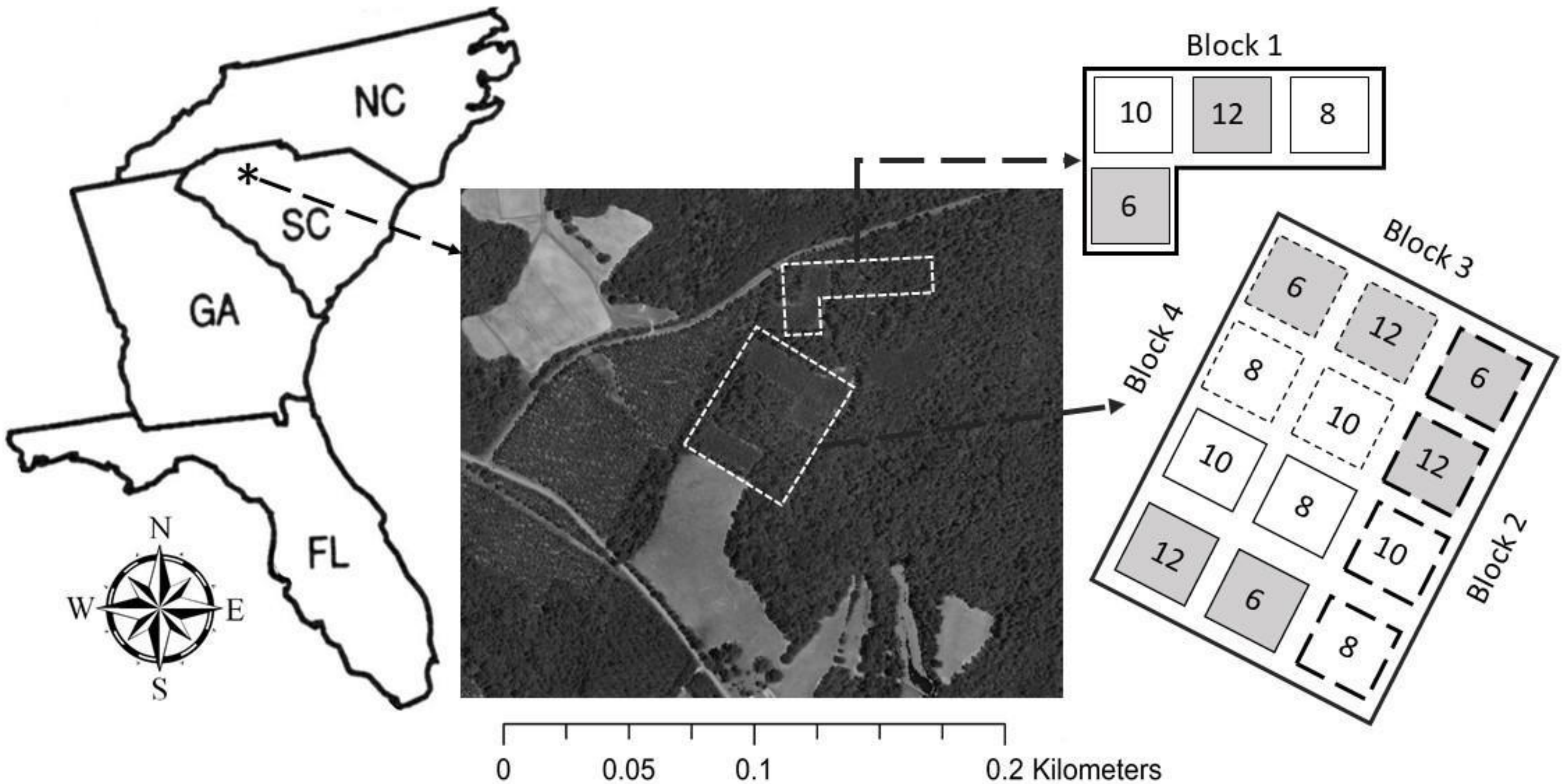

Figure 4.1. Long-term Soil Experiment (LTSE) established in 1957 as a loblolly pine (*Pinus taeda* L.) spacing study with four blocks and four different spacings at the Calhoun Experimental Forest. In 2007, 6 and 12 ft spacings of each block were harvested and replanted in 2009 ("cut plots") whereas 8 and 10 ft spaces were not cut ("uncut plots").

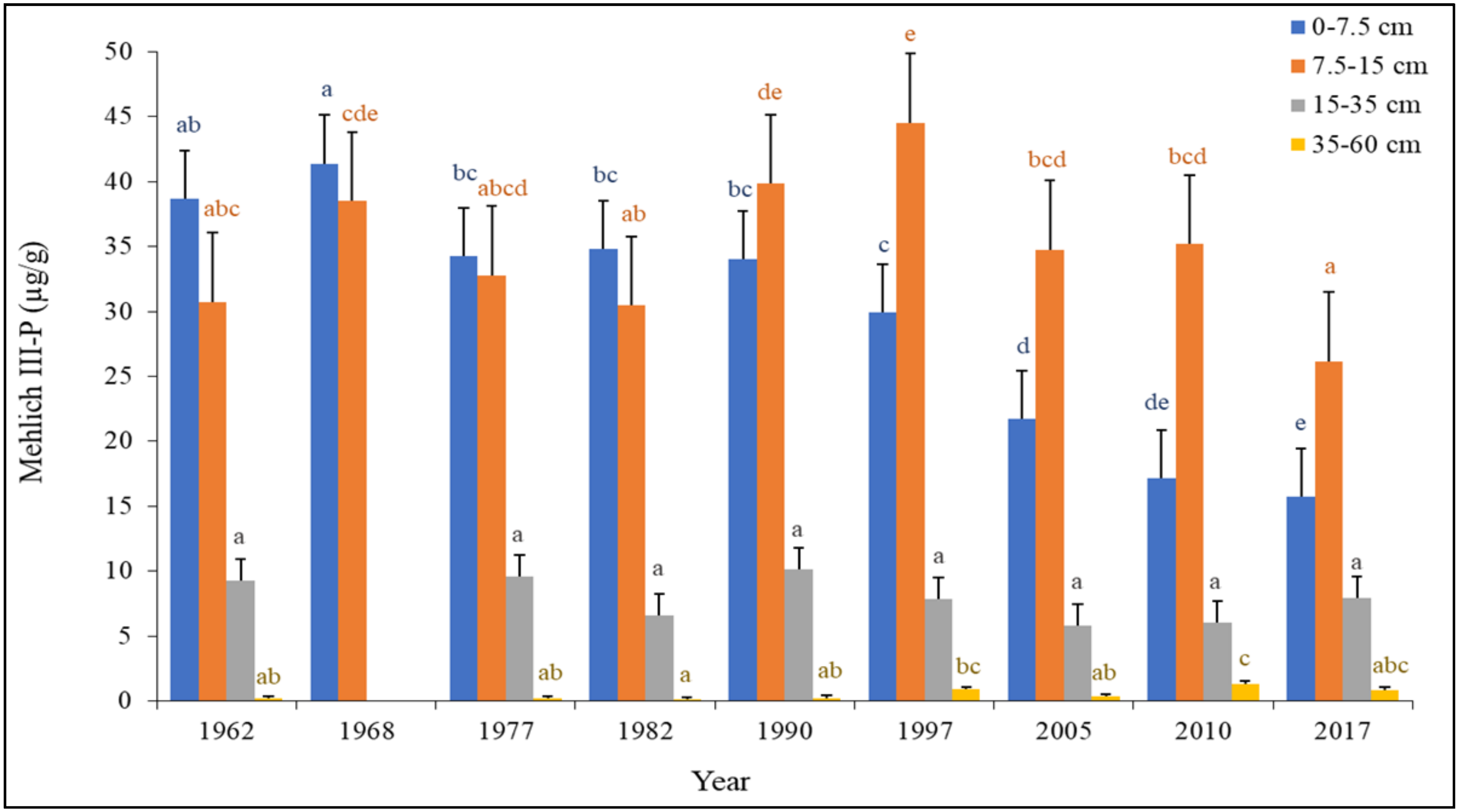

Figure 4.2. Mehlich III extractable phosphorus concentration (mean ± SE) for four soil depths (0-7.5, 7.5-15, 15-35, and 35-60 cm) in eight permanent, uncut plots at the Calhoun Experimental Forest, South Carolina. Sample size for each depth within each year = 8 (soil samples were not collected from >15 cm depth in 1968). The extractable P from 1962-2005 was measured and reported in a previous paper (Richter et al., 2006).

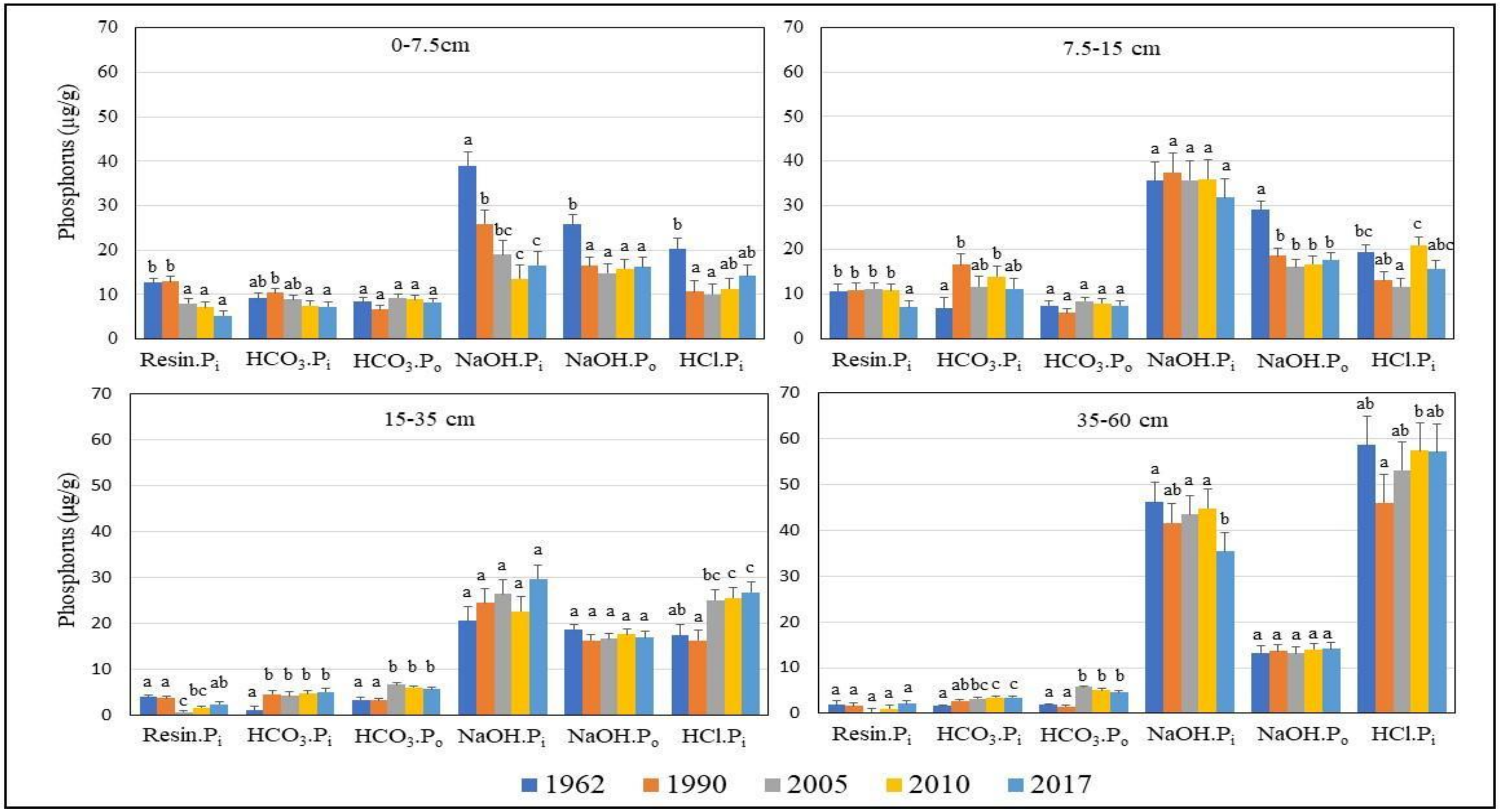

Figure 4.3. Soil phosphorus fractions (mean ± SE) in 8 permanent, uncut plots for the four soil layers (0-7.5, 7.5-15, 15-35, and 35-60 cm) at the Calhoun Experimental Forest, South Carolina over five decades. Sample size for each depth within each year = 8.

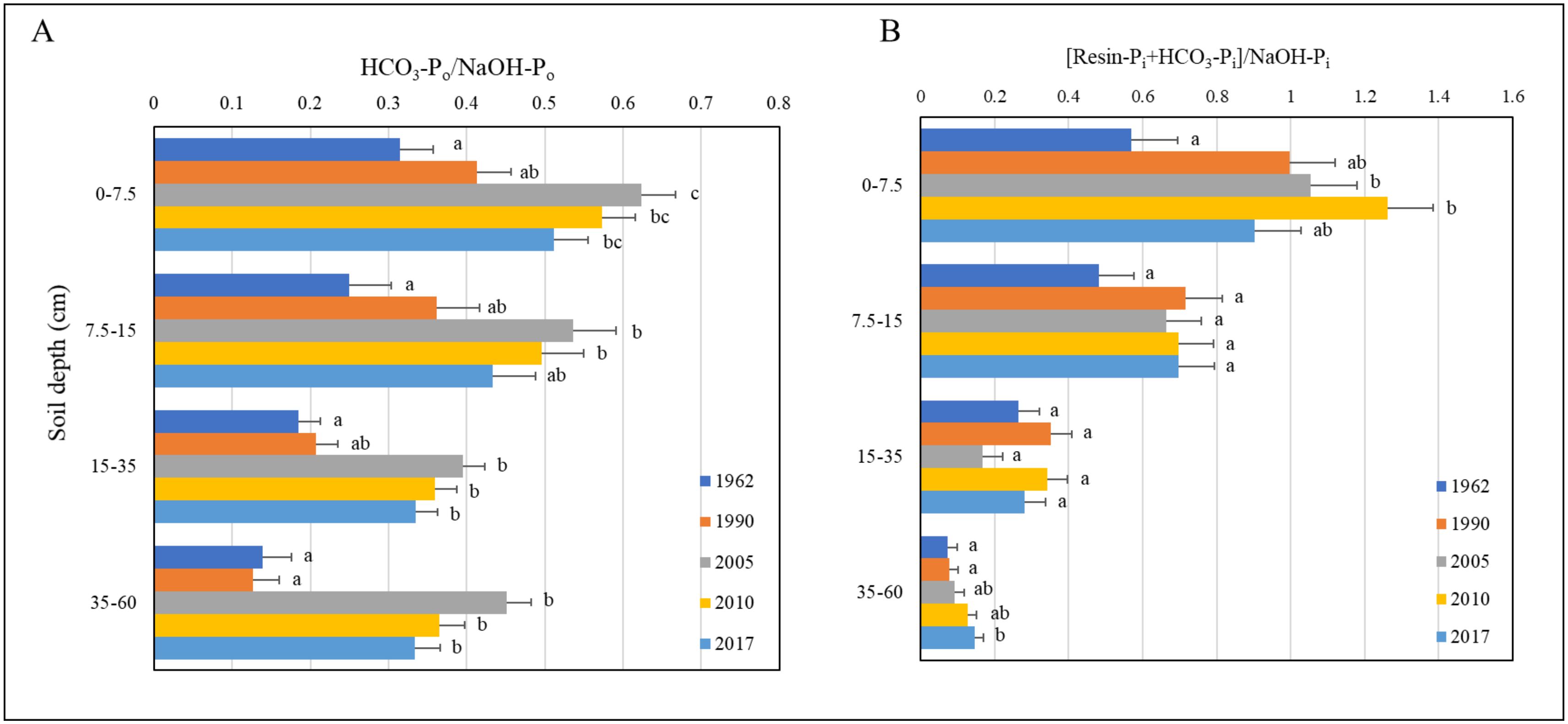

Figure 4.4. Relatively labile inorganic and organic phosphorus fractions relative to slower cycling fractions (mean ± SE) in 8 permanent uncut plots at the Calhoun Experimental Forest, South Carolina.

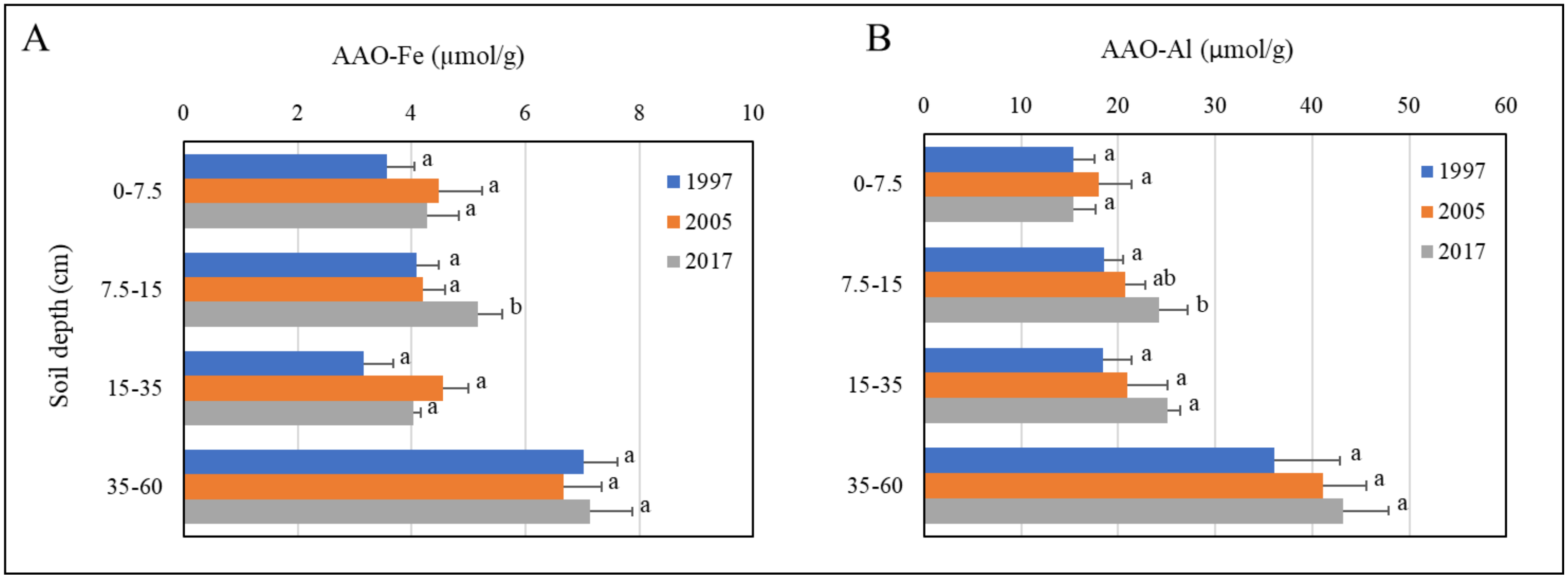

Figure 4.5. Acid Ammonium Oxalic extractable Fe and Al in four-soil layer of 8 uncut plots at the Calhoun Experimental Forest, South Carolina.

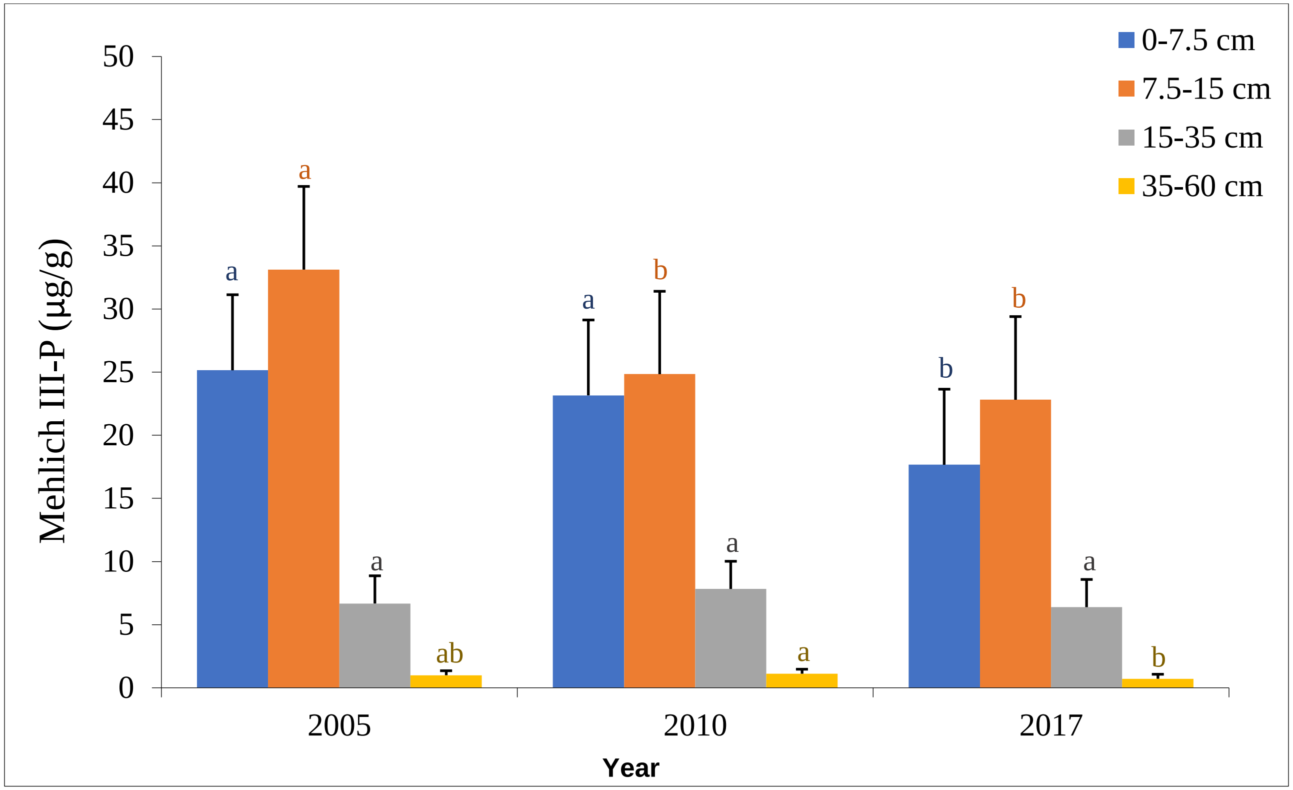

Figure 4.6. Mehlich III extractable phosphorus concentration (mean ± SE) for the four soil layers in eight permanent cut plots at the Calhoun experimental Forest, South Carolina over five decades. Sample size for each depth within each year = 8.

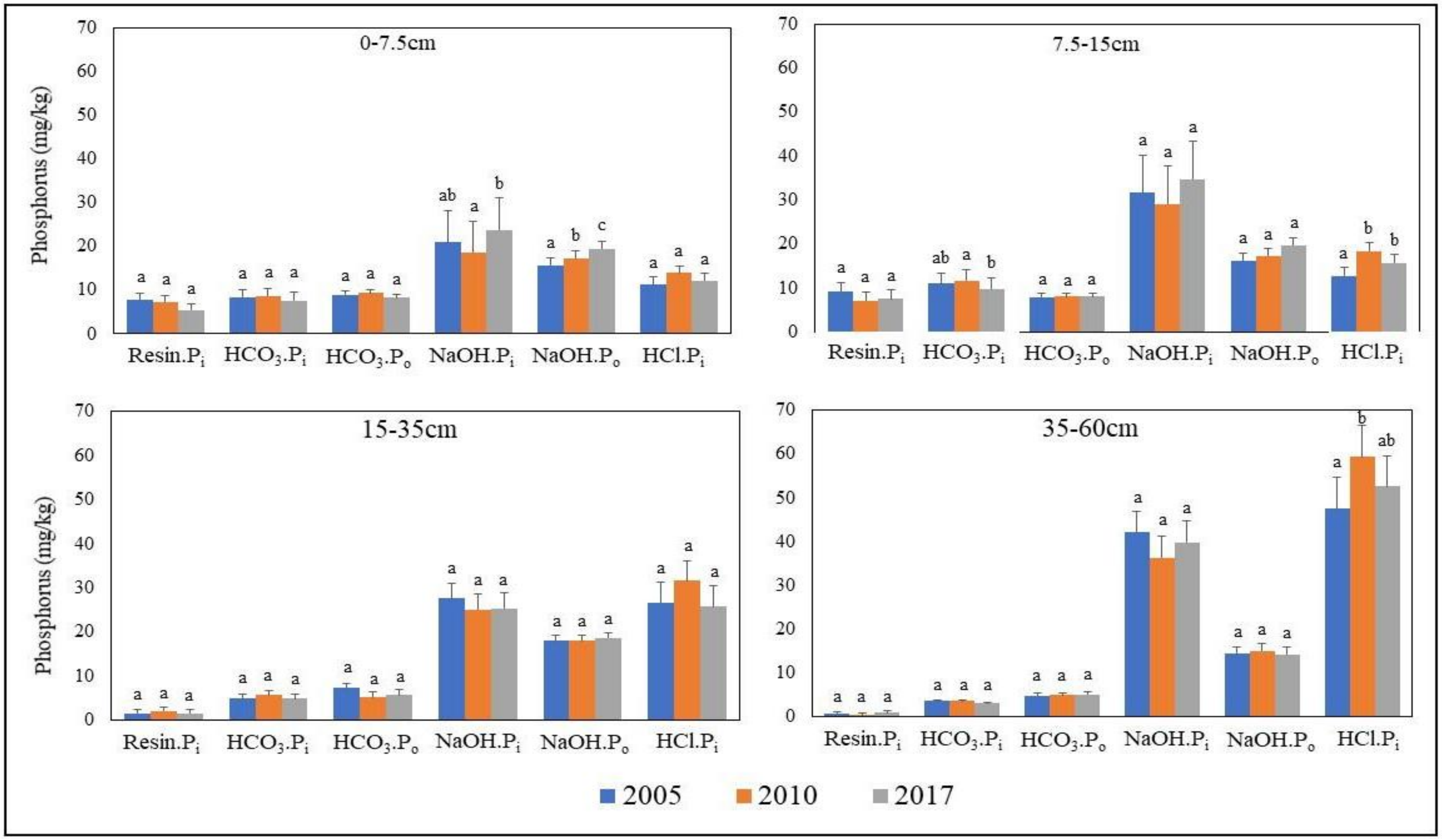

Figure 4.7. Soil phosphorus fractions (mean ± SE) in 8 permanent cut plots for four soil layers at the Calhoun Experimental Forest, South Carolina. Sample size for each depth each within year = 8.

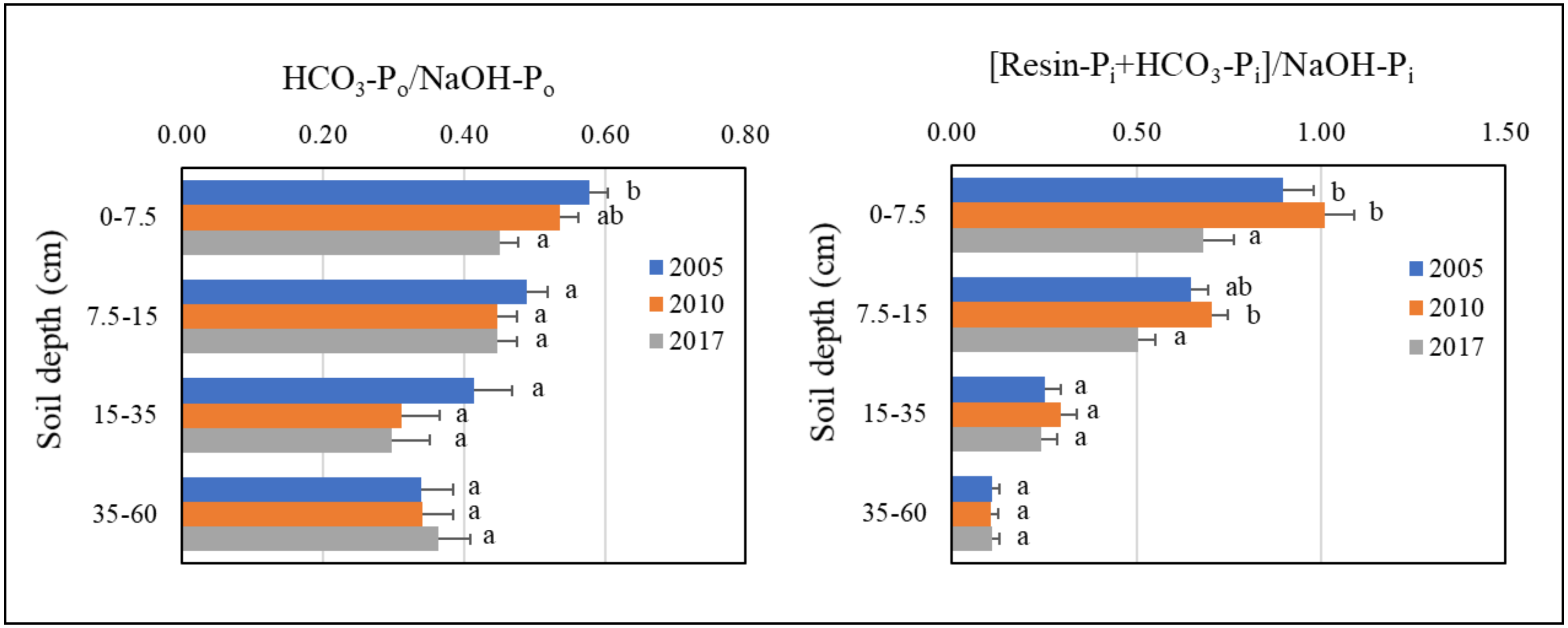

Figure 4.8. Relatively labile inorganic and organic phosphorus fractions relative to slower cycling fractions (mean ± SE) in 8 permanent cut plots at the Calhoun Experimental Forest, South Carolina.

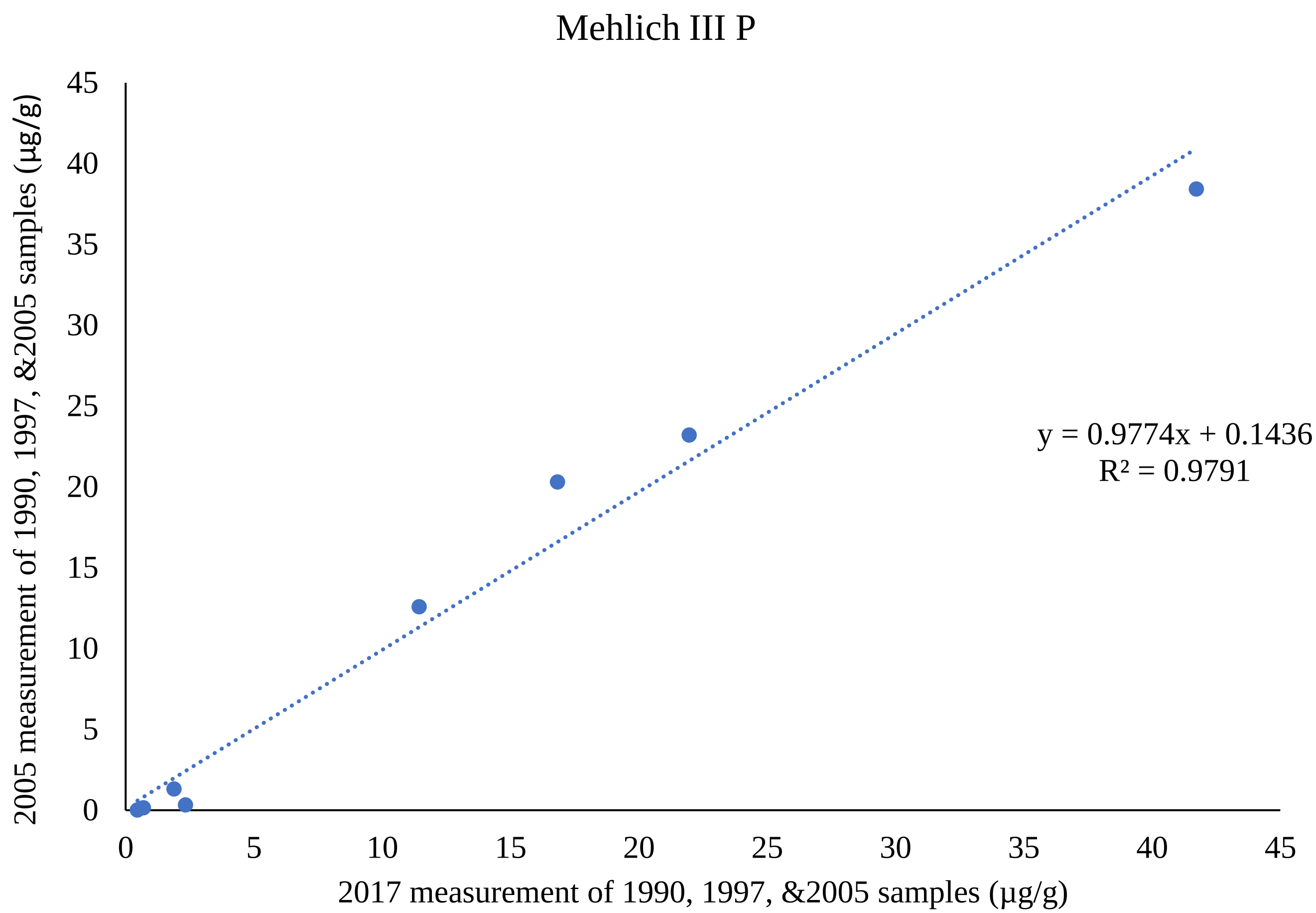

Supplementary Figure 4.1. Linear regression lines between Mehlich III phosphorus measured in 2005 and 2017 of different samples collected from 8 permanent uncut plots in 1990, 1997, and 2005.

A

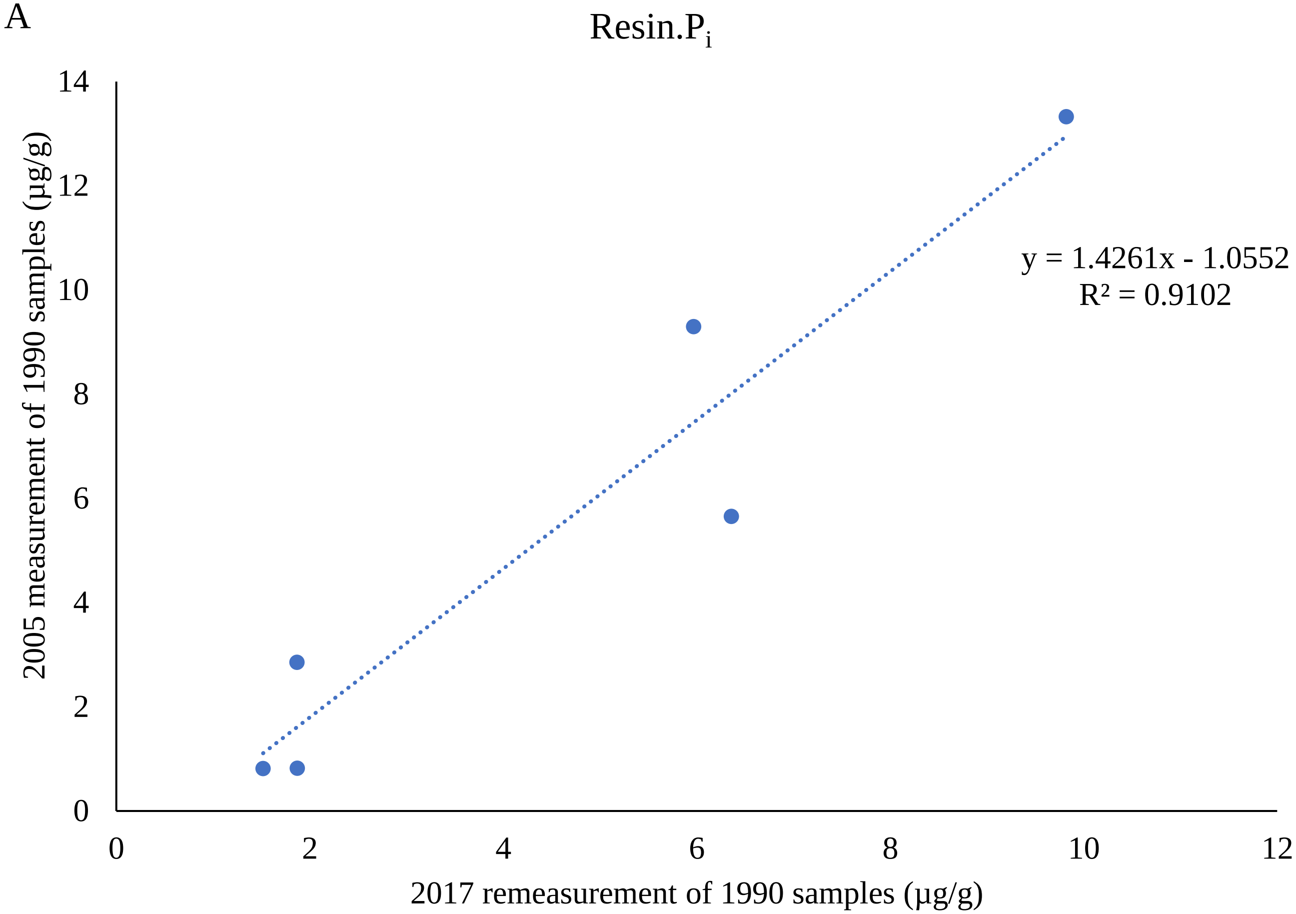
Resin.Pi
14
12
10
8
6
4
2
0
2005 measurement of 1990 samples (µg/g)
y = 1.4261x - 1.0552
R² = 0.9102
0
2
4
6
8
10
12
2017 remeasurement of 1990 samples (µg/g)

B

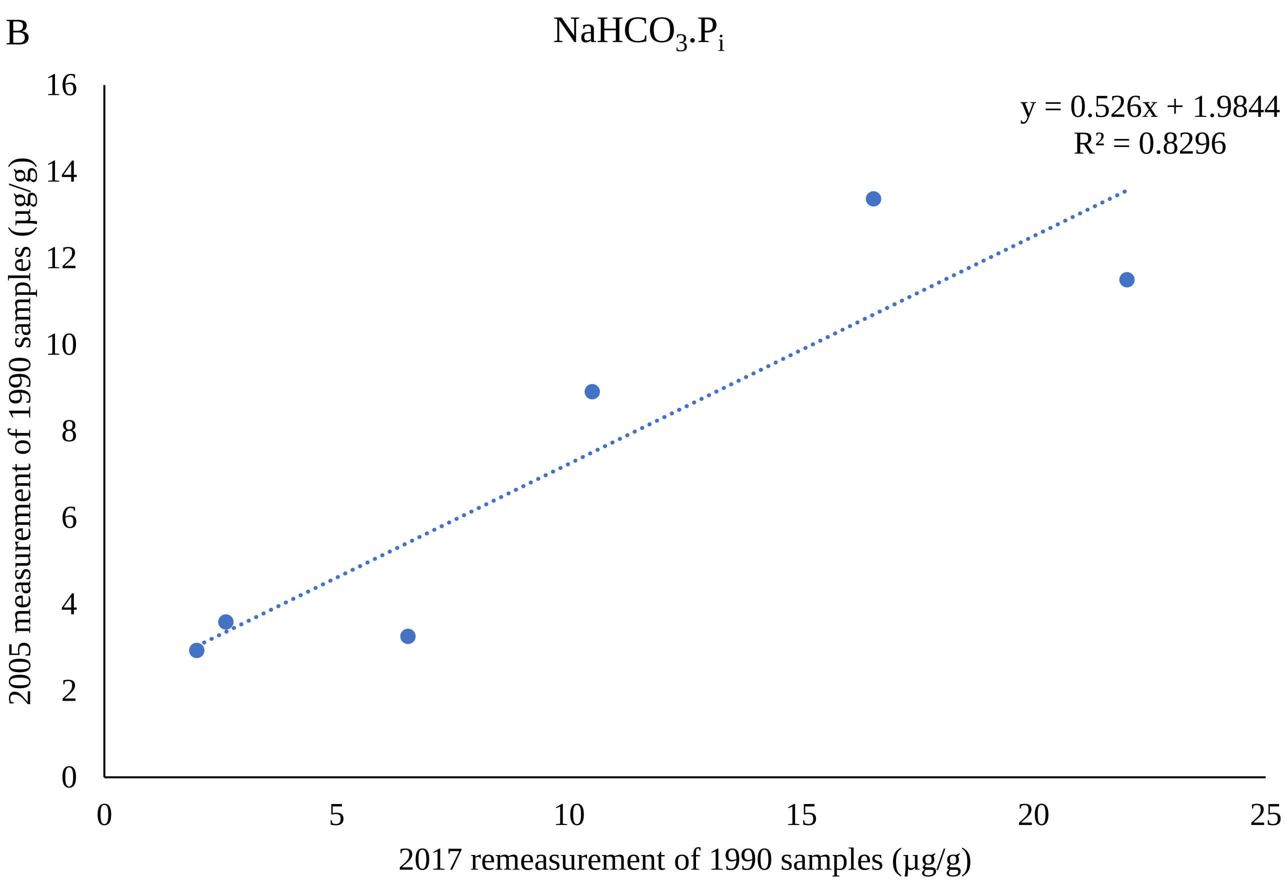
NaHCO3.Pi
y = 0.526x + 1.9844
R² = 0.8296
2005 measurement of 1990 samples (µg/g)
0
2
4
6
8
10
12
14
16
0
5
10
15
20
25
2017 remeasurement of 1990 samples (µg/g)

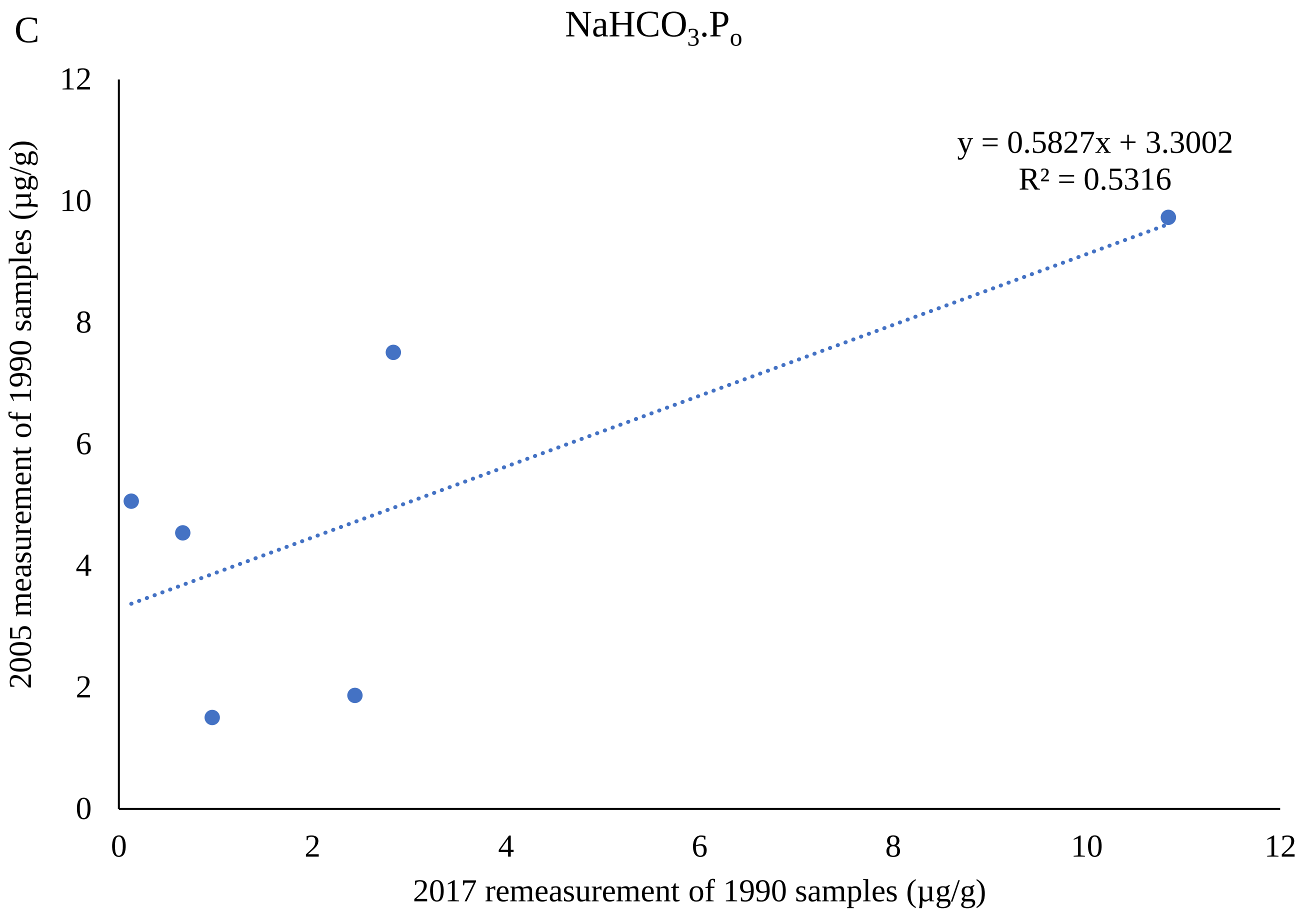
C
NaHCO3.Po
y = 0.5827x + 3.3002
R² = 0.5316
2005 measurement of 1990 samples (µg/g)
2017 remeasurement of 1990 samples (µg/g)
0
2
4
6
8
10
12

D

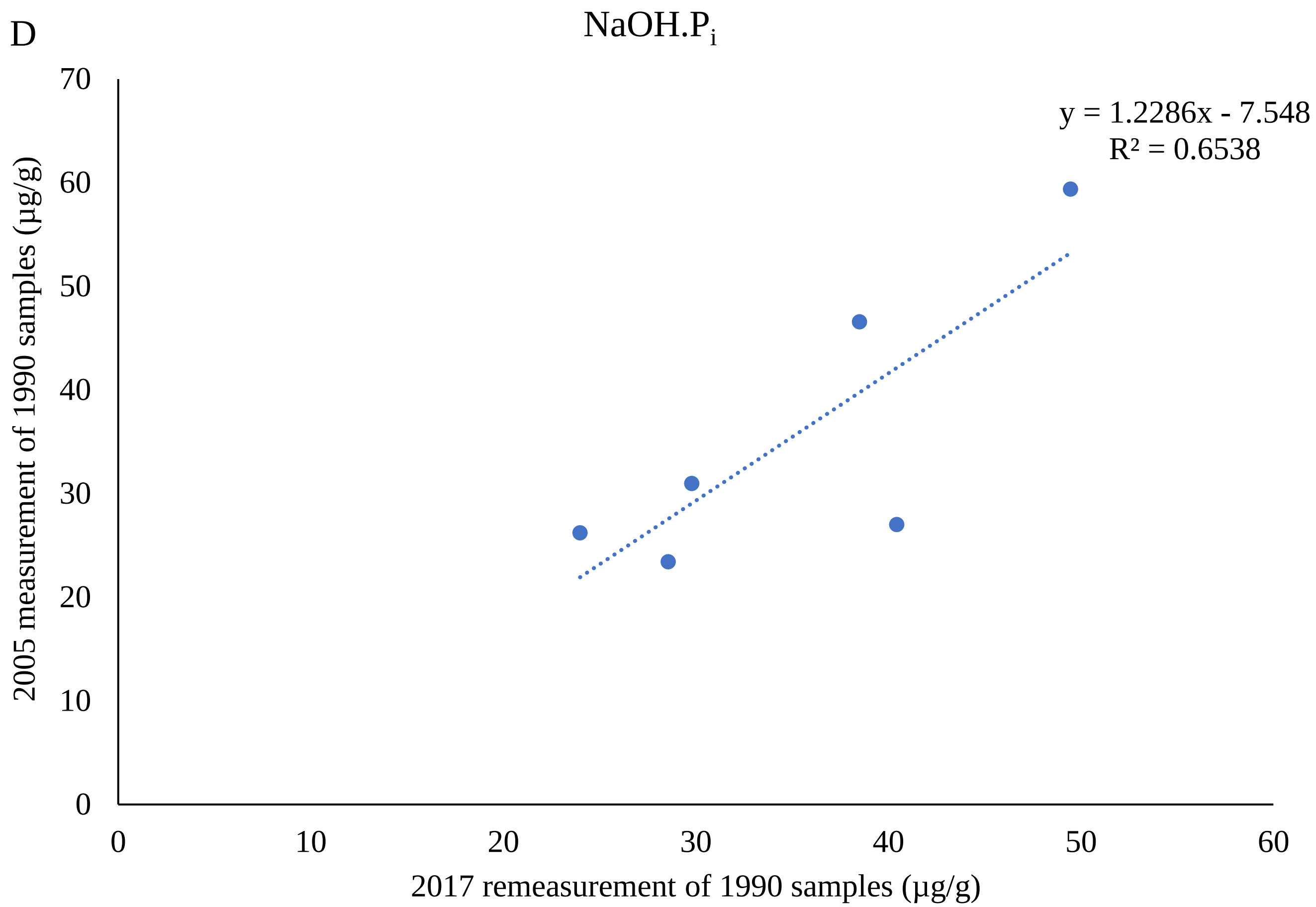
NaOH.P_i
y = 1.2286x - 7.548
R^2 = 0.6538
2005 measurement of 1990 samples (µg/g)
2017 remeasurement of 1990 samples (µg/g)
0
10
20
30
40
50
60
70

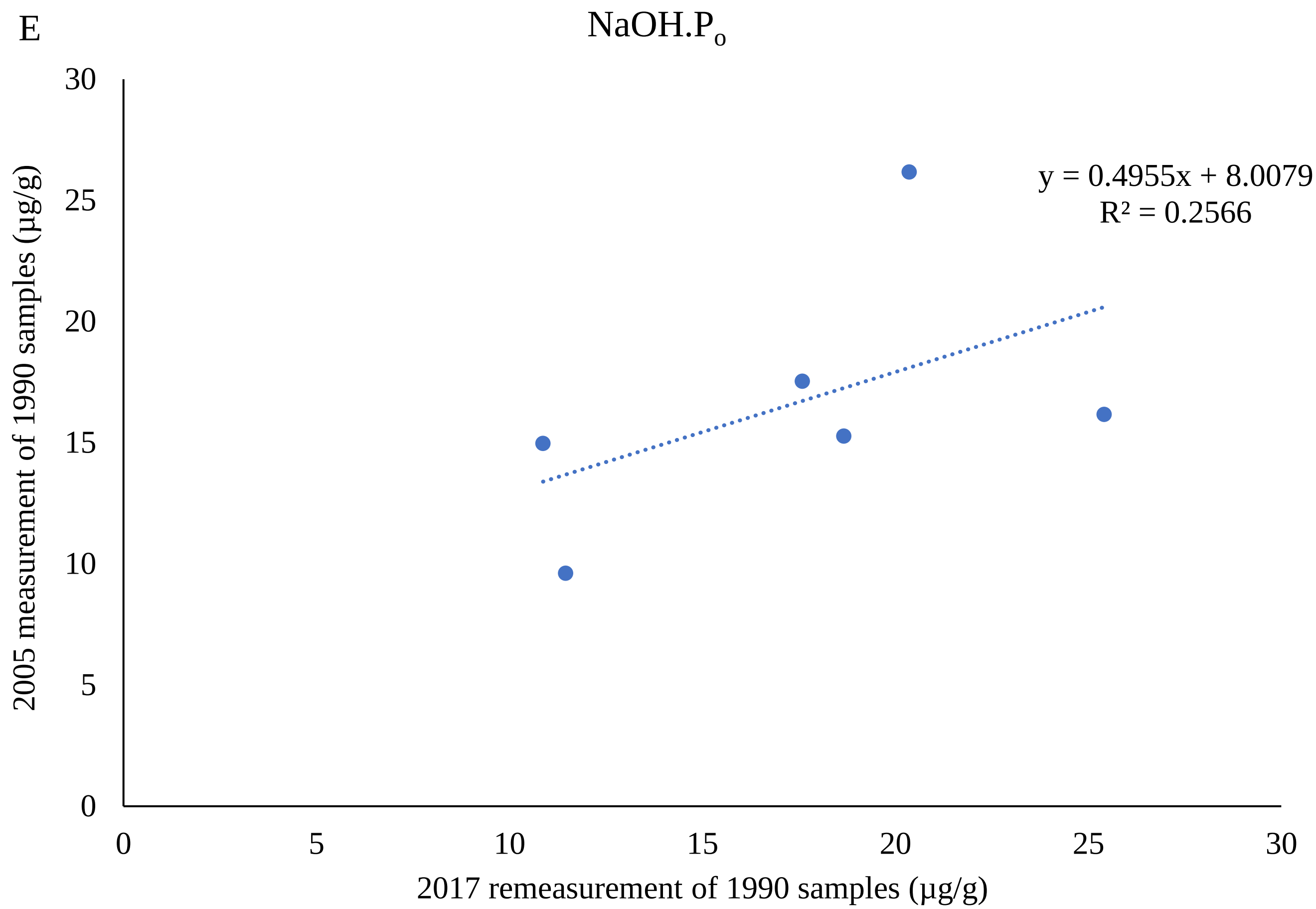

E
NaOH.P$_o$
y = 0.4955x + 8.0079
R^2 = 0.2566
2005 measurement of 1990 samples (µg/g)
2017 remeasurement of 1990 samples (µg/g)
0
5
10
15
20
25
30

F

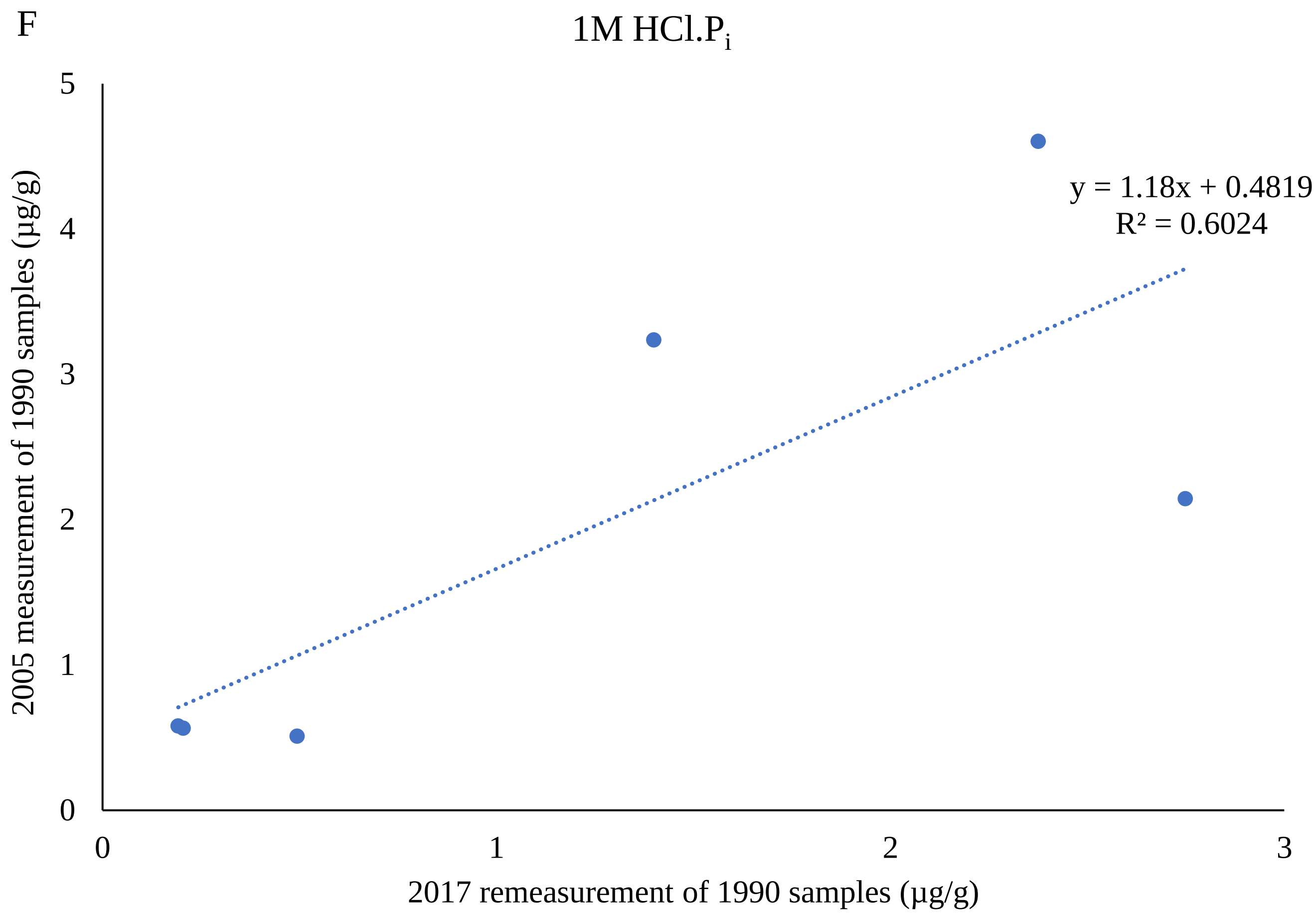
1M HCl.P_i
y = 1.18x + 0.4819
R^2 = 0.6024
2005 measurement of 1990 samples (µg/g)
2017 remeasurement of 1990 samples (µg/g)
0
1
2
3
4
5
0
1
2
3

G

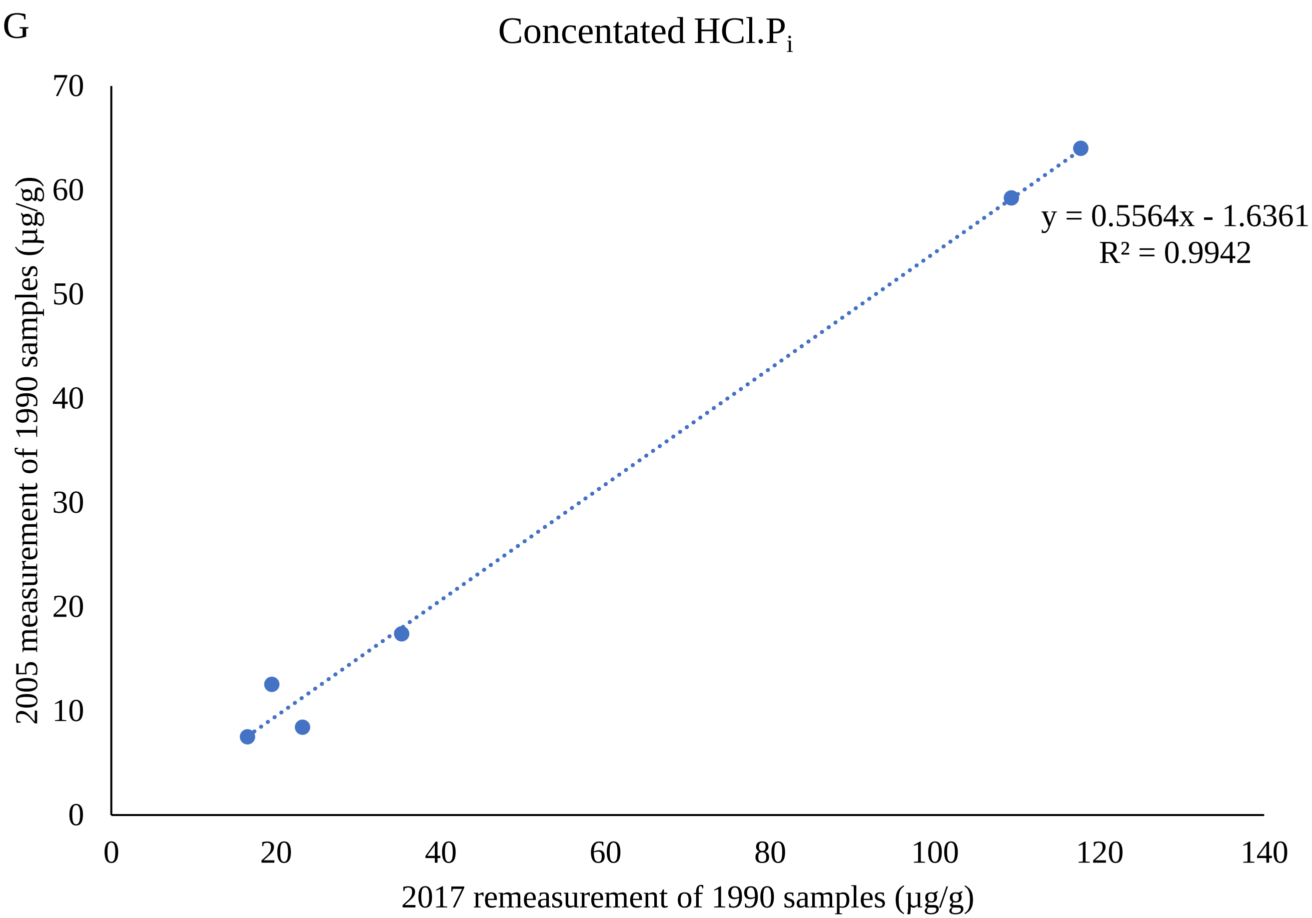

Concentated HCl.P$_i$
70
60
50
40
30
20
10
0
2005 measurement of 1990 samples (µg/g)
0
20
40
60
80
100
120
140
2017 remeasurement of 1990 samples (µg/g)
y = 0.5564x - 1.6361
R² = 0.9942

H

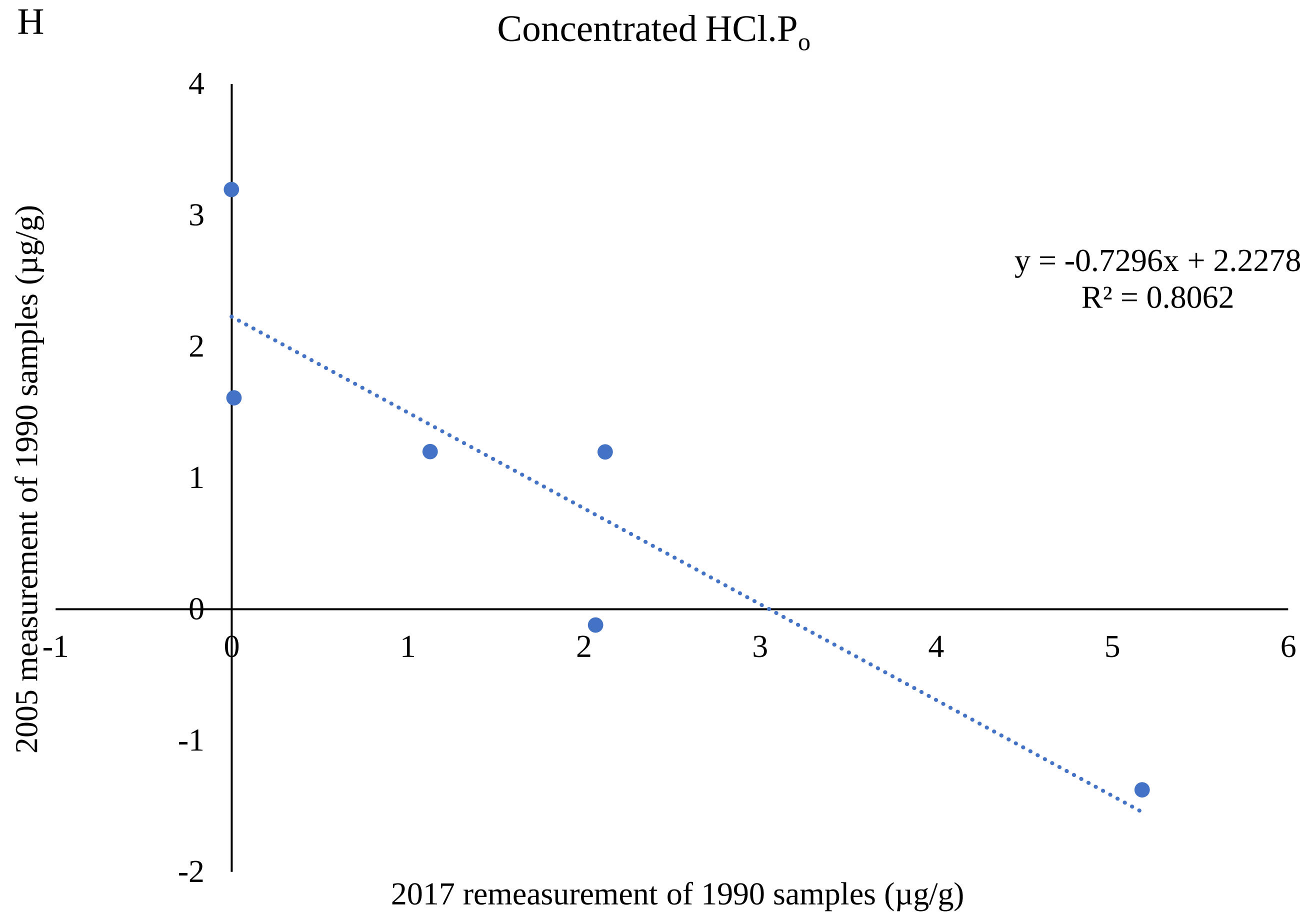

Concentrated HCl.P$_o$
4
3
2
1
0
-1
-2
-1
0
1
2
3
4
5
6
y = -0.7296x + 2.2278
R² = 0.8062
2005 measurement of 1990 samples (µg/g)
2017 remeasurement of 1990 samples (µg/g)

I

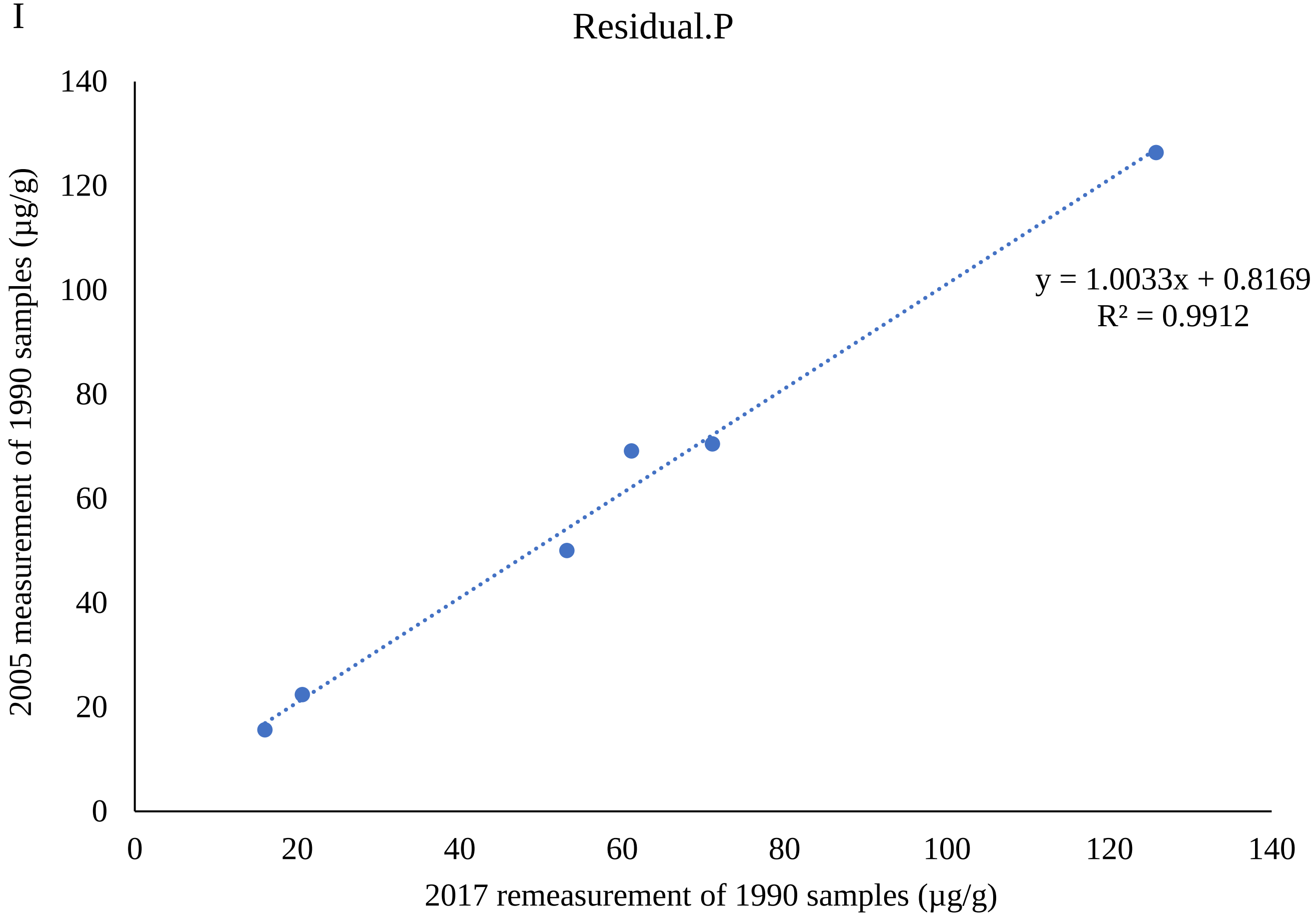
Residual.P
y = 1.0033x + 0.8169
R² = 0.9912
2005 measurement of 1990 samples (µg/g)
2017 remeasurement of 1990 samples (µg/g)
0
20
40
60
80
100
120
140

J

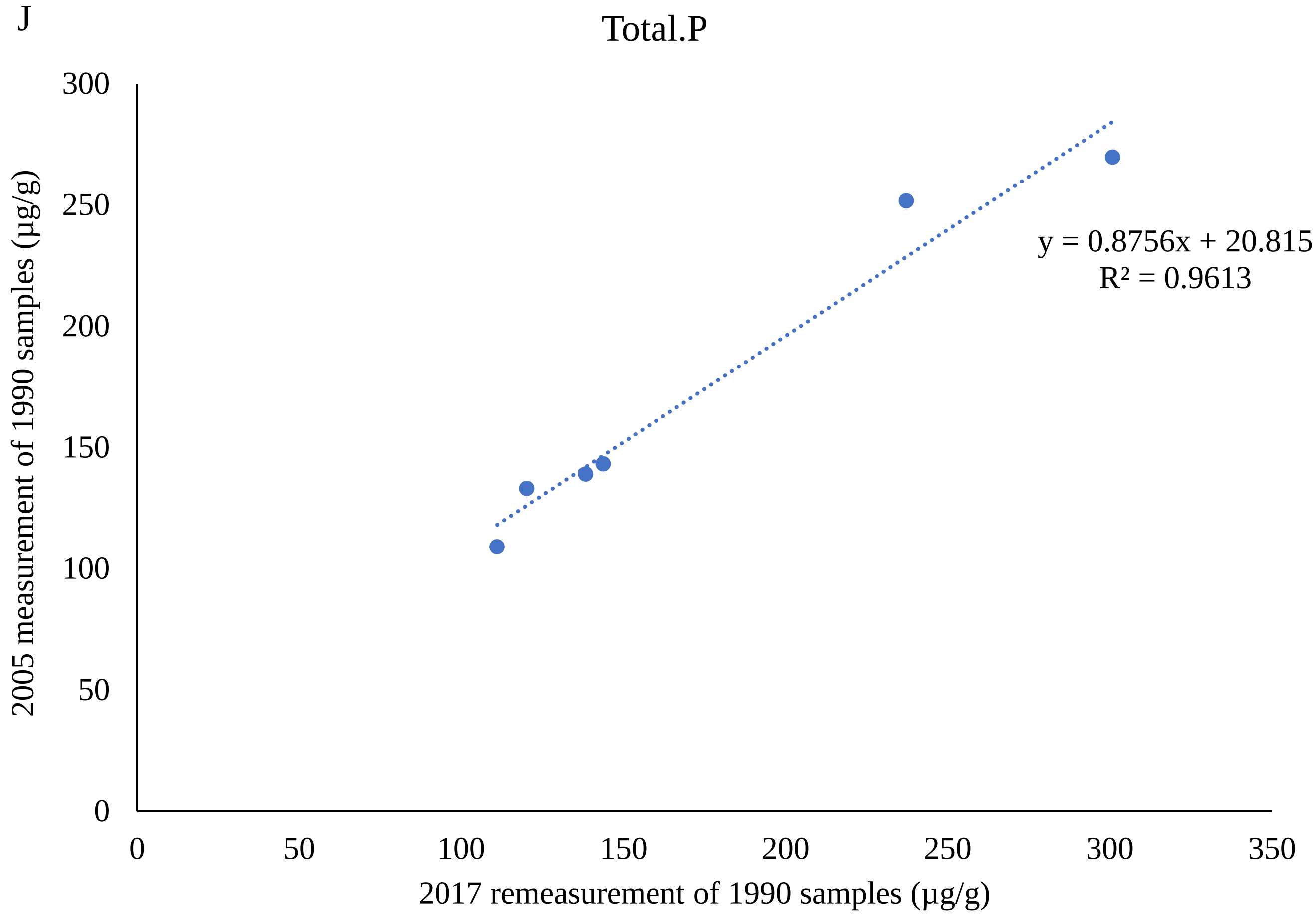

Supplementary Figure 4.2. Linear regression lines between phosphorus fractions measured in 2005 and 2017 of different samples collected from 8 permanent uncut plots in 1990 (Figures A-J).

A

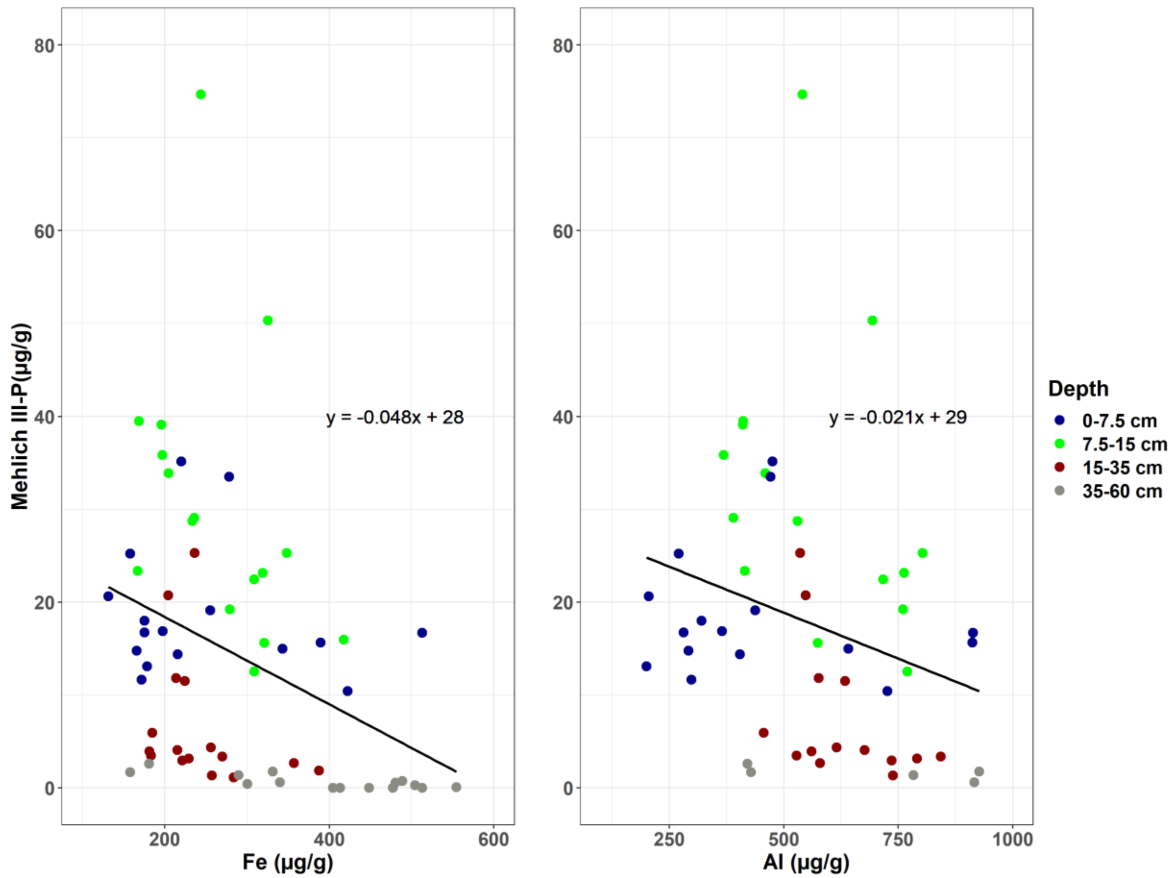
Mehlich III-P(μg/g)
80
60
40
20
0
200
400
600
Fe (μg/g)
y = -0.048x + 28
250
500
750
1000
Al (μg/g)
y = -0.021x + 29
Depth
0-7.5 cm
7.5-15 cm
15-35 cm
35-60 cm

B

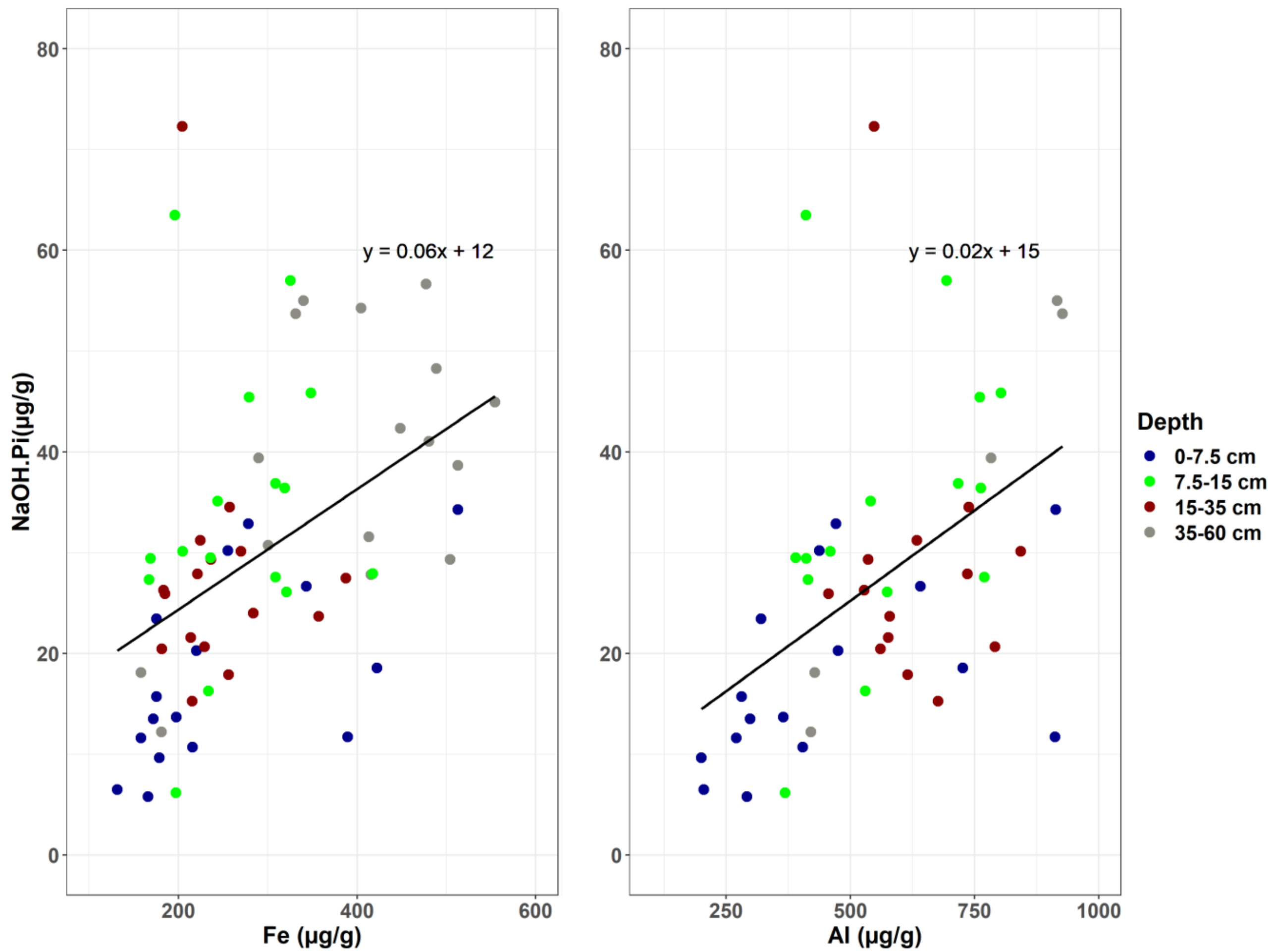
y = 0.06x + 12
y = 0.02x + 15
NaOH.Pi(µg/g)
Fe (µg/g)
Al (µg/g)
Depth
0-7.5 cm
7.5-15 cm
15-35 cm
35-60 cm

C

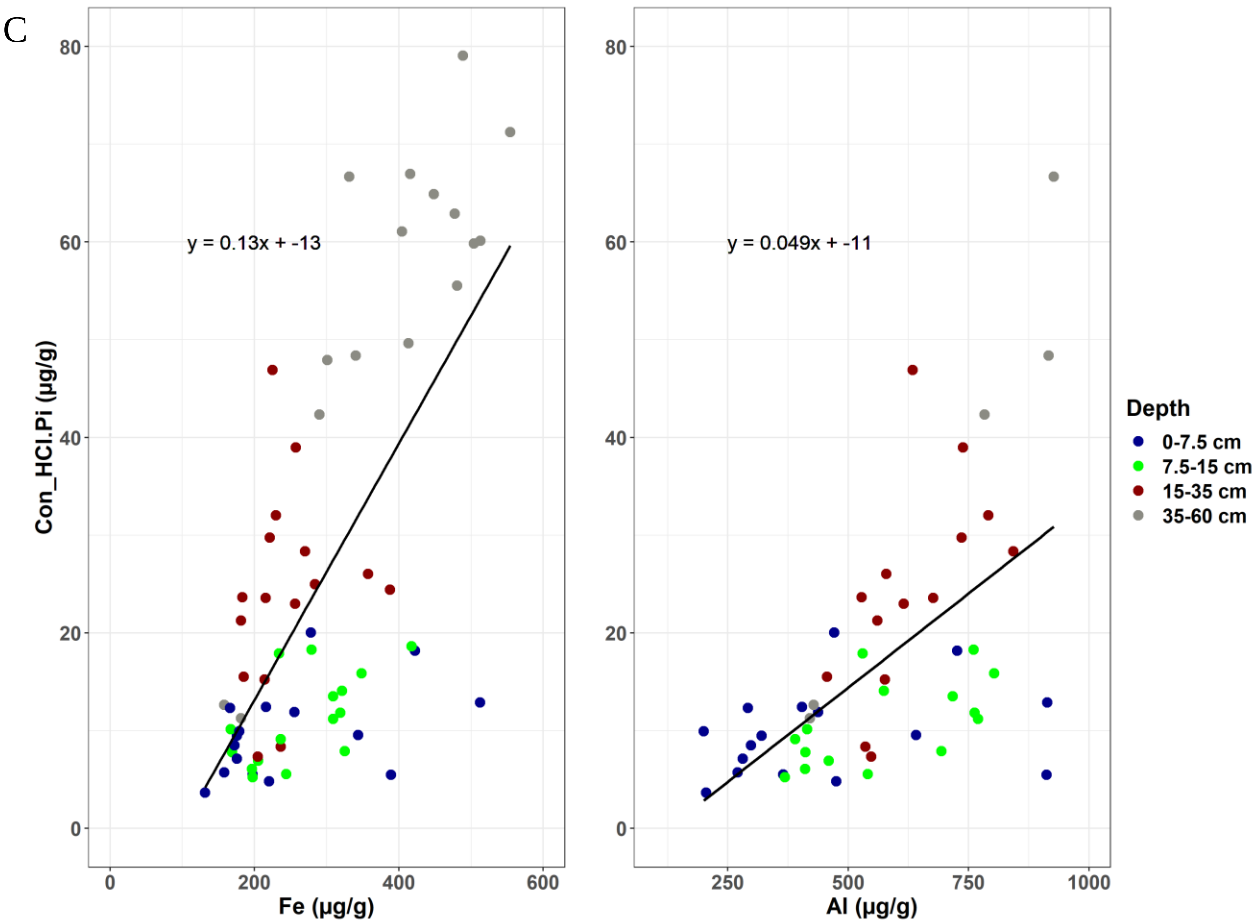

Supplementary Figure 4.3. Regression line between phosphorus extracted with Mehlich III (Figure A), NaOH (Figure B), and Concentrated HCl (Figure C) with iron (Fe), and aluminum (Al) extracted with Acid Ammonium Oxalic (AAO) of 8 permanent uncut plots in 1997, 2005 and 2017 at the Calhoun Experimental Forest, South Carolina.

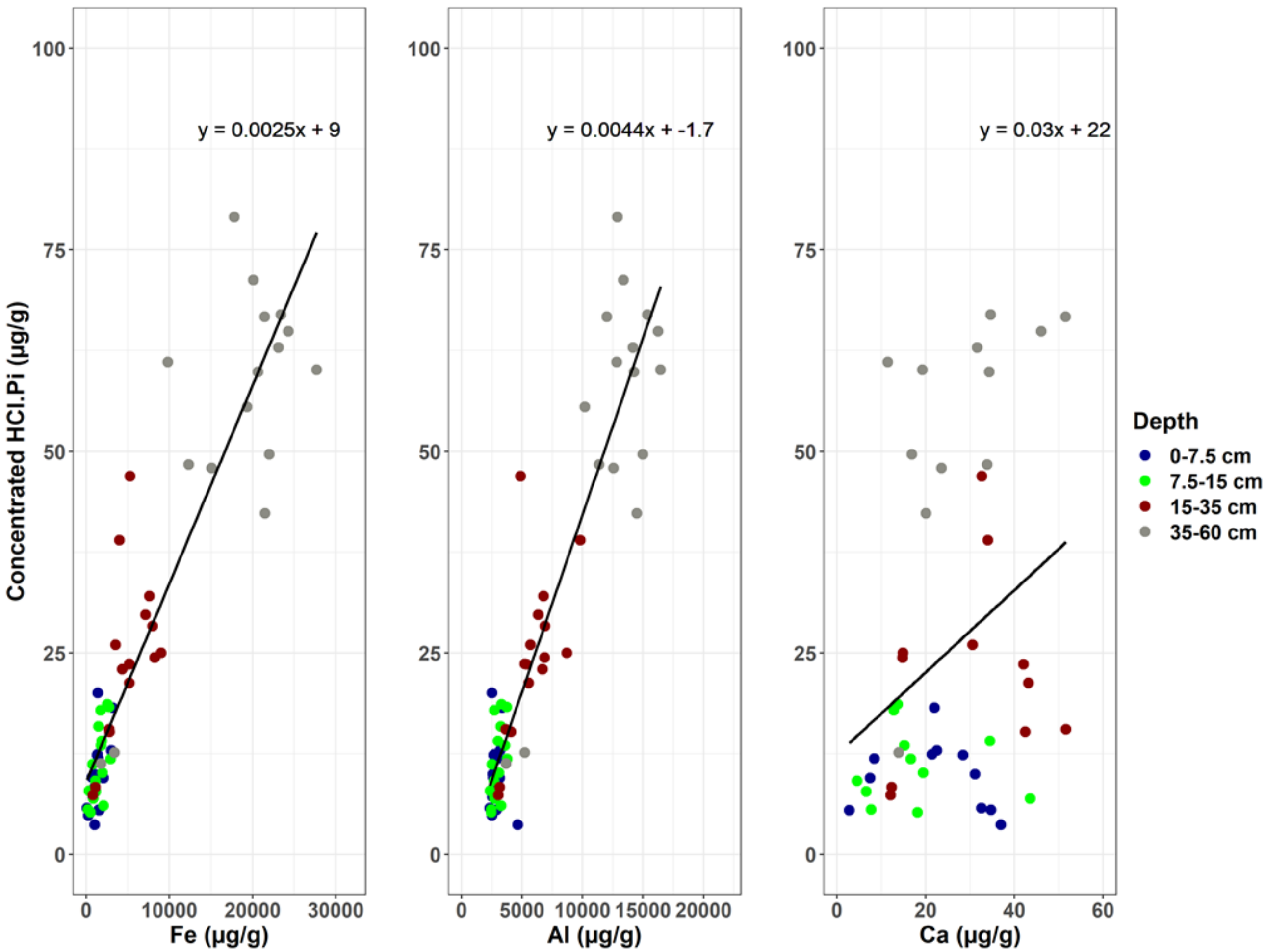

Supplementary Figure 4.4. Regression line between phosphorus (P) with iron (Fe), aluminum (Al), and calcium (Ca) extracted with concentrated HCl of 8 permanent uncut plots from 2005 and 2017 at the Calhoun Experimental Forest, South Carolina.

CHAPTER 5

THE IMPACTS OF HISTORICAL LAND USE ON PHSPHORUS MOVEMENT IN THE CALHOUN CRITICAL ZONE OBSERVATORY IN THE SOUTHEASTERN US PIEDMONT[1]

[1] M. Foroughi, J. Mallard, D. R. Nelson, L. A. Sutter, and D. Markewitz. To be submitted to Journal of Environmental Quality.

Abstract

Human interactions with the critical zone through land use can alter soil phosphorus (P) cycling and distribution. These P changes occur through both time and space as P is taken up by plants, and as added P fertilizer is translocated downslopes throughout the soil profile by erosion and leaching. In the southeastern US Piedmont, a more than one-hundred-year period of forest clearing and farming that included P fertilization caused severe surface erosion prior to reforestation. This history resulted in elevated surface soil P in farmed ridge tops, even after 70 years of reforestation, but little data exists on redistribution of this P downslope or down profile during these 70 years. The objective of this study is to investigate the effect of different land use histories on P losses over time. Combined with multiple years of current site data on soils, soil solutions, and stream waters from two small watersheds in the Calhoun Critical Zone Observatory (Calhoun CZO) in South Carolina, USA, we use the soil and water assessment tool (SWAT) to simulate different land use trajectories (mature deciduous forest, upland agriculture and lowland forest, agricultural land, afforestation with upland agriculture, pine forest, and mixed-forest) on P movement. We expected that P movement in watersheds during farming with fertilization would be high relative to forested conditions (mature deciduous, pine, or mixed) and that periods of agriculture with forest (upland agriculture with afforestation or lowland forests) would be intermediate. Also, we expected that intensive rainfall would accelerate surface erosion having a non-linear, positive effect on P redistribution. Results indicated the annual total P loss under 100% agriculture (3.7 kg $ha^{-1}yr^{-1}$) was six times greater than under 100% forest land cover (0.6 kg $ha^{-1}yr^{-1}$) while intermediate conditions were only 1/3 of loss under agriculture. Furthermore, the model predicted range of P leaching in the soil profile was 0.036 to 0.1 kg ha^{-1} yr^{-1}, which could

account for 7-20 kg ha^{-1} of vertical P movement over 200 years. This rate of leaching is consistent with differences in extractable soil P measured through 2m under farmed and never farmed locations. Simulation under high rainfall indicated more P could be mobilized during wet periods (i.e., hurricanes). These land use change simulations demonstrate how historical land use could impact soil P re-distribution downslope and down profile.

1. Introduction

Transformation of forest land to agricultural use and return to forest cover has left a legacy of impacts on forest soils (Richter and Markewitz, 2001; McLauchlan, 2006). Land use and land management influence soil chemistry, soil erosion, and soil nutrient runoff to surface water (Johnes and Heathwaite, 1997; Grieve, 2001; Wang *et al.*, 2010). Given a period of agricultural crop production and fertilization, these activities have particularly influenced soil P and its landscape distribution (Alt *et al.*, 2011; Aguiar *et al.*, 2013; Foroughi *et al.*, in review). A variety of attributes and actions impact P movement in watersheds such as inherent soil P concentration, P loading to the soil through fertilization or organic amendments, watershed land cover and clearing, tillage, topography, soil erodibility, and precipitation quantity and intensity (Dillon and Kirchner, 1975; Sharpley *et al.*, 1981; Osborne, 1988; Sharpley and Smith, 1990). For example, Sharpley *et al.* (1996) demonstrated how P loading that results in Mehlich III soil P concentrations of >200 mg kg^{-1} are excessive and likely to generate P runoff. Similarly, Elrashidi *et al.* (2005) exhibited increased water (1122 vs 939 m^3 ha^{-1}) and P (217 vs 190 g-P ha^{-1}) runoff in croplands compared to native grasslands. Finally, Sharpley (1985) revealed a clear link between increasing rainfall intensity (50-150 mm h^{-1}) and slope (2-20%) with the effective depth of surface soil generating P runoff (2-14 mm).

Two centuries of land use history in the eastern US has followed a trajectory of forest to agriculture to afforestation that has extensively influenced soil properties (Compton and Boone, 2000; Foster *et al.*, 2003). The southeastern Piedmont of the US was particularly altered due to an extended era of cotton farming (Wear and Greis, 2013). Land use and land management changed in the Southeast from the 1700s to 1800s with a transition from mature forest to crop land. Subsequently, the abandonment of agricultural land to afforestation occurred after the 1900s

(Brender, 1952; Cowell, 1998). More than half of the Eastern forest of the US was cleared and converted to farm, pasture, and industry in the 17th century (Williams, 1992). By the 18th century, however, the proportion of agricultural land in the southeastern Piedmont of the US began to decline (Hart, 1980). For example, coniferous and deciduous forest covered less than 19% of the Georgia Piedmont in the 1930s when agricultural land comprised 81% (Turner and Ruscher, 1988). By 1980, agricultural land declined to 36% whereas the coniferous forest distribution increased to 41%. Recently, in 2016 forests covered more than 67% of Georgia and South Carolina (Vogt and Smith, 2017).

Well-known soil legacies of this history of land clearing and farming in the southeastern US include excessive surface soil erosion (Ireland *et al.*, 1939; Hall, 1949; Trimble, 1974) and P enrichment (Richter and Markewitz, 2001; Richter *et al.*, 2006). Nearly 17 cm of surface soil is estimated to have eroded from hillslopes in the Southeast between 1750-1950 (Trimble, 2008). During this period, there was increasing P fertilization in upland locations (Ruffin, 1852) and surface soil available P is still elevated due to these practices (Richter and Markewitz, 2001). For example, in the Piedmont of South Carolina in 2017, when comparing hardwood forest soils that were never farmed to forest soil under 70-year-old afforesting crop fields available soil P was still 50-100% greater (4 to 6 ug-P g-soil^{-1} in surface soil or 2 to 4 ug-P g-soil^{-1} in subsoil); a difference evident through 2 m of soil (Foroughi *et al.*, in review). Phosphorus enrichment in the top-soil layers of agricultural land can lead to P leaching loss and P movement with soil erosion (Hurtt *et al.*, 2006), and a strong correlation between agricultural land use and P movement into streams has been demonstrated (Nielsen *et al.*, 2012). On the other hand, in the South Carolina location noted above, after 70 years of afforestation soil solution P was lower in abandoned sites compared to the never farmed reference and 1st order streams in afforested watersheds were typically < 1 µmol P

L^{-1} (Foroughi *et al.*, in review). The mechanism for high P fluxes during agriculture transitions to low P fluxes under afforestation while retaining elevated soil P is difficult to resolve given a lack of long-term measurements.

Recent reviews of agricultural legacies on soil and solution P (MacDonald *et al.*, 2012; Deng *et al.*, 2017; Goyette *et al.*, 2018) have all addressed the dichotomy observed above of the potential for high P loss during agricultural use but with a long-term persistence of soil P enrichment, which suggests limited P losses. MacDonald *et al.* (2012), for example, using a meta-analysis of 94 studies demonstrated a clear increase in soil P in abandoned agricultural land compared to reference sites with no farming history (similar to results documented above for South Carolina) but also found that abandoned areas, depending on land use, had lower soil P than current agricultural areas. This suggests that although soil P is enriched after abandonment some soil P continues to be lost and land use might influence the rate of loss. Deng *et al.* (2017) specifically looked at abandoned agricultural areas in 220 independent sampling sites that had been afforesting. In these areas, they noted an overall decline in total soil P content (12% on average) with afforestation but no measurable change in available P concentrations (~27 µg-P g-soil^{-1}), highlighting a continued loss of P but also a buffering of the available P pool (Schmidt *et al.*, 1997; Richter *et al.*, 2006). They also highlighted that total P declined most in afforesting tropical sites suggesting that rainfall inputs may play an important role in P loss. Finally, Goyette *et al.* (2018) reconstructed 110 years of P fluxes in 23 watersheds and concluded that the time to eliminate legacy P in runoff might range from 100 to 2000 years. They also suggest this variance is a function of rainfall and land use.

In the southeastern US Piedmont today, we find P enriched soils through 2 m but also limited soil solution P and first order stream water P concentrations (Foroughi *et al.*, in review).

The quantify of P lost to streams or leached through the soil profile when these lands where transforming from active agricultural to afforestation over a 200-year period is not well known. Modeling P solution fluxes through soils and to streams during these land use changes may help us to understand these land use dynamics (Veldkamp and Verburg, 2004). Previous modeling studies have investigated the impact of future land use and climate changes on runoff and P flows (Wilson and Weng, 2011; Mehdi *et al.*, 2015; Jiang *et al.*, 2018). For example, Mehdi *et al.* (2015) highlighted how combining land use and climate change scenarios could increase loss of total P by 8-foldcompared to climate change scenarios alone. Similarly, Wilson and Weng (2011) tested the effect of future urban land use and climate changes on water quality in the Chicago metropolitan area. They found that total P concentration should decline in watershed streams as a result of a reduction in agricultural land (2-18%), industrial (1-3%), medium density residential (4-7%), or low density residential (2-7%) uses.

The objectives of this modeling study were to:1) assess the legacy effect of land use changes on the surface and subsurface movement of P and 2) determine the impact of precipitation inputs on surface and subsurface P movement under these different land use scenarios. We expected that cultivation and P fertilization would cause P movement to the surface water due to runoff and soil erosion. Thereafter, loss of P would decrease with agricultural land abandonment and afforestation. In addition, during this period we expected part of the applied fertilizer P would be leached through the soil profile. We also expected that total P fluxes would be increased when the precipitation rate was increased, especially when land was still under agricultural use due to more soil and sediment runoff to the stream. Finally, we hypothesized that leaching of soluble P would be greater in afforested land because of historical agricultural use.

2. Methods

2.1 Study site

Our study watersheds, W4 of 8.75 ha and W3 of 10.3 ha, are situated in the Calhoun Critical Zone Observatory (Calhoun CZO) within the Sumter National Forest (34° 7' 55.36" N, 82°18' 36.17" W) in Union County, SC (Fig. 5.1). Elevation ranges from 125 to 172 m and nearly 85% of the watershed slope is 0-30% (Fig. 5.2). The average temperature and annual precipitation of this region between 2011-2018 was 17°C and 1185 mm, respectively (Clinton, SC; https://www.ncdc.noaa.gov/cdo-web/). Approximately, 93% of this watershed is covered by forest (deciduous and pine) and 7% by grasses (Fig. 5.2).

2.2 Land use history data and scenarios

Land use history data for the Calhoun CZO revealed that hardwood forest declined from ~85% to <10% between 1790 to 1910 while open land (i.e., agricultural land) increased to ~90% in 1910. Thereafter, between 1910 to 1940 open land declined to ~50% while hardwood and pine forest has developed slowly to cover ~25 and 10% of the landscape, respectively (Fig. 5.3). The data in Fig. 5.3 were derived from US Forest Service (USFS) archives that contained legal descriptions, maps, deed abstracts, and other records pertaining to land acquisition by the US Forest Service. At the time of purchase, the USFS recreated deed chains for each of the properties, going back to the original land grants, whenever possible. When land transactions occurred, whether through sale, inheritance, partitioning, or other mechanism, surveyors mapped the property using the metes and bounds system (Pettus, 1995). The metes and bounds surveys fixed property boundaries based on landscape features (including trees, rivers, and later, as trees became scarcer, stakes and rocks) and compass bearings. The land use data are from 60 out of 518, randomly selected properties. For each property, the landscape features were recorded for each historical transaction, and later aggregated into hardwood, pine, open, and water categories. The category counts for each decade represented the sum of transaction records for the previous 10 years (e.g., 1850 includes data from 1841-1850). The Calhoun Experimental Forest was covered with mixed hardwood forest before 1800, then the upland forest was converted to agricultural land (Ruffin, 1852; Gray and Thompson, 1933; Metz, 1958). Furthermore, farmers applied P fertilizer and lime to the land after intensive deforestation (Taylor, 1953; Sheridan, 1979). Most of the agricultural lands were abandoned and then converted to regrowth forest or pasture in the early 20th century (Metz, 1958; Richter and Markewitz, 2001). Based on these specific records for the Calhoun CZO and other historical accounts for the region scenarios for model simulation where developed.

Six land use scenarios were simulated (Fig. 5.4) to approximate the forest to cropland to afforestation trajectory. The starting watershed condition is covered with mature deciduous forest (FRSD). Thereafter, flatter, upland areas that were likely cleared first are converted to agricultural land for a mixed land use watershed (FRSD+AGRR). The next step assumes less desirable lands (i.e., steeper) were cleared and brought into agriculture such that 100% of watershed area is converted to agricultural land (AGRR). As economic and environmental conditions changed it is presumed some of the less desirable lands were abandoned and pine forests started to develop on these hillslopes (AGRR+FRSE). We then abandoned agriculture in the uplands and the whole watershed area is covered with pine forest (FRSE). Finally, the most recent land use that approximates current conditions is a mixture with the pine trees persisting in the flatter upland and hillslopes reverting to deciduous forest (FRSD+FRSE) (Fig. 5.4). The current land cover map contains around 7% grassland, but it was not considered for the simulation scenarios.

Each scenario is simulated for a ten-year period and the results are reported as an average over the ten-year period. Initial soil P was set at measured reference conditions (2 ug g^{-1}). Reported rates of historical fertilization indicate that farmers normally applied 200-300 lb/ac (224-336 kg ha^{-1}) fertilizer with 11-20-13 (N-P-K) or 500 to 600 lb/ac (560-673 kg ha^{-1}) 4-10-6 fertilizer (Taylor, 1953; Sheridan, 1979). Based on these reports, agricultural land area in each scenario received annual inputs of 230 lb/ac (250 kg ha^{-1}) fertilizer application of N-P-K (11-20-13). Initial soil P was increased to 20 ug g^{-1} after agricultural abandonment based on reported values after afforestation on prior agricultural land at the Calhoun CZO (Richter *et al.*, 2006). Similarly, available P was set to 5 ug g^{-1} for the current land use scenario based on measurements from the watersheds in 2017 (Foroughi *et al.*, in review). All these land use scenarios were simulated based on two different precipitation conditions (i.e., normal and high). The normal precipitation was an annual input of 1169 mm, while the higher precipitation was 2688 mm. This is consistent with the highest rainfalls recorded between 1979-2014 (https://www.ncdc.noaa.gov/cdo-web/).

2.3 SWAT model description

The Soil and Water Assessment Tool (SWAT) was implemented to determine the influence of land management activity on streamflow (discharge), P loss into runoff, and P leaching in soil layers (Arnold *et al.*, 1993; Arnold *et al.*, 1998). The SWAT model predicts the effect of different land use and land management on the quantity and quality of water and soil over multiple years (Arnold *et al.*, 1998; Neitsch *et al.*, 2011). SWAT employs a daily time step that can be aggregated to report monthly output (Wilson and Weng, 2011). The study watershed is divided into sub-watersheds based on a digital elevation model (DEM) and each sub-watershed includes multiple hydrological response units (HRU), which increases simulation accuracy. Each sub watershed and HRU has a unique soil type, land use, and slope. In addition, SWAT needs information on hydrology, maximum and minimum air temperature, precipitation, erosion, plant growth, initial nutrient concentrations, pesticide and fertilize inputs, and specific agricultural management (Gassman *et al.*, 2007). In this study, we only tracked outputs for discharge, P loss into stream, and P leached in the soil profile.

2.3 SWAT input data

The ArcSWAT 2012 interface was used to build this model using a DEM with 1×1 m resolution, a land use map obtained from the National Land Cover Dataset (http://www.mrlc.gov), and the Soil Survey Geographic Database (SSURGO) extracted from the web soil survey (https://websoilsurvey.sc.egov.usda.gov/). Climate data were gathered from the National Oceanic and Atmospheric Administration (https://www.ncdc.noaa.gov/cdo-web/) using the nearby Clinton, SC station including maximum and minimum temperature, and precipitation. In addition, onsite precipitation data for 2015 and 2016 were available and utilized [(Mallard, 2017); unpublished data]. According to the soil map, most parts of the watersheds (87.8%) are loamy, mixed, active, thermic, shallow Typic Hapludalfs with a small portion (12.2%) of the upland as fine, mixed, active, thermic Ultic Hapludalfs (12.2%). The soil layers are generally A (=< 7.6 cm), E (7.6- 20 cm), Bt or Be (15-53 cm), Bt1 (25-84 cm), or Bc (33-122 cm).

2.4 Model calibration and validation

Stream discharge was consistently measured in watersheds W3 and W4 during 2015-2017 and these data were used to calibrate and validate the model for streamflow [(Mallard, 2018); unpublished data]. Furthermore, monthly stream samples were collected in these same watersheds to measure P concentration through 2014-2017. SWAT was calibrated using W4 for daily and monthly streamflow, monthly total P, and monthly inorganic P with the SWAT Calibration and Uncertainty Program (SWAT-CUP) version 5.2 using the SUFI2 (sequential uncertainty fitting) version 2 (Abbaspour *et al.*, 2007; Abbaspour, 2013). The daily and monthly streamflow were initially calibrated with 15 parameters, then the P concentration parameters were calibrated. According to the calibration process, the sensitive parameters for streamflow and P were adjusted in SWAT (Table 5.1). The validation model was performed for daily and monthly discharge and monthly P for W3 with the same condition of soil type, land cover, hydrology, and slope (Fig. 5.2). The coefficient of determination (R^2), Root Mean Square Error (RMSE), and Nash-Sutcliffe Efficiency (NSE) were used as the primary objective functions for calibration and validation.

3. Result

3.1 Calibration and validation

The calibration between observed and simulated discharge in daily and monthly time steps were generally well correlated (Figure 5.5 and 5.6, respectively). Occasionally, peak observed and predicted discharge values were not well correlated, which may relate to the lack of onsite rainfall data. The correlation and NSE between daily observed and simulated streamflow were ≥0.59 for both W4 and W3 (Table 5.2). Similarly, the NSE of monthly calibration and validation for streamflow were 0.72 and 0.55, respectively (Table 5.2). Observed and simulated total P and inorganic P were also generally well aligned (Figure 5.7). The monthly calibration had NSE with a range of 0.39 for total P and 0.46 for inorganic P. For the validation the NSE ranged from 0.34 to 0.31 for monthly total P and inorganic P, respectively (Table 5.2).

3.2 Streamflow under land use and precipitation changes

Using the calibrated model based on the current conditions described above we simulated the different land use change scenarios for discharge. The model simulation starting with FRSD found 38% (453 mm) of annual precipitation as runoff. As uplands were initially cleared

(FRSD+AGGR) runoff increased to 41% percent (482 mm). After 100% of the watershed was converted to agriculture (AGRR), runoff reached the highest amount of 563 mm or 48% as runoff (Fig. 5.8). During initial agricultural abandonment under AGRR+FRSE with secondary pine forests on the hillslope, runoff declined again to 37%. As land use reverted to fully forested conditions under FRSE and FRSE+FRSD runoff was 36% (418-420 mm).

For the high rainfall simulations using the same land use scenarios, although the amount of precipitation increased only two-fold relative to average rainfall years, streamflow increased around three-fold. Streamflow increased from 453 to 1371 mm per year under FRSD and from 562 to 1620 mm with AGRR land cover (Fig. 5.8). The other forested conditions (FRSE, FRSE+FRSD) were similar to FRSD, which also shared greater similarity to the mixed land covers of FRSD+AGRR and AGRR+FRSE with lower increases than the 200% increase observed under AGRR.

3.3 Patterns of P loss under land use and precipitation changes

For total P runoff to streams, the results of the simulations from the different scenarios indicated that the total P loss increased by ~ six-fold from 0.6 to 3.7 kg ha^{-1} yr^{-1} when 100% mature hardwood forest (FRSD) was converted to 100% agricultural land (AGRR) that included application of P fertilizer (Fig. 5.8). This increase in P runoff from fully forested (FRSD) to fully agriculture (AGGR) followed a rising and falling pattern with land use conversion and recovery. In contrast to the discharge patterns mixed land uses had an intermediate level of P runoff compared to FRSD and AGGR. When upland portions of the watershed were agriculture, but the rest was covered with forest (FRSD+AGRR and AGRR+FRSE), the total P loss ranged from 1 to 1.2 kg ha^{-1} yr^{-1}. As land returned to fully forested (FRSE and FRSD+FRSE) loss of total P ranged from 0.6-0.9 kg ha^{-1} yr^{-1}.

The response of total P loss to rainfall quantity indicated that the loss of P increased from 0.6 to 1 kg ha^{-1} yr^{-1} on average when the watershed was covered with mature hardwood forest (FRSD). Under higher rainfall, the total P loss increased by ~1.5 fold (1.2 to 1.7 kg ha^{-1}) when uplands were initially cleared (FRSD+AGGR). The highest loss of total P occurred when the watershed was AGRR with high rainfall (4.46 kg ha^{-1}). Thereafter, along the trajectory but still with higher rainfall, the total P loss to surface water increased from 1.0 to 1.6 kg ha^{-1} (AGRR+FRSE). Finally, total P loss in forest land after complete abandonment of agricultural land (FRSE and FRSD+FRSE) increased from 0.9 to 1.2 kg ha^{-1} (FRSE) and 0.6 to 1.0 kg ha^{-1}(FRSD+FRSE) with two-fold higher rainfall (Fig. 5.8).

Inorganic P runoff to streams followed the same pattern as total P under average precipitation conditions. The model predicted that inorganic P loss increased during forest clearing and conversion to agricultural land. Under FRSD inorganic P loss was 0.02 kg ha^{-1} while the highest loss of inorganic P was 0.18 kg ha^{-1} when the entire watershed was under cultivation (Fig. 5.8). Again, inorganic P loss trended up and down with forest loss (FRSD+AGRR and AGRR) and recovery (AGRR+FRSE, FRSE, and FRSE+FRSD). Interestingly, inorganic P loss was higher under FRSE and FRSE+FRSD compared to FRSD, likely due to historical application of P to agricultural land that increased initial soil P in model parameterizations. The content of inorganic P loss with the two-fold increase under high rainfall increased proportionally such that fluxes were 50-60% higher for all land use scenarios.

3.4 *Soil P leaching*

The model predicted that 0.06 kg ha^{-1} of soluble P leached annually from the first soil layer to the second soil layer (below 7.5 cm) when land use was mature hardwood forest (FRSD). Leaching of P into the soil declined to 0.05 kg ha^{-1} when the upland part of the watershed converted to agriculture (FRSD+AGRR). Phosphorus leaching was even slightly lower (0.036 kg ha^{-1}) when the entire watershed was converted to agricultural land, AGRR. Leaching of soluble P increased to 0.092 kg ha^{-1} with early afforestation in most of the watershed (AGRR+FRSE). Similarly, P leached around 0.1 kg ha^{-1} when the watershed covered to pine forest (FRSE); however, it declined to 0.06 kg ha^{-1} after the watershed was covered with FRSE+FRSD mixed forest (Fig. 5.8). Under high precipitation P leaching increased by 0.05 to 0.27 kg ha^{-1} under FRSD, FRSD+AGRR, and FRSD+FRSE.

The response of P leaching to high rainfall was increased P translocation to the second soil layer from 0.06 to 0.27 kg ha^{-1} when the watershed was FRSD and FRSD+AGRR. The highest content of leached P was associated with P leaching under AGRR, which increased from 0.036 to 0.33 kg ha^{-1} when the amount of precipitation was two times greater than normal years. Under agriculture abandonment (AGRR+FRSE) P leaching increased 3-fold due to high rainfall. Similarly, P leaching increased from 0.1 or 0.05 kg ha^{-1} to >0.3 kg ha^{-1} FRSE and FRSD+FRSE, respectively (Fig. 5.8).

4. Discussion

Using model simulations, we tried to assess how the historic land use trajectory in the southeast US from forest to agriculture to afforestation may have influenced loading of P into streams and through soils over time. Furthermore, we wanted to assess how periods of high rainfall (or possibly individual events such as hurricanes) may have altered these rates of P runoff and leaching. Overall, our calibrations and validations of current surface runoff and P loss provide confidence that inference under historic scenarios should be possible (Figs. 5.5 and 5.6). Further, in general, patterns when converting mature hardwood forest to agricultural land that led to increased P loss from surface soil to stream and increased with rainfall amounts are consistent with previous research and our expectation. Specifically, the results indicated 1) that the highest P loss occurred when the watershed was under agriculture with P fertilization; 2) soluble P leaching in to the soil increased after abandonment from agricultural, and 3) high rainfall simulations helped to accelerate P loss into stream and through soils. To address our objectives, however, we apply these outputs to help quantify the potential quantity of P movement to stream and into the soil profile along this historical trajectory.

4.1 Land use and precipitation changes on streamflow

The simulation of different land use scenarios with SWAT indicated that streamflow through the study watershed increased between 3 to 10% when 20% of the upland area was converted to agricultural use (Fig. 5.8). Decreasing forest or increasing agricultural cover in watersheds is consistently related to increases in stream flow (Hornbeck *et al.*, 1993; Brown *et al.*, 2005). Less soil organic matter in and on the topsoil decreases the infiltration rate and low evapotranspiration from agricultural land compared with forest land both lead to a greater part of precipitation moving to surface runoff. In the current model simulation runoff increased 9-12% when 100% of the watershed was agricultural (AGRR) land in comparison with forest land use, a result within the range of previous studies. For example, a simulation on the effect of land use change on stream discharge in a Philippino watershed predicted an 11 to 17% increase in runoff volume when 50 or 100% of pasture cover was converted to agricultural land (Alibuyog *et al.*, 2009). Similarly, deforestation due to expanding urbanization or agricultural use from 1995 to 2005 in Vietnam caused an increase in surface runoff of up to 160 mm (Ngo *et al.*, 2015). Thus, it is evident that the conversion from forest to agriculture increased surface runoff and erosion in the Southeast during this trajectory of land use change.

The interaction of land use with precipitation rate on stream discharge varied across land use scenarios. When the annual precipitation rate increased two-fold the model predicted a runoff increase of 8.5-11.5% under forest and >12% increase under agricultural land. The greatest difference in percent runoff was between agricultural land with high precipitation compared with forest land use under average precipitation (Fig. 5.8). Both land use and precipitation affect streamflow as similarly demonstrated in a South Nation watershed in Ontario, Canada that had 8.5-11.2% increase in streamflow due to precipitation changes and 1.2-2.6% increase in streamflow due to land use changes (El-Khoury *et al.*, 2015). In another model simulation conducted in Brazil, watershed stream discharge decreased 39-57% due to a 20-32% reduction of precipitation (Von Randow *et al.*, 2019). In a study in the southeast USA the range of observed streamflow in Piedmont forest was 24-39 cm ha^{-1} yr^{-1} while the discharge from Piedmont agricultural land was 63-65 cm ha^{-1} yr^{-1} (Bradshaw *et al.*, 2005). Overall, the simulated model prediction of increasing streamflow when mature hardwood forest (FRSD) was cleared and converted to AGRR followed by streamflow reduction with afforestation after abandonment of agricultural provide a solid basis for considering historic P movement.

4.2 Land use and precipitation changes on P loss

The impact of land use changes on inorganic and total P predicted that P loss to the stream increase annually around 42% for inorganic P and 50% for total P when 20% of the upland forests of the watershed were converted to agricultural land (Fig. 5.8). According to land use histories for the southern US Piedmont, watersheds similar to those in the Calhoun CZO were cultivated for ~150 years. This time trajectory suggests that ~560 kg ha^{-1} P could have been lost over a 150-year period in comparison to a similar period of forest (FRSD or FRSD+FRSE) cover where just 90 kg ha^{-1} would have exited. The greater loss of P to stream water in agricultural land results largely due to annual applications of P fertilizer but harvesting activities, the loss of deep tree roots in forests, and the accelerated erosion of soil P with sediments also contribute. Multiple prior studies have quantified the role of current agricultural activities in causing soil erosion and transport of soil nutrients to streams (Sharpley and Withers, 1994; Carpenter *et al.*, 1998).

The accumulation of soil P when P fertilizer is applied to agricultural land increases the potential for P movement from soil to stream (Sharpley *et al.*, 1996; Elrashidi *et al.*, 2005). Historical research about the southeastern Piedmont reported that farmers added animal manure to the land until about 1870-1873 when superphosphate fertilizer production was begun in Charleston, SC (Sheridan, 1979). We used this information to simulate 250 kg ha^{-1} of 11-20-13 fertilizer application or 50 kg ha^{-1} of P. Given the various sources of P (manure and superphosphate) as well as uncertain formulations of superphosphate it is hard to estimate exactly how much P as fertilizers was added to our Calhoun CZO watershed over 150 years. If, however, we assumed sustained inputs of 50 kg ha^{-1} for 150 years the total input is 7,500 kg ha^{-1}. Currently, measured total soil P through 2 m of soil with an agricultural history has ~4000-6000 kg ha^{-1} but this is not greater than profiles measured in areas without previous agriculture (Foroughi *et al.*, in review). As such, we might expect high rates of P loss when 100% of the simulation watershed was agricultural land with 50 kg ha^{-1} P fertilization added to the surface soil. Under this condition, however, only 3.7 kg ha^{-1} yr^{-1} total P moved annually from soil to stream. In addition to stream export (3.7 kg ha^{-1} yr^{-1}) plant P uptake may account for an additional ~5.8 kg ha^{-1} yr^{-1} of fertilizer inputs based on model output, which still leaves 82% of P fertilization in soil mineral stocks. After 70-yrs of afforestation, current total soil P measurements do not account for any of this un-exported fertilizer P.

Given the limited P loss relative to inputs noted above, we combined land use changes with precipitation conditions addressing whether periods of high rainfall (or specific high rainfall events such as hurricanes) may have a disproportionate effect on P loss. Under the simulated model conditions, the highest total P loss to the stream was 4.6 kg $ha^{-1}yr^{-1}$ when 100% of forest (FRSD) was transformed to agricultural land (AGRR) with high precipitation, a loss rate four-fold higher than under forest land use but only 25% higher than agriculture under average rainfall (Fig. 5.8). Increasing discharge in streams can dilute P concentrations but there is a strong correlation between stream flow volume and loss of P (r = 0.47 - 0.82), which persisted for all the different land use scenarios. Combining land use and precipitation changes can cause a larger increase in runoff and nutrient loss to streamflow (Tong *et al.*, 2012). For example, in Pheasant Branch watershed Dane County, Wisconsin total P movement increased 6-fold during a storm event compared to a period of average rain fall (7 kg ha^{-1} yr^{-1}) when comparing pastureland and cultivated crop land (Huisman and Karthikeyan, 2012). Similar storm event sampling in pastureland in the Georgia Piedmont showed an average of 0.062-0.18 kg total P movement to streams per day that increased to 0.47 kg just after each storm (Byers *et al.*, 2005).

In the Calhoun CZO, changing land use history under high rainfall conditions could account for 735 kg ha^{-1} total P loss over 150 year when the watershed was agricultural land compared to 560 kg ha^{-1} total P loss under average condition reported above. Thus, loss P into stream and plant uptake could account around 1600 kg ha^{-1} P over 150 years when watershed was agriculture land. After agricultural abandonment and afforestation 69 kg ha^{-1} P could be lost over 70 years under the high rainfall situation compared to ~55 kg ha^{-1} P under average rainfall. The high rainfall simulation indicates that to the extent these years or events occurred they likely drove more P from the watershed, but the differences estimated here still do not account for 7,500 kg ha^{-}

^{1} of fertilizer P inputs. Suggesting lower P inputs or underestimated loss rates over this land use trajectory.

4.3 *Land use and precipitation changes on P leaching through soil*

While land use changes influence P movement with surface runoff, both through soil erosion and dissolved in surface runoff, a part of P movement is vertical as solution leaching through the soil profile. The simulation of land use scenarios predicted P leaching rates to the subsurface layer (i.e., below 7.5 cm) of 0.05-0.08 kg ha^{-1} yr^{-1}. In contrast with P in runoff that was highest under AGRR, rates of P leaching were lowest in AGRR being 28% less than under forest land uses. When the watershed was afforesting to AGRR+FRSE and FRSE, P leaching into the subsurface was greater than under other land uses (Fig. 5.8). Less volume of surface runoff was predicted under forest land uses due to greater surface infiltration compared with agricultural land that resulted in increased P leaching. The amount of P leaching is influenced by land cover, management activities, and the quantity of fertilizer application (Leinweber *et al.*, 1999). Hydrologic flow rates are also a primary driver with P moving slowly through the soil profile under low flow (Akhtar *et al.*, 2003). Finally, soil clays including iron and aluminum oxides can fix or adsorb P slowing it's down profile movement (Parfitt, 1978).

Consistent with historical land use changes in the Calhoun CZO, we previously found elevated extractable P in upper (0-30 cm) surface layers (Richter and Markewitz, 2001) that we presume is a response to prior fertilization. More recently, however, when comparing soil through 2m in lands known to have been farmed previously relative to reference sites we found increase in Mehlich-III extractable P throughout the profile (Foroughi *et al.*, in review). We presume this is a result of vertical soil P leaching, although this is inconsistent with expected P fixation in the iron oxide rich Bt. Based on the model output, rates of P leaching into the soil profile over a 150 yr period of agriculture and afforestation account for ~7-20 kg ha^{-1} P. In Foroughi *et al.* (in review) measured available P (Mehlich-III P) in watersheds of the Calhoun CZO that have historical agricultural land was 33 kg ha^{-1} (through 2m soil profile) greater than profiles in hillslopes with no agricultural history. This result suggests vertical P leaching over decades may account for the observed increase in subsoil available P.

Incorporating high precipitation into model simulations for the various land uses resulted in the content of P leaching to subsoil layers to increase 5 to 9-fold largely due to an increasing volume of water infiltration. Previous work has similarly demonstrated how periods of saturated soil conditions under forest or agroforestry conditions can enhance P mobility by 50-70% relative to unsaturated soil conditions (Maranguit *et al.*, 2017). Thus, leaching of P into subsoil layers over decades of land use change in the Calhoun CZO may well have been enhanced in high rainfall years or during specific high rainfall events (i.e., hurricanes).

Two centuries of land use history in the Calhoun CZO has followed a trajectory of forest to agriculture to afforestation that has left a legacy of P enrichment and redistribution. Generally, stream water losses of P increased with decreasing forest proportion and inputs of P fertilizer during agriculture while during afforestation P stream water fluxes declined; all expected responses. Phosphorus leaching vertically through soils followed a different pattern with the highest P leaching rates to subsurface soil under afforesting conditions when soil P was elevated but so were surface soil infiltration rates. Model rates of P leaching at the end of the afforestation trajectory were similar to measured rates of 0.48-0.55 μmol L^{-1} phosphate in soil solution at 15 cm and 0.2-0.6 μmol L^{-1} at 60 cm (Foroughi *et al.*, in review). Previous measurement in the Calhoun CZO of total soil P that showed no difference between historically farmed relative to unfarmed watersheds could not be well-explained by P losses even at 4.5 kg ha^{-1} under agriculture with high rainfall rates. If fertilizer inputs were truly 7,500 kg ha^{-1} over the long sweep of 150-yrs loss would account for <1000 kg ha^{-1}. In contrast, subsurface increase in Mehlich III P through 2m of ~ 30 kg-P ha^{-1} were consistent with model leaching estimates over the agriculture to afforestation period of the trajectory. Vertical leaching fluxes of ~40 kg-P ha^{-1} could account for the entire increase.

5. Conclusion

This study revealed how historical land use changes may have effected P movement from soil to streamflow and how increased rainfall has the potential to amplify the loss of P with runoff. Deforestation and cultivation of the watershed increased streamflow and P loss from soil to stream, particularly with agricultural P fertilizer. Intensive rainfall rate has a positive effect on P movement that combined with land use scenarios could exceed P content in streamflow. Phosphorus mobility in water declines due to afforestation after agricultural land abandonment. This historical land use modeling approach constrains estimates of how much P might have been released to stream and into the soil profile when the southeastern Piedmont was under cultivation for 150 years. The model suggested a lower historic P fertilization rate than utilized here and that vertical leaching of P is consistent with currently observed subsoil P increases.

References

Abbaspour, K.C., 2013. SWAT-CUP 2012. SWAT Calibration and Uncertainty Program—A User Manual.

Abbaspour, K.C., Yang, J., Maximov, I., Siber, R., Bogner, K., Mieleitner, J., Zobrist, J., Srinivasan, R., 2007. Modelling hydrology and water quality in the pre-alpine/alpine Thur watershed using SWAT. Journal of hydrology 333, 413-430.

Aguiar, A.d.C.F., Cândido, C.S., Carvalho, C.S., Monroe, P.H.M., de Moura, E.G., 2013. Organic matter fraction and pools of phosphorus as indicators of the impact of land use in the Amazonian periphery. Ecological indicators 30, 158-164.

Akhtar, M.S., Richards, B.K., Medrano, P.A., DeGroot, M., Steenhuis, T.S., 2003. Dissolved phosphorus from undisturbed soil cores. Soil Science Society of America Journal 67, 458-470.

Alibuyog, N., Ella, V., Reyes, M.R., Srinivasan, R., Heatwole, C., Dillaha, T., 2009. Predicting the effects of land use change on runoff and sediment yield in Manupali River subwatersheds using the SWAT model. International Agricultural Engineering Journal 18, 15.

Alt, F., Oelmann, Y., Herold, N., Schrumpf, M., Wilcke, W., 2011. Phosphorus partitioning in grassland and forest soils of Germany as related to land-use type, management intensity, and land use–related pH. Journal of Plant Nutrition and Soil Science 174, 195-209.

Arnold, J.G., Allen, P.M., Bernhardt, G., 1993. A comprehensive surface-groundwater flow model. Journal of hydrology 142, 47-69.

Arnold, J.G., Srinivasan, R., Muttiah, R.S., Williams, J.R., 1998. Large area hydrologic modeling and assessment part I: Model development1. Wiley Online Library.

Bradshaw, J.K., Radcliffe, D.E., Lichtenstein, K., Bakker, M., Jackson, R., Markewitz, D., Risse, L.M., 2005. Land use effects on suspended sediment yield in six small Georgia watersheds. Georgia Institute of Technology.

Brender, E., 1952. From forest to farm to forest again. Am. For 58, 24-25.

Brown, A.E., Zhang, L., McMahon, T.A., Western, A.W., Vertessy, R.A., 2005. A review of paired catchment studies for determining changes in water yield resulting from alterations in vegetation. Journal of hydrology 310, 28-61.

Byers, H.L., Cabrera, M.L., Matthews, M.K., Franklin, D.H., Andrae, J.G., Radcliffe, D.E., McCann, M.A., Kuykendall, H.A., Hoveland, C.S., Calvert, V.H., 2005. Phosphorus, sediment, and Escherichia coli loads in unfenced streams of the Georgia Piedmont, USA. Journal of Environmental Quality 34, 2293-2300.

Carpenter, S.R., Caraco, N.F., Correll, D.L., Howarth, R.W., Sharpley, A.N., Smith, V.H., 1998. Nonpoint pollution of surface waters with phosphorus and nitrogen. Ecological applications 8, 559-568.

Compton, J.E., Boone, R.D., 2000. Long-term impacts of agriculture on soil carbon and nitrogen in New England forests. Ecology 81, 2314-2330.

Cowell, C.M., 1998. Historical change in vegetation and disturbance on the Georgia Piedmont. The American midland naturalist 140, 78-90.

Deng, Q., McMahon, D.E., Xiang, Y., Yu, C.L., Jackson, R.B., Hui, D., 2017. A global meta-analysis of soil phosphorus dynamics after afforestation. New Phytologist 213, 181-192.

Dillon, P.J., Kirchner, W., 1975. The effects of geology and land use on the export of phosphorus from watersheds. Water Research 9, 135-148.

El-Khoury, A., Seidou, O., Lapen, D., Que, Z., Mohammadian, M., Sunohara, M., Bahram, D., 2015. Combined impacts of future climate and land use changes on discharge, nitrogen and phosphorus loads for a Canadian river basin. Journal of environmental management 151, 76-86.

Elrashidi, M., Mays, M., Harder, J., Schroeder, D., Brakhage, P., Peaslee, S., Seybold, C., Schaecher, C., 2005. Loss of phosphorus by runoff for agricultural watersheds. Soil science 170, 543-558.

Foroughi, M., Sutter, L., Markewitz, D., in review. The role of hillslope and land use history on P distribution. Submitted to Biogeochemistry CZO Book, Springer.

Foster, D., Swanson, F., Aber, J., Burke, I., Brokaw, N., Tilman, D., Knapp, A., 2003. The importance of land-use legacies to ecology and conservation. BioScience 53, 77-88.

Gassman, P.W., Reyes, M.R., Green, C.H., Arnold, J.G., 2007. The soil and water assessment tool: historical development, applications, and future research directions. Transactions of the ASABE 50, 1211-1250.

Goyette, J.-O., Bennett, E., Maranger, R., 2018. Low buffering capacity and slow recovery of anthropogenic phosphorus pollution in watersheds. Nature Geoscience, 1.

Gray, L.C., Thompson, E.K., 1933. History of agriculture in the southern United States to 1860.

Grieve, I.C., 2001. Human impacts on soil properties and their implications for the sensitivity of soil systems in Scotland. Catena 42, 361-374.

Hall, A.R., 1949. Terracing in the southern Piedmont. Agricultural History 23, 96-109.

Hart, J.F., 1980. Land use change in a piedmont county. Annals of the association of American geographers 70, 492-527.

Hornbeck, J., Adams, M., Corbett, E., Verry, E., Lynch, J., 1993. Long-term impacts of forest treatments on water yield: a summary for northeastern USA. Journal of Hydrology 150, 323-344.

Huisman, N.L., Karthikeyan, K., 2012. Using radiometric tools to track sediment and phosphorus movement in an agricultural watershed. Journal of hydrology 450, 219-229.

Hurtt, G.C., Frolking, S., Fearon, M., Moore, B., Shevliakova, E., Malyshev, S., Pacala, S.W., Houghton, R., 2006. The underpinnings of land-use history: Three centuries of global gridded land-use transitions, wood-harvest activity, and resulting secondary lands. Global Change Biology 12, 1208-1229.

Ireland, H.A., Sharpe, C.F.S., Eargle, D., 1939. Principles of gully erosion in the Piedmont of South Carolina. US Department of Agriculture.

Jiang, S., Hua, H., Jarvie, H.P., Liu, X., Zhang, Y., Sheng, H., Liu, X., Zhang, L., Yuan, Z., 2018. Enhanced nitrogen and phosphorus flows in a mixed land use basin: Drivers and consequences. Journal of cleaner production 181, 416-425.

Johnes, P., Heathwaite, A.L., 1997. Modelling the impact of land use change on water quality in agricultural catchments. Hydrological processes 11, 269-286.

Leinweber, P., Meissner, R., Eckhardt, K.U., Seeger, J., 1999. Management effects on forms of phosphorus in soil and leaching losses. European Journal of Soil Science 50, 413-424.

MacDonald, G.K., Bennett, E.M., Taranu, Z.E., 2012. The influence of time, soil characteristics, and land-use history on soil phosphorus legacies: a global meta-analysis. Global Change Biology 18, 1904-1917.

Mallard, J.M., 2017. CZO Dataset: Calhoun CZO - Precipitation (2014-2017).Retrieved 23 Jun 2019,. http://criticalzone.org/calhoun/data/dataset/6421/.

Mallard, J.M., 2018. Calhoun CZO Stream Discharge/Runoff, HydroShare. https://www.hydroshare.org/resource/ad719c838a7b44e8bbacb33d2c4dd95f/.

Maranguit, D., Guillaume, T., Kuzyakov, Y., 2017. Land-use change affects phosphorus fractions in highly weathered tropical soils. Catena 149, 385-393.

McLauchlan, K., 2006. The nature and longevity of agricultural impacts on soil carbon and nutrients: a review. Ecosystems 9, 1364-1382.

Mehdi, B., Ludwig, R., Lehner, B., 2015. Evaluating the impacts of climate change and crop land use change on streamflow, nitrates and phosphorus: a modeling study in Bavaria. Journal of Hydrology: Regional Studies 4, 60-90.

Metz, L.J., 1958. The Calhoun experimental forest. unknown.

Neitsch, S.L., Arnold, J.G., Kiniry, J.R., Williams, J.R., 2011. Soil and water assessment tool theoretical documentation version 2009. Texas Water Resources Institute.

Ngo, T.S., Nguyen, D.B., Rajendra, P.S., 2015. Effect of land use change on runoff and sediment yield in Da River Basin of Hoa Binh province, Northwest Vietnam. Journal of Mountain Science 12, 1051-1064.

Nielsen, A., Trolle, D., Søndergaard, M., Lauridsen, T.L., Bjerring, R., Olesen, J.E., Jeppesen, E., 2012. Watershed land use effects on lake water quality in Denmark. Ecological applications 22, 1187-1200.

Osborne, L.L., 1988. Empirical relationship between land use/cover and stream water quality in an agricultural watershed. J Environ Manage 26, 9-27.

Parfitt, R., 1978. Anion adsorption by soils and soil materials. Adv. Agron 30, 50.

Pettus, L., 1995. Surveying practices in early South Carolina. Backsights Magazine.

Richter, D.D., Allen, H.L., Li, J., Markewitz, D., Raikes, J., 2006. Bioavailability of slowly cycling soil phosphorus: major restructuring of soil P fractions over four decades in an aggrading forest. Oecologia 150, 259-271.

Richter, D.D., Markewitz, D., 2001. Understanding soil change : soil sustainability over millennia, centuries, and decades. Cambridge University Press, Cambridge.

Ruffin, E., 1852. An essay on calcareous manures. JW Randolph.

Schmidt, J., Buol, S., Kamprath, E., 1997. Soil phosphorus dynamics during 17 years of continuous cultivation: a method to estimate long-term P availability. Geoderma 78, 59-70.

Sharpley, A., 1985. Depth of Surface Soil-runoff Interaction as Affected by Rainfall, Soil Slope, and Management 1. Soil Science Society of America Journal 49, 1010-1015.

Sharpley, A., Ahuja, L., Menzel, R., 1981. The Release of Soil Phosphorus to Runoff in Relation to the Kinetics of Desorption 1. Journal of Environmental Quality 10, 386-391.

Sharpley, A., Daniel, T., Sims, J., Pote, D., 1996. Determining environmentally sound soil phosphorus levels. Journal of soil and water conservation 51, 160-166.

Sharpley, A.N., Smith, S., 1990. Phosphorus transport in agricultural runoff: the role of soil erosion. Soil erosion on agricultural land. Proceedings of a workshop sponsored by the British Geomorphological Research Group, Coventry, UK, January 1989. John Wiley & Sons Ltd., pp. 351-366.

Sharpley, A.N., Withers, P.J., 1994. The environmentally-sound management of agricultural phosphorus. Fertilizer research 39, 133-146.

Sheridan, R.C., 1979. Chemical fertilizers in southern agriculture. Agricultural History 53, 308-318.

Taylor, R.H., 1953. Fertilizers and Farming in the Southeast, 1840-1950: Part I: 1840-1900. The North Carolina Historical Review 30, 305-328.

Tong, S.T., Sun, Y., Ranatunga, T., He, J., Yang, Y.J., 2012. Predicting plausible impacts of sets of climate and land use change scenarios on water resources. Applied Geography 32, 477-489.

Trimble, S.W., 1974. Man-induced soil erosion on the southern Piedmont. Soil Conservation Society of America.

Trimble, S.W., 2008. Man-induced soil erosion on the Southern Piedmont, 1700-1970. Soil and Water Conservation Society.

Turner, M.G., Ruscher, C.L., 1988. Changes in landscape patterns in Georgia, USA. Landscape ecology 1, 241-251.

Veldkamp, A., Verburg, P.H., 2004. Modelling land use change and environmental impact. Elsevier.

Vogt, J.T., Smith, W.B., 2017. USDA Forest Inventory and Analysis Fiscal Year 2016 Business Report. https://bit.ly/3302zrn.

Von Randow, R.C.S., Rodriguez, D.A., Tomasella, J., Aguiar, A.P.D., Kruijt, B., Kabat, P., 2019. Response of the river discharge in the Tocantins River Basin, Brazil, to environmental changes and the associated effects on the energy potential. Regional environmental change 19, 193-204.

Wang, X., Shang, S., Yang, W., Clary, C.R., Yang, D., 2010. Simulation of land use–soil interactive effects on water and sediment yields at watershed scale. Ecological Engineering 36, 328-344.

Wear, D.N., Greis, J.G., 2013. The southern forest futures project: Technical report. Gen. Tech. Rep. SRS-GTR-178. Asheville, NC: USDA-Forest Service, Southern Research Station. 542 p. 178, 1-542.

Williams, M., 1992. Americans and their forests: a historical geography. Cambridge University Press.

Wilson, C.O., Weng, Q., 2011. Simulating the impacts of future land use and climate changes on surface water quality in the Des Plaines River watershed, Chicago Metropolitan Statistical Area, Illinois. Science of the Total Environment 409, 4387-4405.

Table 5.1. Streamflow and phosphorus parameters, fitted values, and P-value used for calibration of the model in SWAT-CUP (Soil and Water Assessment Tool Calibration and Uncertainty Program)

Parameter	Description	Fitted value	P-value
<u>Flow parameters</u>			
r__CN2.mgt	Runoff curve number II	-0.095	$1.34e^{-66}$
v__ALPHA_BF.gw	Exponential decay factor for groundwater flow to the stream (1/day)	0.598	0.579
v__GW_DELAY.gw	Ground water delay time (days)	70.48	0.265
v__GWQMN.gw	Threshold depth of water in the shallow aquifer (mm)	0.075	0.714
v__GW_REVAP.gw	Groundwater re-evaporation coefficient	0.175	0.220
v__TRNSRCH.bsn	Fraction of transmission losses from main channel (m^3/s)	0.487	$2.74e^{-27}$
v__CH_K2.rte	Effective hydraulic conductivity of the alluvium in the main channel (mm/hr)	11.30	$1.34e^{-66}$
v__CH_K1.sub	Effective hydraulic conductivity in tributary channel alluvium (mm/hr)	197.5	0.638
v__CH_N2.rte	Manning's roughness coefficient of the main channel	0.157	0.024
v__SURLAG.bsn	Surface runoff lag coefficient	4.144	0.546
r__SOL_K().sol	Saturated hydraulic conductivity (mm/hr)	0.223	0.252
r__SOL_AWC().sol	Available water capacity of the soil layer (mm H_2O/mm soil)	1.140	0.243
r__SOL_BD().sol	Moist bulk density (g/cm^3)	-0.090	1.884
v__ESCO.bsn	Soil evaporation compensation factor	0.498	0.831
v__EPCO.bsn	Plant uptake compensation factor	0.170	0.570
<u>Phosphours parameters</u>			
v__PPERCO.bsn	Phosphorus percolation coefficient	13.05	0.107
v__PSP.bsn	Phosphorus sorption coefficient	0.824	0.789
v__ERORGP.hru	Organic P enrichment ratio	4.791	$1.56e^{-15}$
v__RSDCO.bsn	Residue decomposition coefficient	0.006	0.937
v__PHOSKD.bsn	Phosphorus soil partitioning coefficient	164.1	$2.65e^{-07}$

Table 5.2. Statistical criteria used as primary objective functions to evaluate the loss of P in land use and streamflow for calibration and validation.

Items[1]	Time	Criteria[2]	Calibration	Validation
Streamflow (m^3/s)	Daily	RMSE	0.003	0.005
		NSE	0.620	0.590
		R^2	0.620	0.480
Streamflow (m^3/s)	Monthly	RMSE	0.001	0.001
		NSE	0.720	0.550
		R^2	0.750	0.590
Total P (kg/ha)	Monthly	RMSE	1.420	0.970
		NSE	0.390	0.340
		R^2	0.520	0.820
Inorganic P (kg/ha)	Monthly	RMSE	0.040	0.020
		NSE	0.460	0.310
		R^2	0.500	0.830

[1] P: phosphorus
[2] NSE: Nash-Sutcliff Efficiency, R^2: Coefficient of determination, RMSE: Root mean square error

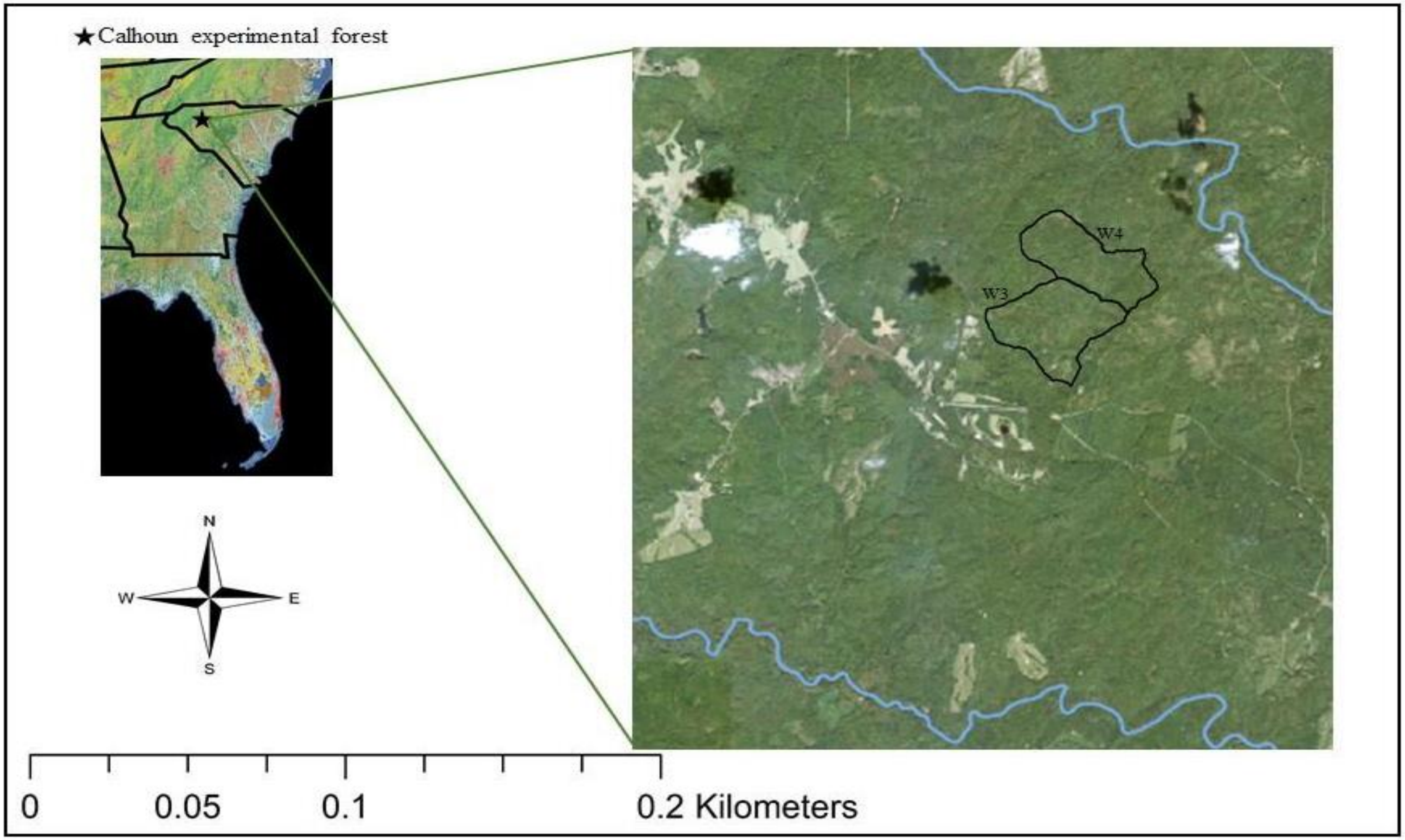

Figure 5.1. Study watershed (W4) location in Calhoun Critical Zone Observatory in Union county, South Carolina (SC). W4: Study watershed, W3: Validate watershed

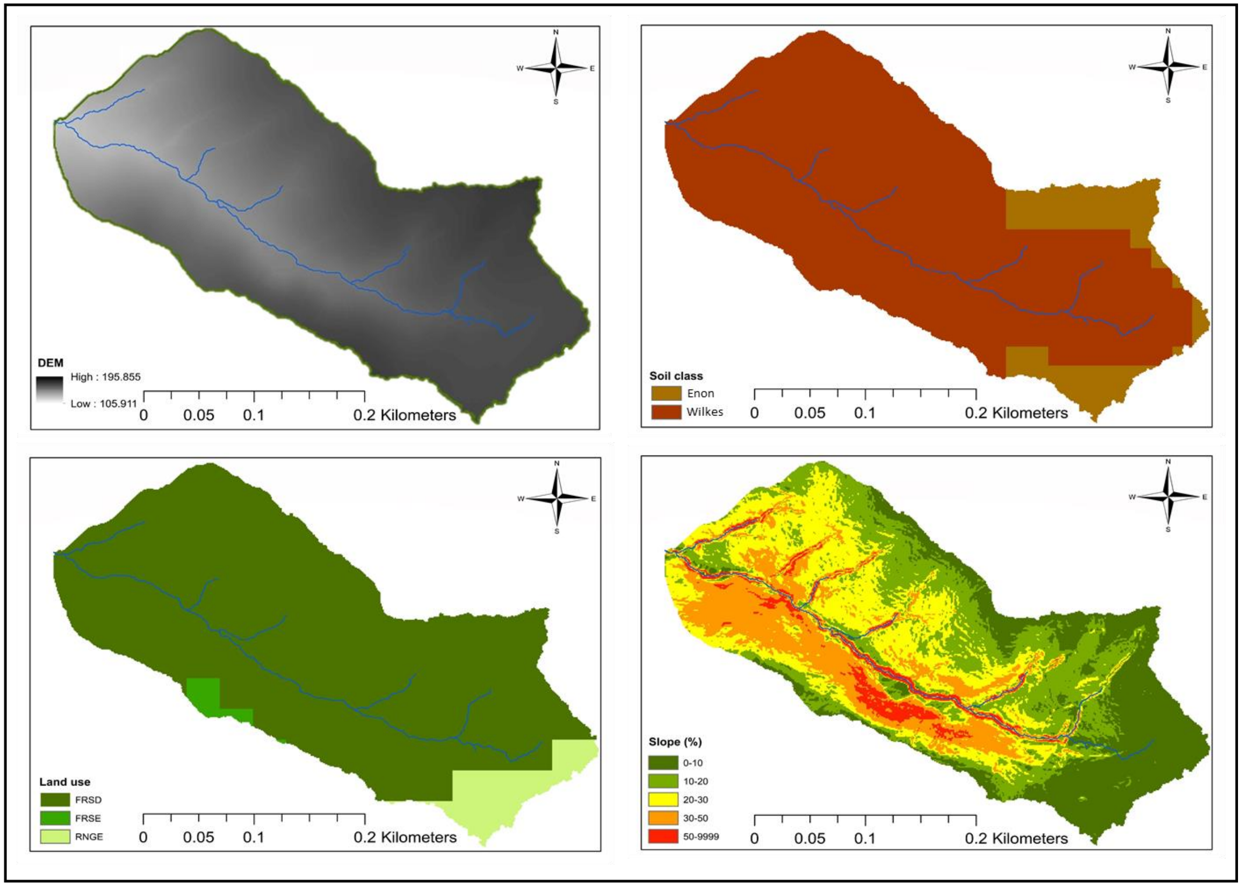

Figure 5.2. ArcSWAT input map data for study watershed W4 in Calhoun Critical Zone Observatory in Union county, South Carolina (SC). DEM: Digital elevation map, FRSD: deciduous forest, FRSE: evergreen forest, RNGE: grasslands

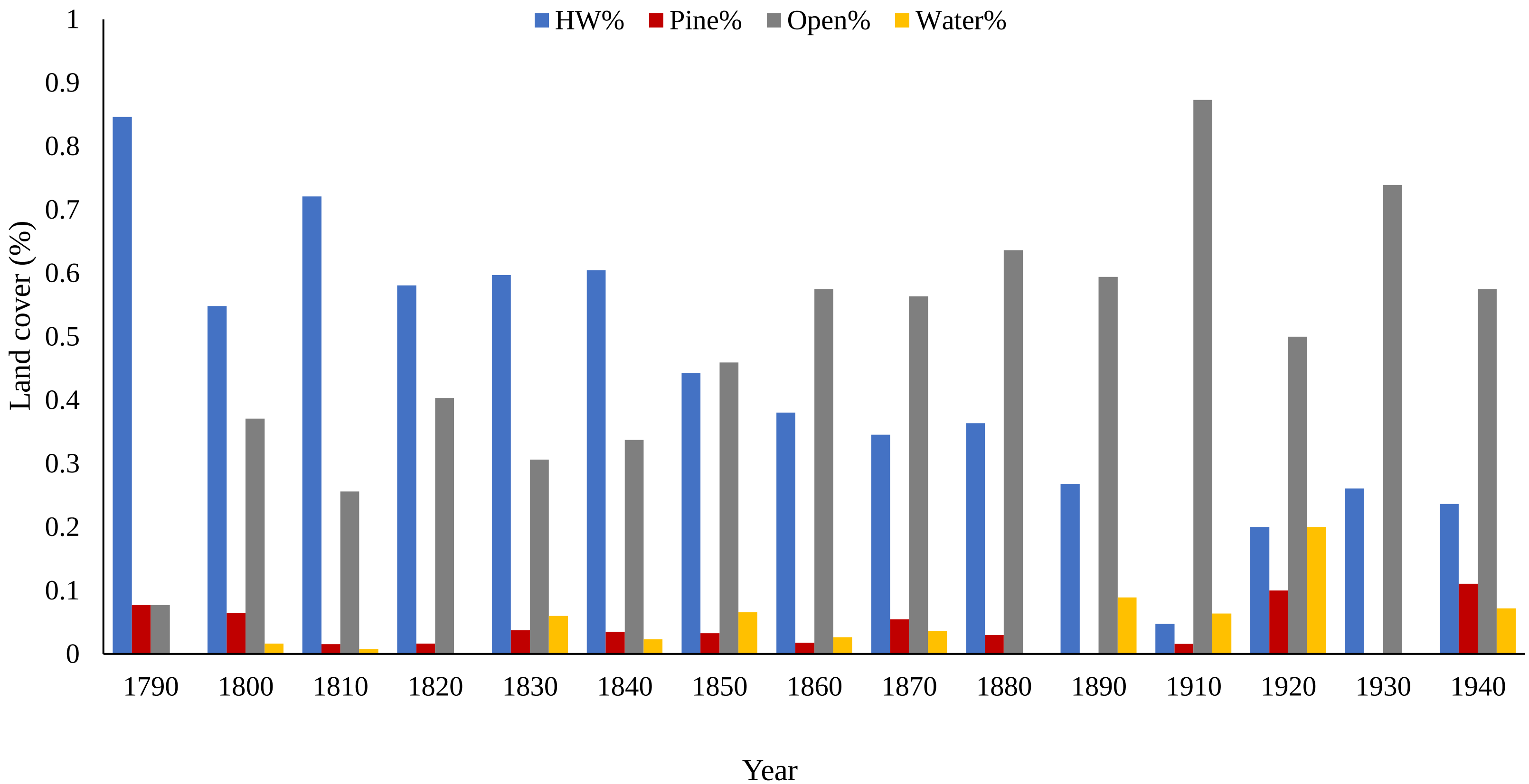

Figure 5.3. Land cover changes at Calhoun Critical Zone Observatory in Sumter national forest, South Carolina, US from 1790 to 1940.

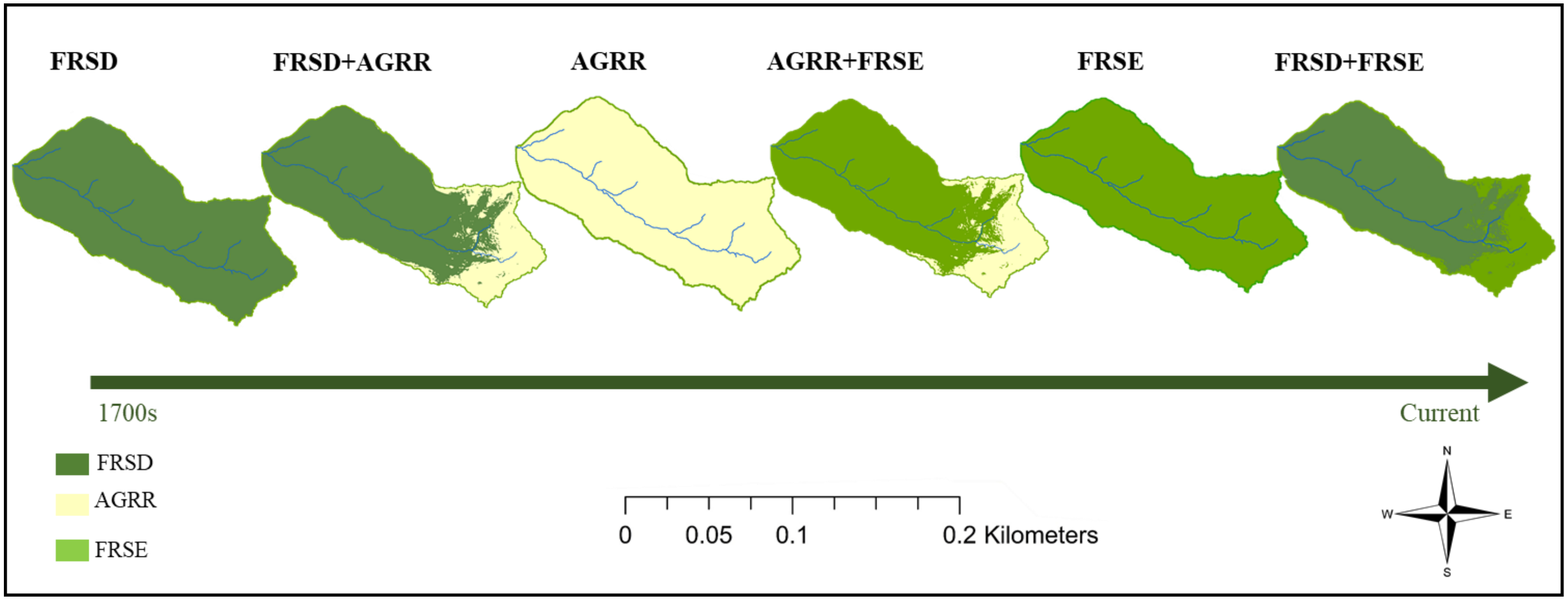

Figure 5.4. Land use scenarios of the study watershed W4 in Calhoun Critical Zone Observatory in Union county, South C FRSD: Deciduous forest, AGRR: Agricultural land, and FRSE: Pine forest.

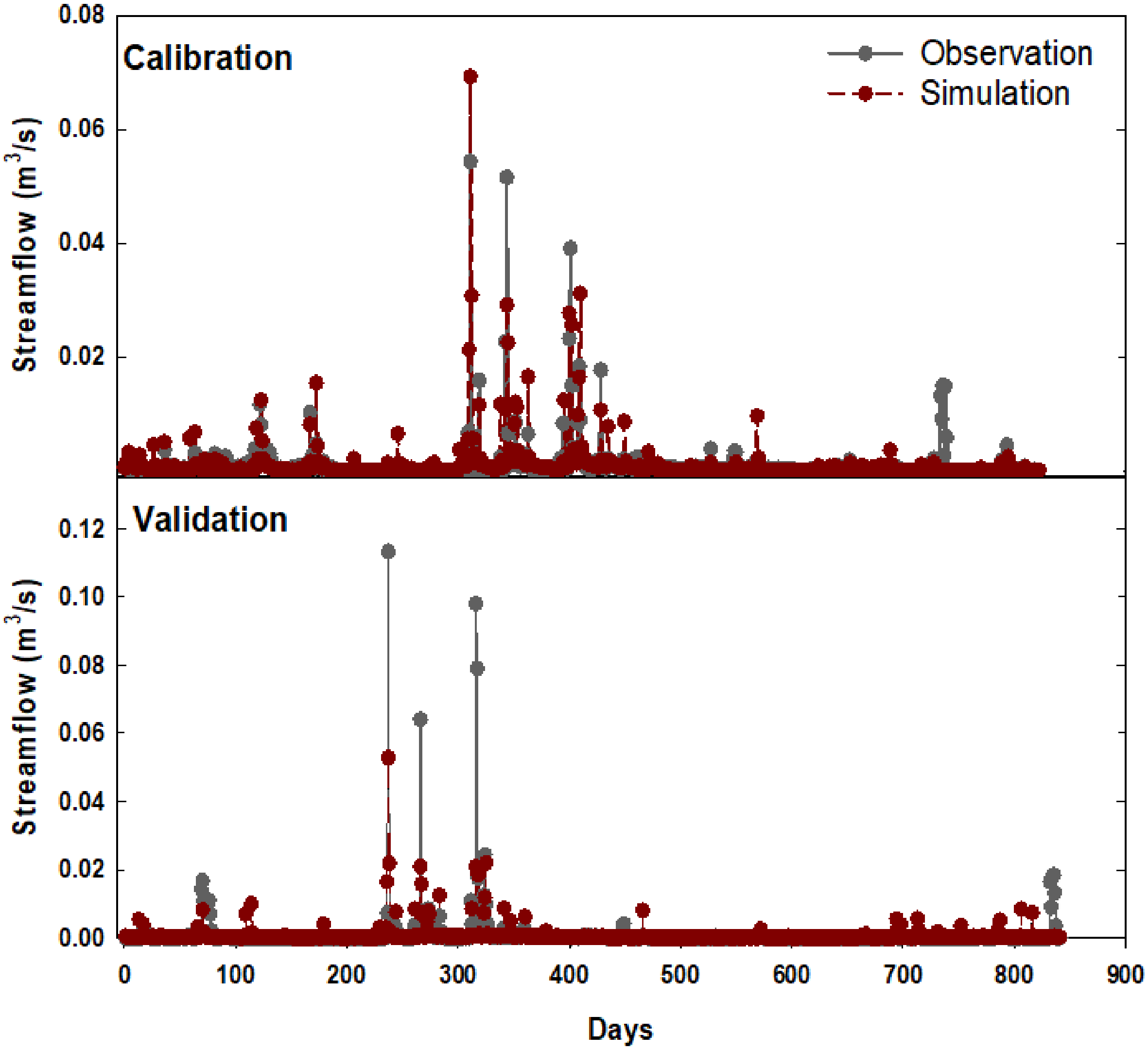

Figure 5.5. The observed and simulated plots of daily streamflow of model calibration and validation in the Calhoun CZO.

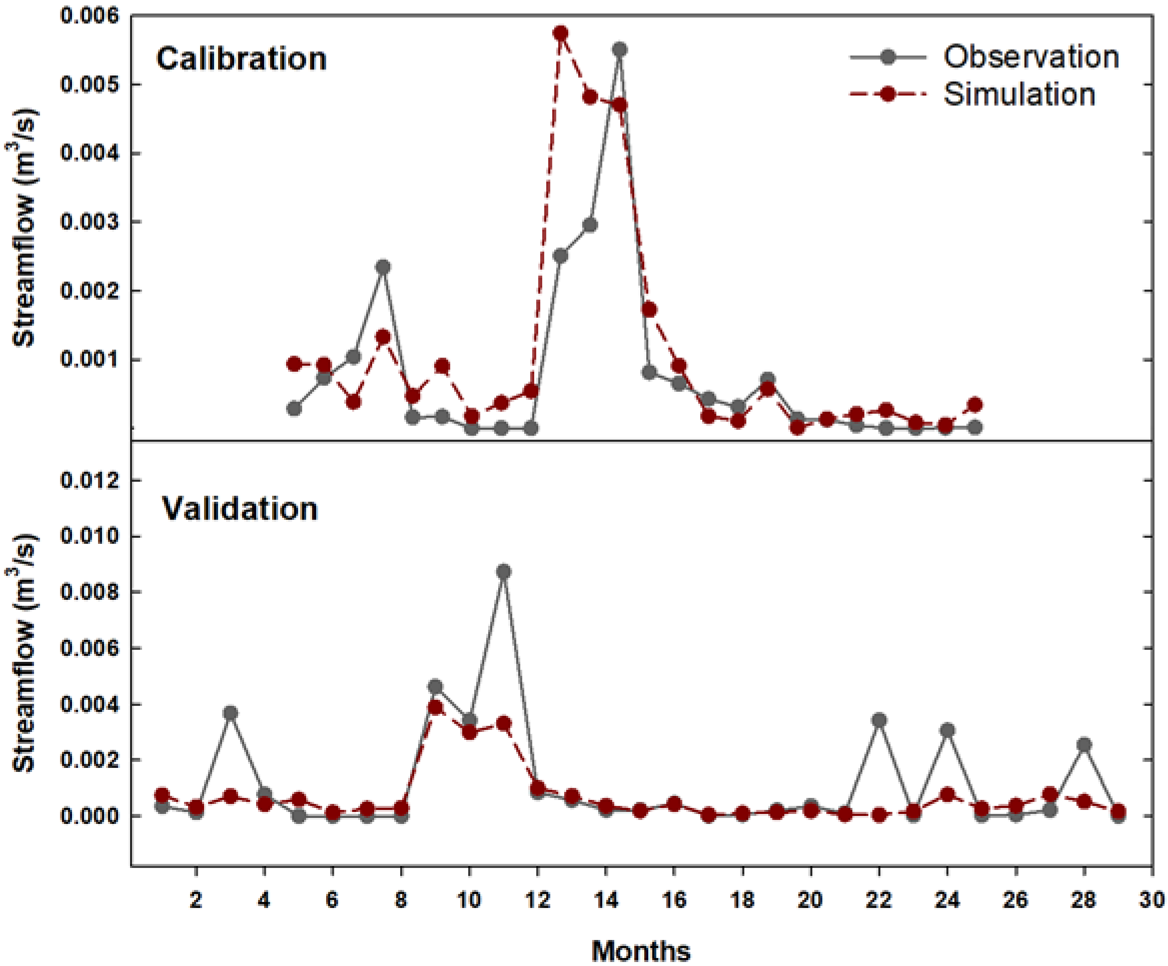

Figure 5.6. The observed and simulated plots of monthly streamflow of model calibration and validation in the Calhoun CZO.

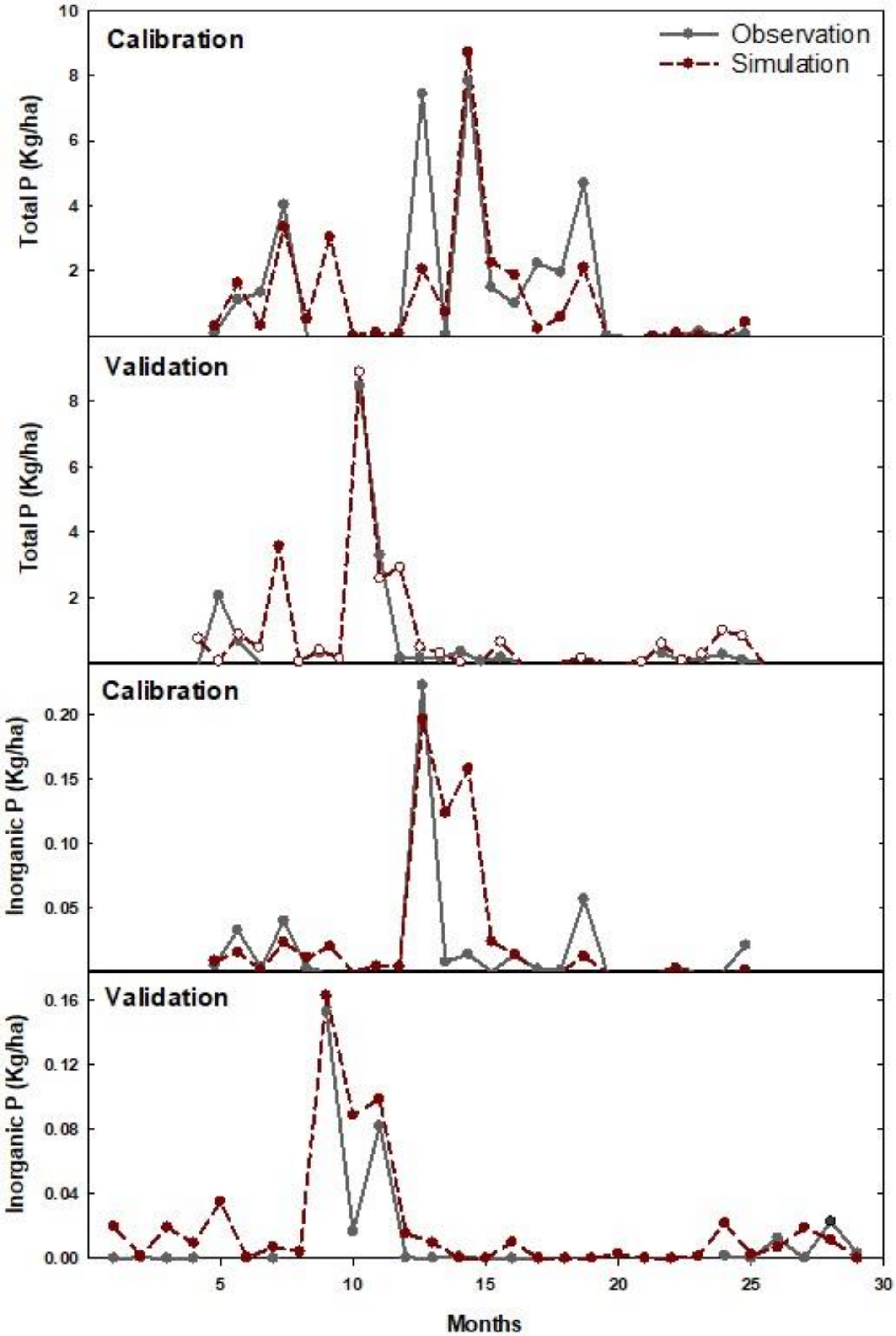

Figure 5.7. The observed and simulated plots of total and inorganic phosphorus of model calibration and validation in the Calhoun CZO.

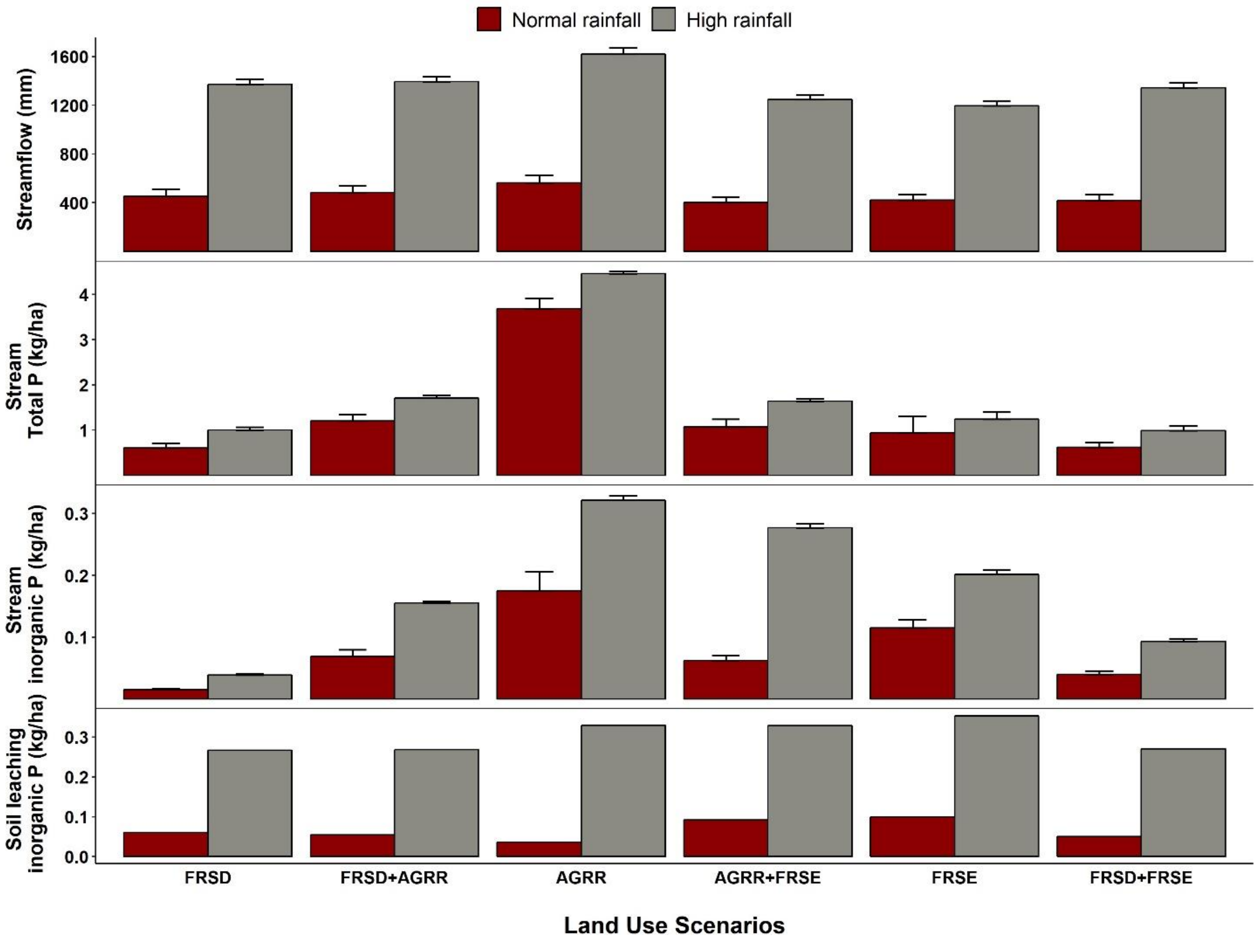

Figure 5.8. Simulated streamflow (mm), total and inorganic phosphorus (P) in streams, and soil leaching inorganic P in subsoil layer for different land use and climate scenarios in the study area. FRSD: Deciduous forest, AGRR: Agricultural land, FRSE: Pine forest.

CHAPTER 6

CONCLUSIONS

This study investigated P distribution in a Southeastern US Piedmont forest to answer questions about the effect of historical land use changes, topography, and forest development on soil P fractions over time. With this in mind, three individual studies addressed P redistribution. Chapter 3 describes the role of hillslope and land use history on P distribution in the critical zone; Chapter 4 describes dynamics of soil phosphorus distribution over sixty years of forest development in the in the critical zone Observatory in the Southeastern US Piedmont; Chapter 5 models the impacts of historical land use on phosphorus movement in the Calhoun Critical Zone in the Southeastern US Piedmont.

The effects of historical land use changes and topography on soil P were determined by comparing soil P fractions in three hillslope positions of watersheds with historical agricultural activity and hardwood forest with no prior farming use. Soil solutions were also collected from four hillslope positions at the same watersheds. Besides soil solutions, streams samples were collected from different streams of different orders to follow P movement in this area. The P fractions results showed the available P quantity in ridge tops that were farmed was greater than reference ridges through a 2 m soil profile due to P input and vertical leaching of P over several decades. In contrast, soil solution had higher P release in reference sites compared to agricultural hillslopes possibly due to no loss of organic matter and a retention of roots in these areas. Overall, a limited accumulation of soil P in downslope locations can be due to P washing into streams and being lost from the soil system. The anthropogene effects on soil P biogeochemistry is still evident in the Calhoun Critical Zone Observatory (Calhoun CZO).

The effects of forest regeneration on prior agricultural land relating to P distribution were studied by collecting soil samples from 1962 to 2017 for four different soil depths (through 60 cm) from 8 permanent uncut plots. Similarly, soil samples were collected from 8 permanent plots cut in 2007. Phosphorus data indicated the Mehlich-III P pools declined from 1962 (39 μg g^{-1}) to 2017 (16 μg g^{-1}) in the surface layer (0-7.5 cm) in uncut plots. The same P fraction reduced from 2005 (25.2 and 33.1 μg g^{-1}) to 2017 (17.7 and 22.8 μg g^{-1}) in the top 2 soil layers (0-7.5 and 7.5-15 cm, respectively) of cut plots. Slowly cycling P fractions (NaOH and HCl) also declined (~80 kg ha^{-1}) during this 55 year period. Despite these decreases, estimates of P accumulation in trees and forest floor exceeded these changes in soil P content. As such, the recycling of organic P due to accumulating organic matter in these regenerating forests appears necessary to meet P demand. Overall, the slowly cycling P fractions and decomposition of litterfall and trees debris have a critical role in soil P sustainability.

Long term land use changes in the southeastern US Piedmont forests effects on soil P concentration on top ridge and P leaching into the soil profile with application P fertilization. Also, land use changes impact on P movement to downslope with soil erosion. The P measurement indicated the soil solution P in old pine forest with historical agricultural land was lower than hardwood forest with no prior farm use, however, the current available P pools in old pine forest was greater than hardwood forest. Modeling determined how historical land use changes in the southeastern US Piedmont impacted on soil P movement at this area over 200 years. The model includes six different land use scenarios (FRSD, FRSD+AGRR, AGRR, AGRR+FRSE, FRSE, and FRSD+FRSE) with two rainfall rates (Normal and high). The output of the model indicated deforestation and conversion to agricultural land caused more than 550±200 kg ha^{-1} P movement from soil into streams for 150 years while the reverted land from agriculture to forest reduced the P movement to 69 kg ha^{-1} for the next 70 years. The amount of soluble P leached around 38±10 kg ha^{-1} in soil profile for 200 years during land use change in the Southeastern Piedmont forest. The highest P content leached into soil profile observed after regenerating forest due to prior application P fertilization. Changing the rainfall rate has a positive effect on P movement into streams and soil profile. Overall, modeling historical land use could explain the current difference of soil P distribution between watersheds with historical agricultural land and hardwood forest with no prior farm activities in the Southeastern US Piedmont.